



# GEOLOGY OF THE INTERMOUNTAIN WEST

*an open-access journal of the Utah Geological Association*

ISSN 2380-7601

Volume 10

2023

## STRATIGRAPHY, SEDIMENTOLOGY, AND PALEOCLIMATIC PROXIES OF THE UPPER JURASSIC MORRISON FORMATION OF CENTRAL MONTANA

Dean R. Richmond



This is an open-access article in which the Utah Geological Association permits unrestricted use, distribution, and reproduction of text and figures that are not noted as copyrighted, provided the original author and source are credited. Email inquiries to [GIW@utahgeology.org](mailto:GIW@utahgeology.org).



# GEOLOGY OF THE INTERMOUNTAIN WEST

*an open-access journal of the Utah Geological Association*

ISSN 2380-7601

Volume 10

2023

## Editors

Douglas A. Sprinkel Azteca Geosolutions 801.391.1977 GIW@utahgeology.org dsprinkel@gmail.com	Thomas C. Chidsey, Jr. Utah Geological Survey 801.824.0738 tomchidsey@gmail.com
Bart J. Kowallis Brigham Young University 801.380.2736 bkowallis@gmail.com	John R. Foster Utah Field House of Natural History State Park Museum 435.789.3799 johnfoster@utah.gov
Steven Schamel GeoX Consulting, Inc. 801.583-1146 geox-slc@comcast.net	

## Production

Cover Design and Desktop Publishing  
Douglas A. Sprinkel

Cover

*Fossil dinosaur bones were first discovered in the Upper Jurassic Morrison Formation near the town of Grass Range, Montana, in 1987. The first excavation commenced in 2003 by the Judith River Dinosaur Institute. The discovery of numerous fossil dinosaur bones and ongoing excavations prompted geologic research in the area. The photograph is of the 2017 Judith River Dinosaur Institute Quarry 3 excavation. The quarry is stratigraphically 28 m above the underlying Swift Formation. Large, disarticulated sauropod bones can be seen exhumed from a gray mudstone bed. Scales are 1 m and 0.5 m.*



Geology of the Intermountain West (GIW) is an open-access journal in which the Utah Geological Association permits unrestricted use, distribution, and reproduction of text and figures that are not noted as copyrighted, provided the original author and source are credited.

## 2023–2024 UGA Board

President	Eugene Szymanski	eugenes@utah.gov	801.537.3364
President-Elect	Keilee Higgs	keileeann@utah.gov	801.678.3683
Program Chair	Chris Stallard	cstallard@utah.gov	801.386.0976
Treasurer	Aubry DeReuil	aubry@zanskar.us	850.572.2543
Secretary	Trae Boman	tbowman@teamues.com	801.648.5206
Past President	Rick Ford	rford@weber.edu	801.915.3188

## UGA Committees

Environmental Affairs	Craig Eaton	eaton@ihi-env.com	801.633.9396
Geologic Road Sign	Greg Gavin	greg@loughlinwater.com	801.541.6258
Historian	Paul Anderson	paul@pbageo.com	801.364.6613
Outreach	Greg Nielsen	gnielsen@weber.edu	801.626.6394
Public Education	Zach Anderson	zanderson@utah.gov	801.537.3300
	Matt Affolter	gfl247@yahoo.com	
Publications	Paul Inkenbrandt	paulinkenbrandt@utah.gov	801.537.3361
Publicity	Paul Inkenbrandt	paulinkenbrandt@utah.gov	801.537.3361
Social/Recreation	Roger Bon	rogerbon@xmission.com	801.942.0533

## AAPG House of Delegates

2024–2026 Term	David A. Wavrek	dwavrek@petroleumsystems.com	801.322.2915
----------------	-----------------	------------------------------	--------------

## State Mapping Advisory Committee

UGA Representative	Bill Loughlin	bill@loughlinwater.com	435.649.4005
--------------------	---------------	------------------------	--------------

## Earthquake Safety Committee

Chair	Grant Willis	gwillisgeol@gmail.com	801.537.3355
-------	--------------	-----------------------	--------------

## UGA Website — [www.utahgeology.org](http://www.utahgeology.org)

Webmaster	Paul Inkenbrandt	paulinkenbrandt@utah.gov	801.537.3361
-----------	------------------	--------------------------	--------------

## UGA Newsletter

Newsletter Editor	Bill Lund	uga.newsletter@gmail.com	435.590.1338
-------------------	-----------	--------------------------	--------------

*Become a member of the UGA to help support the work of the Association and receive notices for monthly meetings, annual field conferences, and new publications. Annual membership is \$30 and annual student membership is only \$5. Visit the UGA website at [www.utahgeology.org](http://www.utahgeology.org) for information and membership application.*

*The UGA board is elected annually by a voting process through UGA members. However, the UGA is a volunteer-driven organization, and we welcome your voluntary service. If you would like to participate please contact the current president or committee member corresponding with the area in which you would like to volunteer.*



## Stratigraphy, Sedimentology, and Paleoclimatic Proxies of the Upper Jurassic Morrison Formation of Central Montana

Dean R. Richmond

Sam Noble Museum, University of Oklahoma, Norman, OK 73072 USA; [drrichmond@ou.edu](mailto:drrichmond@ou.edu).

### ABSTRACT

Since the discovery of dinosaurs in the late 19th century, the Upper Jurassic Morrison Formation has received considerable scholarly attention. However, the formation in central Montana needed to be sufficiently investigated. Recent dinosaur excavations from exposed Morrison strata on the southern flank of Spindletop dome near the town of Grass Range, Montana, prompted a review of the formation's geology, paleobotany, and paleoclimate. A review of historical stratigraphic measurements of the formation in Montana reveals a considerable variance in measured thicknesses. Stratigraphic measurements and regional log data indicate that the formation averages 71 m thick across central Montana. A new regional isopach map of the formation from well-log data illustrates a broad distributive fluvial system that migrated from the southwest toward the northeast. The formation is divided into two informal facies in the study area: lower and upper depositional facies. The lower depositional beds represent the mud-rich distal-most distributive fluvial facies that overlies the stranded muddy tidal flat of the Swift Formation. An increased sandstone:mudstone ratio and small isolated fluvial channel and crevasse splay beds indicate that the upper depositional beds represent the slow progression of the distributive fluvial system. However, a review of the regional field stratigraphy and well-log data did not provide a regional correlatable facies change to warrant subdividing the formation into members.

The stratigraphic positions and climatic interpretations for lithologic, faunal, and floral paleoclimatic proxies are specified. The compilation of climate proxy data from central Montana demonstrates that the climate in this region was wetter than in southern parts of the Morrison foreland basin. The climatic proxies signify that the environmental conditions were variable during the Late Jurassic in central Montana, displaying changing temperatures with mesic and xeric intervals of unknown duration.

### INTRODUCTION

The Upper Jurassic Morrison Formation, an expansive sequence of terrestrial sediments deposited in foreland basins formed by the North America Cordilleran orogenic system, covers approximately 1.5 million km<sup>2</sup> of the North American Intermountain West (Dodson and others, 1980). The formation has been intensely

studied for uranium (Turner-Peterson and Fishman, 1986), coal (Harris, 1966; Silverman and Harris, 1966), oil and gas (Norwood, 1965; Johnson, 2005), and dinosaurs (Foster, 2007). Since the Dinosaur Bone Wars of Othniel Charles Marsh and Edward Drinker Cope during the 1870s in the newly-opened American West, dinosaurs have been the focus of research and imagina-

*Citation for this article.*

Richmond, D.R., 2023, *Stratigraphy, sedimentology, and paleoclimatic proxies of the Upper Jurassic Morrison Formation of central Montana: Geology of the Intermountain West*, v. 10, p. 223–276, <https://doi.org/10.31711/giw.v10.pp223-276>.

tion. Dinosaurs have been discovered in every U.S. state where the Morrison Formation is exposed (Turner and Peterson, 1999).

The Morrison Formation is widespread in Montana, but formation surface exposures are limited (Woodruff and Foster, 2017). As a result, the Morrison and the dinosaurs of this northern part of the Jurassic foreland basin still need to be better understood. Early studies of the Morrison Formation in Montana mentioned dinosaur bones, bone fragments, gastroliths, freshwater bivalves, fossil plants, and seeds (Calvert, 1909; Fisher, 1909; Gardner and others, 1945; Brown, 1946; Vine, 1956; Knechtel, 1959). Moreover, in the Rocky Mountains of southwestern Montana, exposures of the Morrison strata have been investigated (Malone and Suttner, 1991; Cooley, 1993; Smith and others, 2006). However, the stratigraphy and sedimentology of the formation in central Montana have received inadequate attention. For example, recently newly discovered carbonate mound springs (i.e., tufa deposits) were described from the formation in central Montana (Richmond and others, 2021b); however, the stratigraphy and sedimentology of the region were only superficially discussed.

Montana is well known for its Cretaceous-age dinosaurs (Sahni, 1972; Giffen and others, 1988; Horner, 1988; Maxwell, 1993; White and others, 1998; Schott and others, 2009; Jackson and Varricchio, 2010; Wosik and others, 2017; Prieto-Marquez and Guenther, 2018); limited studies, however, have focused on the Jurassic Morrison Formation and the dinosaurs of the northern part of the foreland basin (Turner and Peterson, 1999). A new diplodocoid dinosaur, *Suuwassea emilieae*, was discovered in the Morrison in south-central Montana and described (Harris and Dodson, 2004; Harris, 2006a, 2006b, 2007). Several papers describe and discuss the recently discovered *Hesperosaurus mjosi* (previously *Stegosaurus*) from Quarry 2 of the Judith River Dinosaur Institute (Saitta, 2015 [reported as the JDRI 5ES Quarry therein]; Maidment and others, 2016, 2018; Woodruff and others, 2019). Woodruff and Foster (2017) described a remarkably well-preserved *Camarasaurus* dinosaur discovered, excavated, and prepared by Judith River Dinosaur Institute from Quarry 1. Storrs and others (2012), in their taphonomic assessment of the Mother's Day Quarry south of Billings, Montana,

discuss an assemblage of 13 disarticulated subadult *Diplodocus* dinosaurs.

Various invertebrates have been discovered from different localities and described (Calvert, 1909; Fisher, 1909; Yen, 1952; Evanoff and others, 1998; Good, 2004; Richmond and others, 2017). Additionally, several fossil wood genera have recently been described from central Montana (Richmond and others, 2019b, 2019c, 2019d, 2021a, 2022).

## GEOLOGIC SETTING

The field study area is located in the southeastern part of Fergus County, Montana (red box on figure 1A), whereas the subsurface interpretation extends into parts of the surrounding five counties (dashed box on figure 1A). Spindletop dome is a small anticline on the eastern flank of the Big Snowy Mountain uplift at the convergence of the Rocky Mountains and Great Plains provinces (figure 1B). The Morrison Formation is exposed along the southwestern hinge zone limb of Spindletop dome and in limited outcrops in the surrounding region (figure 1C). The Morrison Formation is stratigraphically underlain by the Middle to Upper Jurassic Ellis Group, comprising carbonate and clastic marine deposits of the Piper (Sawtooth), Rierdon, and Swift Formations. These marine formations were deposited during the inundation and withdrawal of the Late Jurassic Sundance sea. The mid-late Oxfordian Swift Formation consists of shallow-marine shelf sandstone deposits that accumulated during the final transgressive-regressive marine sequence (Imlay, 1954; Khalid, 1990; Fuentes and others, 2011). The Swift Formation can be divided into four parasequences based on well-log data ( $n = 212$ ). The first three (offshore, lower, and upper shoreface) are open marine parasequences and coarsen upward (figure 2). The fourth uppermost parasequence is a fining-upward, tidal flat facies (Richmond, 2022) (figure 3A). The tidal sequence sandstones are glauconitic, calcite-cemented, angular (0.91), well sorted (0.46), fine-grained (2.76  $\Phi$ ) quartz arenites ( $n = 8$ ; figures 4A and 4B). The northward retreat of the seaway established a flat planation surface on which the northern Morrison sediments were deposited (Richmond and others, 2019d). The J-5 unconformity (Pip-

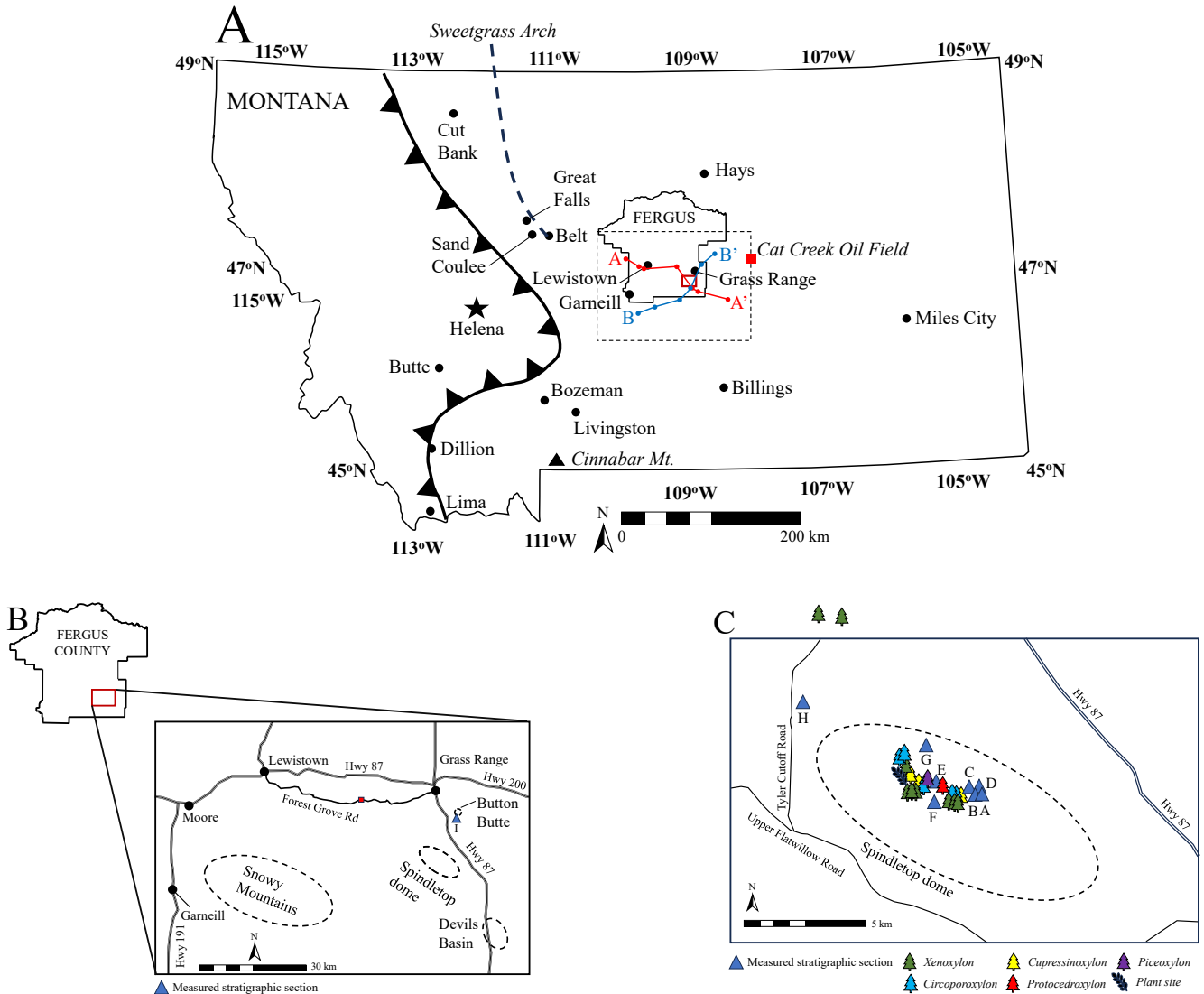


Figure 1. (A) Montana regional index map with the main field study area of the Morrison Formation is highlighted by the red box near the small town of Grass Range in southeastern Fergus County. The map includes locations referenced in the paper as well as index cities. The dashed black box represents the area reviewed with subsurface well-log data. Well-log cross sections A-A' and B-B' are constructed across central Montana (figures 8 and 9). (B) Index map of the local research area including some of the physiographic structures referred to in the text. The main focus area is the southern and western limbs of a Laramide-age anticline known as Spindletop dome. The red box along Forest Grove Road designates a field stratigraphic measurement of the formation. The blue triangle represents the location of the partial stratigraphic measured section I (see figure 10). (C) Spindletop dome index map showing the stratigraphic measured sections A through H. Section I was measured near Button Butte (figure 1B). The trees represent the locations of the different fossil wood genera and the plant icon represents the location of the fossil plant site.

irringos and O'Sullivan, 1978), present at the base of the Morrison Formation in most southern states, is absent in central Montana (Dekalb, 1922; Imlay, 1954; Uhlir and others, 1988; Khalid, 1990; Meyers and Schwartz, 1994; Fuentes and others, 2011; this study).

The Morrison Formation in central Montana is undifferentiated and consists of non-marine variegated illitic mudstones, thin carbonaceous shale, siltstone, sandstone, freshwater limestone, and coal beds. Rapid lateral transitions of terrestrial facies impede the cor-

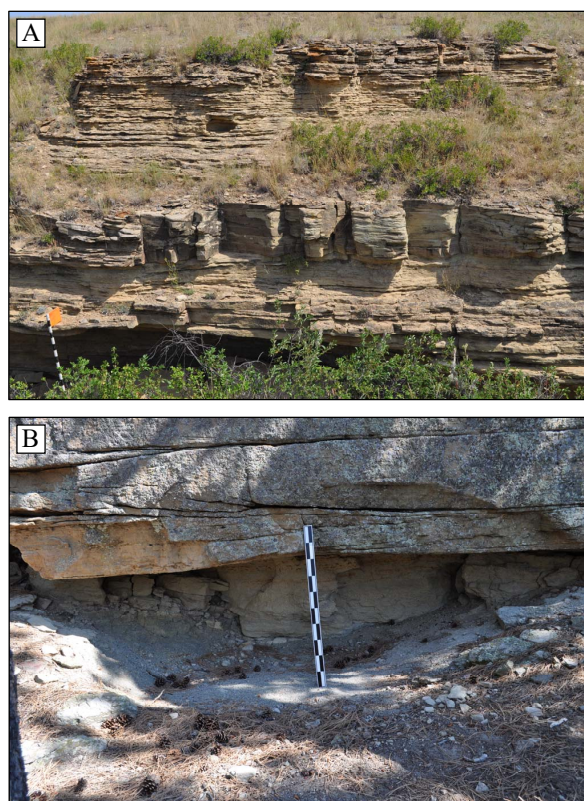
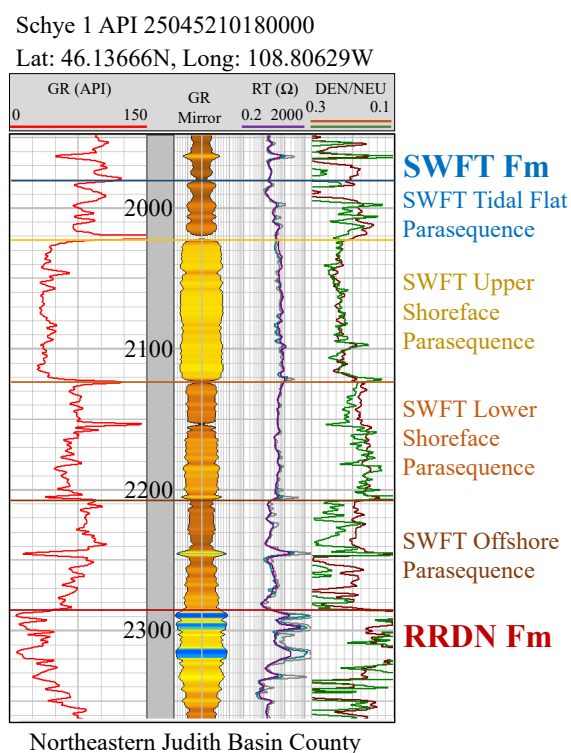


Figure 2. The Schye 1 well log (API 25045210180000) from the northeastern Judith Basin County displays the four marine parasequences of the Oxfordian Swift Formation that are present throughout central Montana. Subsea depths are measured in feet. Formation abbreviations are as follows: Rierdon (RRDN) and Swift (SWFT).

Figure 3. (A) Photograph of the uppermost tidal parasequence of the Jurassic Swift Formation. The uppermost inter-laminated siltstone/mudstone beds of the Swift tidal mudflat are conformable with the overlying Jurassic Morrison Formation. 1.5 m Jacob's staff for scale. (B) Photograph of the K-1 unconformity and the sediments that underly the Lower Cretaceous Kootenai Formation's basal sandstone bed. The fluvial sandstone bed is usually flat-bottomed. Meter scale.

relation of strata over an extensive distance (Moritz, 1951). Unlike the well-exposed strata of the Morrison Formation of the Colorado Plateau, the Morrison strata of central Montana are usually covered by Great Plains mixed prairie grasses, dominated by western wheat-grass (*Pascopyrum smithii*) and Ponderosa pine (*Pinus ponderosa*).

On the Spindletop dome, six recently discovered dinosaur quarries are in various stages of excavation. (1) Quarry 1 (36 m above the Swift Formation), where an exceptionally preserved *Camarasaurus* (Woodruff and Foster, 2017) and disarticulated *Hesperosaurus* limb material (Woodruff and others, 2019) was discovered in 2003. (2) Quarry 2 (47 m above the Swift Formation), where a single disarticulated Macronarian sauropod and numerous disarticulated *Hesperosaurus mjosi* (Saitta,

2015) were excavated. Saitta (2015) interpreted the sauropod in Quarry 2 to be deposited after the stegosaurs. (3) Quarry 3 (28 m above the Swift Formation), where a disarticulated sauropod was found. Preliminary observations suggest the sauropod is similar to *Haplocanthosaurus*. (4) Quarry 4 vertebrate fossil material is from an unknown sauropod (approximately 28 m above the Swift). (5) Quarry 5, 18.5 m stratigraphically above the Swift Formation, has produced disarticulated material suggestive of *Camptosaurus*. (6) Quarry 6 is about 36 m above the Swift yielding miscellaneous unidentified vertebrate fossil material. Currently, quarries 4–6 are in the preliminary stages of excavation. All dinosaur excavations have been conducted, and fossil material has

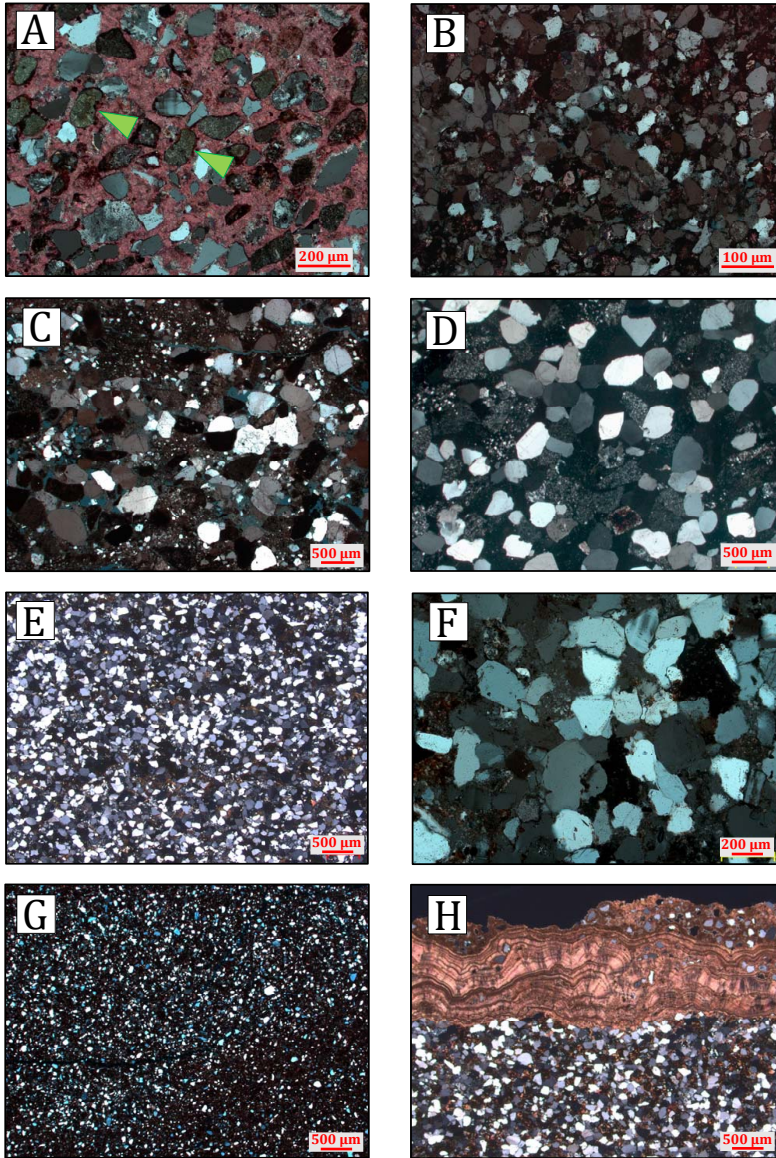


Figure 4. (A) Photomicrograph of a Swift tidal channel sandstone. The sandstone is a calcite-cemented, fine-grained quartz arenite. Glauconite is present in varying amounts (green arrows). Crossed Nichols. (B) Photomicrograph of a Swift muddy tidal flat sandstone. The sandstone is a calcite-cemented, very fine grained quartz arenite. The intergranular porosity is filled with clay. Crossed Nichols. (C) Photomicrograph of the friable sediments beneath the Kootenai basal sandstone (see figure 3B). The sandstone is a medium-grained quartz arenite with mudstone clasts. Crossed Nichols. (D) Photomicrograph of Kootenai sandstone which is calcite-cemented, coarse-grained quartz arenite. (E) and (F) Photomicrographs of Morrison upper depositional facies sandstones. The sandstones are fine-grained quartz arenites. Sutured grain contacts are common, suggesting a metasedimentary source. (G) Photomicrograph of a Morrison lower distal floodplain facies sandstone, which is a coarse-grained, quartz-rich siltstone. (H) Photomicrograph of the uppermost Quarry 2 sandstone bed showing very thin laminae (< 1 cm) of banded microbialite (cyanobacteria, i.e., stromatolitic) that formed atop the sandstone bed. The sandstone is a fine-grained quartz arenite.

been prepared by the Judith River Dinosaur Institute of Billings, Montana (see Saitta, 2015).

The K-1 unconformity (Pipiringos and O'Sullivan, 1978) separates the Upper Jurassic (Kimmeridgian/Tithonian) Morrison Formation from the Lower Cretaceous (Aptian) Kootenai Formation. The amount of time represented by the unconformity is debated. Near Cut Bank, Montana (figure 1A), the pre-Kootenai erosion has removed the Morrison and Swift Formations (Cobban, 1945). Near Great Falls, Montana, the K-1 unconformity is angular (Harris, 1968). In the study area, thinly laminated, friable sediments are present beneath the basal Kootenai sandstone bed, which may represent sedimentation during some stage of the K-1 unconfor-

mity (figure 3B). The friable sandstone is a subangular (1.43), moderately sorted (0.70), medium-grained (1.64  $\Phi$ ) quartz arenite with mudstone clasts (figure 4C). Geochronological data indicates that the missing time from the geologic record represents 20 Ma (Fuentes and others, 2011). However, high-resolution biostratigraphic data from terrestrial ostracodes suggests that the unconformity represents less than 10 Ma (Sames and others, 2008, 2010). The Kootenai Formation is a terrestrial sequence comprised of mudstone deposits, coarse- to medium-grained sandstone beds, and calcrete paleosols and is usually capped by interstratified limestone and dolomite units (Dupree, 2009). In north-central Montana, the Kootenai Formation's lower unit is the Cutbank

Sandstone Member, which consists of cross-bedded, coarse-to medium-grained, quartz arenite sandstone that contains abundant black and gray chert grains (Porter and others, 1996). On the Sweetgrass Arch in northern Montana (figure 1A), the oil-producing basal sandstone is called the Sunburst sand (Collier, 1929).

The Cat Creek anticline oil targets are the Kootenai sandstone beds. The Cat Creek anticline is 64 km northeast of the study area (figure 1A). The sandstone bed targets are locally called the 1<sup>st</sup> and 2<sup>nd</sup> Cat Creek zones (Ames, 1993). The nonproductive 3<sup>rd</sup> Cat Creek sandstone is stratigraphically equivalent to the basal sandstone and is an artesian water zone (Ames, 1993). Historically this sandstone bed has received various names; however, herein, it is referred to as the basal Kootenai sandstone bed. In the study area, the basal sandstone bed has a variable thickness but can be 30 m thick. There is a marked increase in polycrystalline and microcrystalline quartz grains in the sandstones with a visible distinct “salt and pepper” appearance in a hand sample. The basal Kootenai sandstone is a subrounded (2.27), well sorted (0.37), coarse- (0.96  $\Phi$ ) to medium-grained (1.27  $\Phi$ ) quartz arenite ( $n = 2$ ; figure 4D).

## METHODS

Stratigraphic measurements were made using a Jacob's staff and surveyed using a Nikon DTM-322 total station. Following the conventional practice, the Morrison Formation includes the terrestrial mudstone, limestone, and sandstone strata between the underlying Swift Formation and K-1 unconformity (Cobban, 1945). In the field, the contact between the Swift and the Morrison Formations is further defined as the top surface of the uppermost glauconitic sandstone bed of the Swift Formation. In well logs, the top of the Swift is marked at the top of the uppermost sandstone bed, identified by a clean gamma-ray profile. Since the K-1 unconformity is rarely exposed in the field, it is defined as the bottom surface of the basal sandstone bed of the Kootenai Formation. In well logs, the top of the Morrison Formation is selected at the base of a thick, clean gamma-ray profile interpreted to represent the Kootenai Formation basal sandstone bed. The type well log for central Montana is the Gorman 11-19 well (API

25027211260000), 7 km southeast of the Judith River Dinosaur Institute (JRDI) Quarry 1. The type well log (figure 5) displays the interpreted divisions of the Swift and Morrison Formations and the Kootenai Formation basal sandstone bed. The transition between the Swift and the Morrison is often difficult to select in vintage well logs with indistinct curves (e.g., SP, ILD). Therefore, the Swift formational contact was placed at the top of the Swift sandstone/Morrison mudstone demarcation resulting in a maximum thickness for the Morrison Formation. A gamma-ray (GR) > 75° API was used in the well logs to classify the log units as sandstone. The percentage of sandstone for the formation was derived from the formational well-log thickness divided by the total footage where the GR log > 75° API and multiplied by 100.

In the field, 68 sandstone beds were measured for thickness. Twenty-two additional sandstone beds had their width and thickness measured to determine the width:thickness ratio. Sandstones used for thin section analysis were obtained from the measured stratigraphic sections. Thin sections were prepared by Wagner Petrographic (Lindon, Utah) and were examined under a Zeiss petrographic microscope. Grain-size measurements for the well-cemented sandstones were produced using JMicroVision v1.27 from scaled digital thin-section images. A 300-framework grain point count was performed on each sandstone to determine mineralogy and sandstone classification, according to Dott (1964). In thin sections, monocrystalline quartz grains are defined as those consisting of a single crystal. Polycrystalline quartz grains have distinguishable crystal aggregates, whereas microcrystalline quartz (chert) grains have no distinguishable aggregate boundaries. Three hundred framework grains were measured to determine a grain-size distribution. Standard petrology equations (Folk and Ward, 1957) were used to determine grain-size distribution and sorting. A random 100-grain count determined sandstone grain rounding from digital thin-section images. Grains were allocated to a rounding class: 0 – very angular, 1 – angular, 2 – subangular, 3 – subrounded, and 4 – rounded. The average grain roundness was calculated. Carbonates are designated using Folk's classification scheme (Folk, 1959).



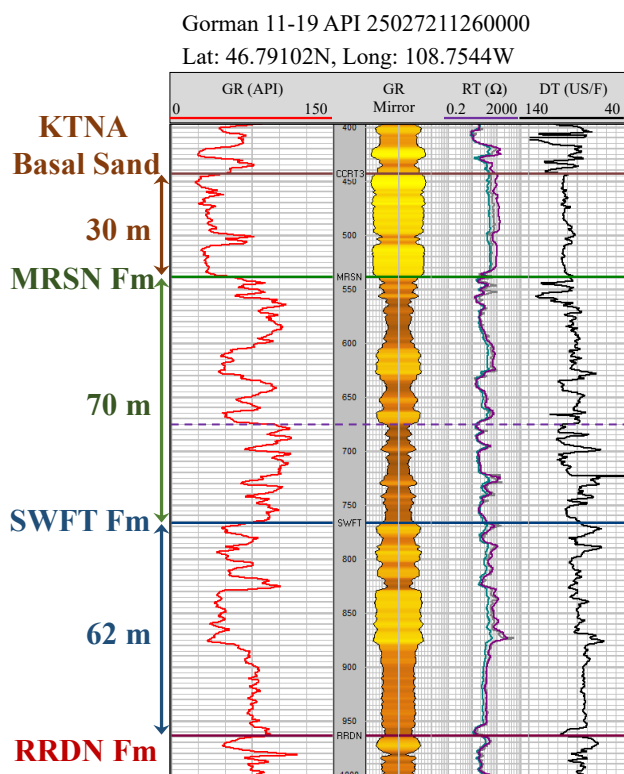


Figure 5. The Gorman 11-19 well log (API 25027211260000) from southeastern Fergus County. The well is 7 km southeast of the Judith River Dinosaur Institute Quarry 1 locality. The well log displays the formation thicknesses and log characteristics of the Swift and Morrison Formations and the basal sandstone bed of the Kootenai Formation. This type well log was the template for the well-derived Morrison formational thicknesses utilized for the central Montana isopach map (figure 7). Formation abbreviations are as follows: Rierdon (RRDN), Swift (SWFT), Morrison (MRSN), and Kootenai (KTNA).

X-ray fluorescence (XRF) and X-ray diffraction (XRD) of Morrison Formation sandstones and mudstones were completed by the Bureau of Economic Geology, the University of Texas at Austin. A Thermo Scientific Niton XL3t Ultra Analyzer XRF gun was used to measure the elemental abundance of the silcrete, a newly discovered rhyolitic ash, and two rhyolite rocks samples from the Yellowstone Basin. The device measured each sample for 210 seconds. Forty-one elements were measured using the XRF tool. However, only the top nine element percentages are shown and account for

greater than 99% of the elements. One hundred meso- and macropore diameters of the rhyolitic ash were measured using a digital caliper from hand samples. Additionally, 300 micropore diameters were measured using JMicroVision v1.27 from scaled digital thin-section images of the ash. All pore sizes are grouped according to the classification of Loucks and others (2012).

Kate Huntington ran the oxygen isotope analyses at the University of Washington, Seattle. Seven carbonate samples were analyzed, but only one produced viable temperature results. Palynology samples were processed by Vera Korasidis at the University of Melbourne, Australia, and were reviewed by Carol Hotton from the National Museum of Natural History.

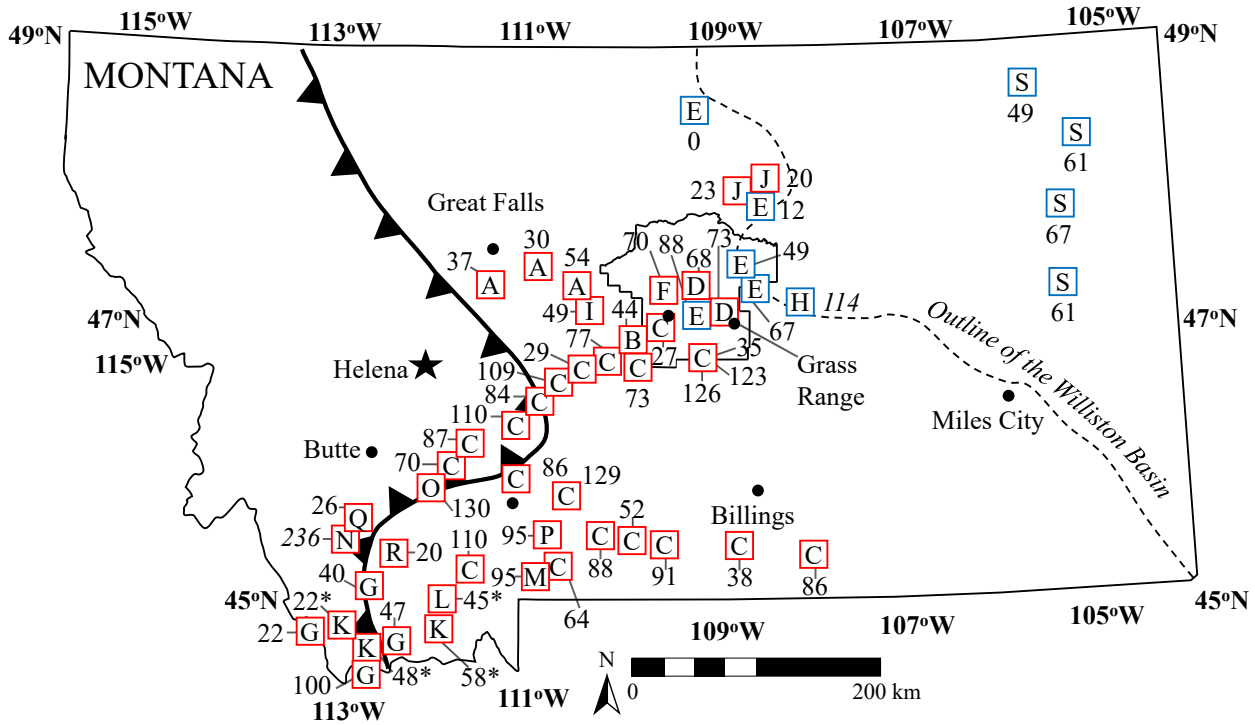
## MORRISON FORMATION STRATIGRAPHY

Stratigraphic measurements of the Morrison Formation have been defined previously for the more southern states. A historical review of the stratigraphic measurements in Montana is presented herein, followed by stratigraphic field measurements and regional well-log data from central Montana.

### Historical Stratigraphic Measurements

The Morrison Formation, named initially by G.H. Eldridge (Emmons and others, 1896), was correlated to Montana by Fisher (1909). A historical review of the formation's measurements is provided herein to show the inconsistencies in the stratigraphic thicknesses of the Morrison Formation across the state (figure 6). Many 20<sup>th</sup>-century researchers reported a formation thickness for their particular study area/region but provided no location details of their stratigraphic measurements (Freeman, 1919; Dekalb, 1922; Harris, 1966, 1968; Silverman and Harris, 1966, 1967; Suttner, 1969; Walker, 1974; Lindsey, 1980). In addition, in some references, the Morrison Formation has been combined with other formations for regional isopach maps (Francis, 1956, 1957; Peterson, 1966, 1981). The review is presented chronologically, reexamining the stratigraphy of central and southwestern Montana and the Williston Basin.

The Morrison Formation coal beds of central Mon-



KEY: **A**-Fisher, 1909; **B**-Calvert, 1909; **C**-Gardner and others, 1945, 1946; **D**-Gardner, 1950, 1959; **E**-Hadley and Milner, 1953; **F**-Miller, 1954; **G**-Scholten and others, 1955; **H**-Hadley, 1956; **I**-Vine, 1956; **J**-Knechtel, 1959; **K**-Moritz, 1951, 1960; **L**-Christie, 1961; **M**-Fraser and others, 1969; **N**-Hobbs, 1967; **O**-Malone and Suttner, 1991; **P**-Cooley, 1993; **Q**-Smith, 2001; **R**-Maidment and Muxworthy, 2019; **S**-Francis, 1957.

Figure 6. Historical stratigraphic measurements of the Morrison Formation in Montana. Each letter refers to the author(s) who published the stratigraphic measurement. See the letter key. The letter(s) placement on the map is where the stratigraphic measurement were made by the author. The majority of the measurements were made along structural features where the formation is uplifted and exposed. Values with an asterisk (\*) indicate interpreted thicknesses. See the text for information pertaining to corrections. The italicized values represent probable erroneous measurements where a corrected estimate could not be determined. Red squares represent field measurements, whereas blue squares are data derived from well-log curves. Thicknesses are in meters.

tana prompted the first stratigraphic measurements in the state. Fisher (1909; A on figure 6) reported thicknesses from 24 to 36 m bordering the Little and Big Belt Mountains. Calvert (1909; B on figure 6) measured the Morrison Formation west of Garneill, Montana, and specified a thickness of 44 m. Lupton and Lee (1921) stated the formation is about 45 m thick east of Lewistown. However, they did not provide a location. Oil finds on the Cat Creek anticline (Lupton and Lee, 1921) and in the Devils' Basin in central Montana prompted

Reeves (1927) to measure the formation in the region, reporting thicknesses between 60 and 90 m. Gardner and others (1945, 1946; C on figure 6) measured numerous stratigraphic sections across south-central and west-central Montana. Additional Morrison stratigraphic measurements can be examined in Gardner and others (1946), but only the data from their 1945 measurements are presented herein. Gardner (1950, 1959; D on figure 6) measured the formation along Forest Grove Road west of Grass Range, Montana. The

thicknesses are 73 and 68 m, respectively. Hadley and Milner (1953; E on figure 6) used well-log data (SP and resistivity curves) to determine the formational thickness from central Montana to south-central Saskatchewan, Canada. They noted that the formation was interbedded with glauconitic sandstones. Their data suggests they included the uppermost Swift Formation sandstone beds in their measurements. Miller (1954; F on figure 6) measured a detailed stratigraphic section northwest of Lewistown, Montana in the South Moccasin Mountains. Scholten and others (1955; G on figure 6) measured the Morrison in the mountains around Lima, Montana. Hadley (1956; H on figure 6) estimated the Morrison to be 114 m from subsurface well logs from the Cat Creek anticline in central Petroleum County. This thicker measurement likely includes strata from the uppermost Swift Formation. The tidal flat parasequence is challenging to delineate in well logs using only vintage SP and resistivity curves. Vine (1956; I on figure 6) measured the formation to be 49 m in central Judith Basin County. Knechtel (1959; J on figure 6) measured the formation thicknesses as 20 and 23 m south of the Little Rocky Mountains, which are east of Hays, Montana. However, Knechtel mentioned glauconitic sandstones were present in the Morrison Formation. This implies that Knechtel, too, may have included the uppermost Swift strata in the measurements.

In southwestern Montana, Moritz (1951, 1960; K on figure 6) measured three sections of the Morrison Formation with variable results: 22, 82, and 119 m. The two thickest sections each have a “salt and pepper” sandstone bed, one of thickness 11 m and one of thickness 23 m. The Kootenai basal sandstone bed is identified in the field by its characteristic “salt and pepper” appearance (Fraser and others, 1969; Walker, 1974; this study). Omitting the “salt and pepper” Kootenai sandstone beds from Moritz’s stratigraphic measurements yields formational thicknesses between 22 and 58 m. Christie (1961; L on figure 6) divided the formation into three informal lithologic units. The basal unit consists of 45 m of “thin-bedded shales, mudstone, limestones, siltstones, and a few sandstones.” The middle unit comprises 45 m of sandstone, and the upper unit includes 61 m of red sandy mudstone. The three units equate to a 151-m Morrison section. The litho-

logic description of the lower unit is analogous to the Morrison strata. However, the middle and upper units convincingly describe the basal sandstone bed and red (maroon-colored) mudstone beds of the Kootenai Formation. Therefore, Christie’s (1961) Morrison Formation measurement likely equates to 45 m. Fraser and others (1969; M on figure 6) measured 95 m of formation thickness at Cinnabar Mountain in Park County. Hobbs (1967; N on figure 6) divided the formation into three informal members northwest of Dillon, Montana, for a total of 236 m. From this description, it is difficult to discern which member should be correctly identified as the Morrison Formation. Hobbs defines the contact between the Morrison and Kootenai Formations as a gradational contact at the base of a gastropod-bearing biomicrite bed. A freshwater gastropod limestone bed has been described in the upper part of the Kootenai Formation (Cobban and others, 1976). Hobbs (1967) likely included most of the Kootenai Formation in the Morrison measurements. Malone and Suttner (1991; O on figure 6) made several Morrison stratigraphic measurements across the Willow Creek fault zone that was active during the Late Jurassic. Their measurements show the formation varies between 120 and 130 m thick in relation to the Willow Creek fault zone. Cooley (1993; P on figure 6) measured the formation south of Livingston, Montana. These measurements specify formation thicknesses between 75 and 95 m. Smith (2001; Q on figure 6) made five stratigraphic measurements of the formation north-northwest of Dillon, Montana, where the formation averaged 26 m in thickness. Maidment and Muxworthy (2019; R on figure 6) published a thickness of approximately 20 m for central and southwest Montana. Francis (1957) generated a Morrison Formation isopach map for Montana and North Dakota and Saskatchewan and Manitoba, Canada. The isopach was generated using well-log data and focused on the Williston Basin. Francis’ north-south Jurassic strata log cross section shows four well logs along the western flank of the Williston Basin in eastern Montana. The four well logs displayed in the cross section were reviewed for the formation thicknesses (Rhodes F-11-6, now the J. Heier F-11-6P, API 25019050140000; East Poplar Unit, 25085050580000; Casterline 1, API 25021051650000; Macioroski 1, API 25079050380000; S on figure 6).

Francis' (1957) isopach map shows the thickest strata in southwestern Montana, which thins eastward with a zero-edge in central North Dakota, southern Saskatchewan, and Manitoba. According to this isopach map, the formation is estimated to be 61 m thick in the current study area.

The review of the historical measurements of the formation shows a wide variation in thickness around the state. The disparity in thicknesses observed on figure 6 is likely related to several factors. First is the possible variation in the paleotopographic surface at the top of the Swift Formation. Second, in some sections, the uppermost Swift parasequence consists solely of mudstone, making it challenging to ascertain the formation top. Third, the possible erosion and downcutting of the Morrison Formation during the K-1 unconformity and the subsequent erosion by the Kootenai basal conglomerate and sandstone beds. Fourth, the basal Kootenai sandstone bed is only sometimes in the section. Fifth, the structural complexities that include compressional and extensional tectonics (i.e., folding, thrust faults, and normal faulting) are common across the state and can contract or expand sections of the formation. And finally, the complicated geology resulting from the previous factors can result in unintentional erroneous measurements.

### **Regional Stratigraphic Thickness From Well Logs**

Two complete stratigraphic measurements of the Morrison Formation were completed in southeastern Fergus County. Due to the structural complexity of Spindletop dome, the first stratigraphic measurement required a composite of several surveyed partial sections made on the southern and western limbs of the anticline. The second section was measured west of Grass Range along the Forest Grove Road (46°59'52.36" N., 109°4'32.92" W.) from the uppermost Swift Formation sandstone bed to the basal Kootenai sandstone bed. Both field measurements determined the formation is 72 m thick in the study area (red triangle on figure 7, Richmond and others, 2021b). Three hundred and ninety-three well logs from six counties in central Montana were reviewed to verify the field measurements (figure

7). The formation thickness, as derived from well-log data, in contrast to the historical field data (figure 6), shows that the formational thickness is relatively consistent across central Montana. The median formational thickness across the six-county area is 71 m. Both log cross section A-A' (figures 1 and 8), which trends northwest-southeast across southern Fergus and northern Musselshell Counties, and log cross section B-B' (figures 1 and 9) that trends southwest-northeast across Wheatland, Fergus, and Petroleum Counties, display a relatively consistent thickness in the formation. No discernible faults in the formation were observed in the well logs.

### **Undivided Morrison Formation**

The Morrison Formation in Montana has yet to be divided into formal members; however, the Morrison Formation has been divided into a total of eleven members in Arizona, Colorado, New Mexico, South Dakota, Utah, and Wyoming. The most recognized members of the Colorado Plateau in stratigraphic order are the Tidwell, Salt Wash, and Brushy Basin Members. The Tidwell Member, named and described by Peterson (1988) and recently described by Carpenter (2022), does not extend northward into Wyoming or Montana. The Salt Wash Member was named for sandstone beds of the McElmo Formation (now Morrison Formation) southeast of the town of Green River, Grand County, Utah (Lupton, 1914) and is restricted to the Colorado Plateau (Mullens and Freeman, 1957; Owen and others, 2015). Gregory (1938) named the Brushy Basin Member for the variegated shales in San Juan County in southeastern Utah. A comprehensive regional investigation of the Brushy Basin Member still needs to be completed, but it likely does not extend north into Montana.

Walker (1974) informally subdivided the Morrison Formation into lower and upper "members" in the area of Great Falls, Montana. The "lower" Morrison consists of mudstone and limestone beds, and the "upper" part of the formation consists of mudstone and sandstone beds. Walker proposed that the "lower" Morrison deposition was lacustrine, whereas fluvial deposition dominated the "upper" part. Malone and Suttner (1991) proposed a tripartite division of the formation for the

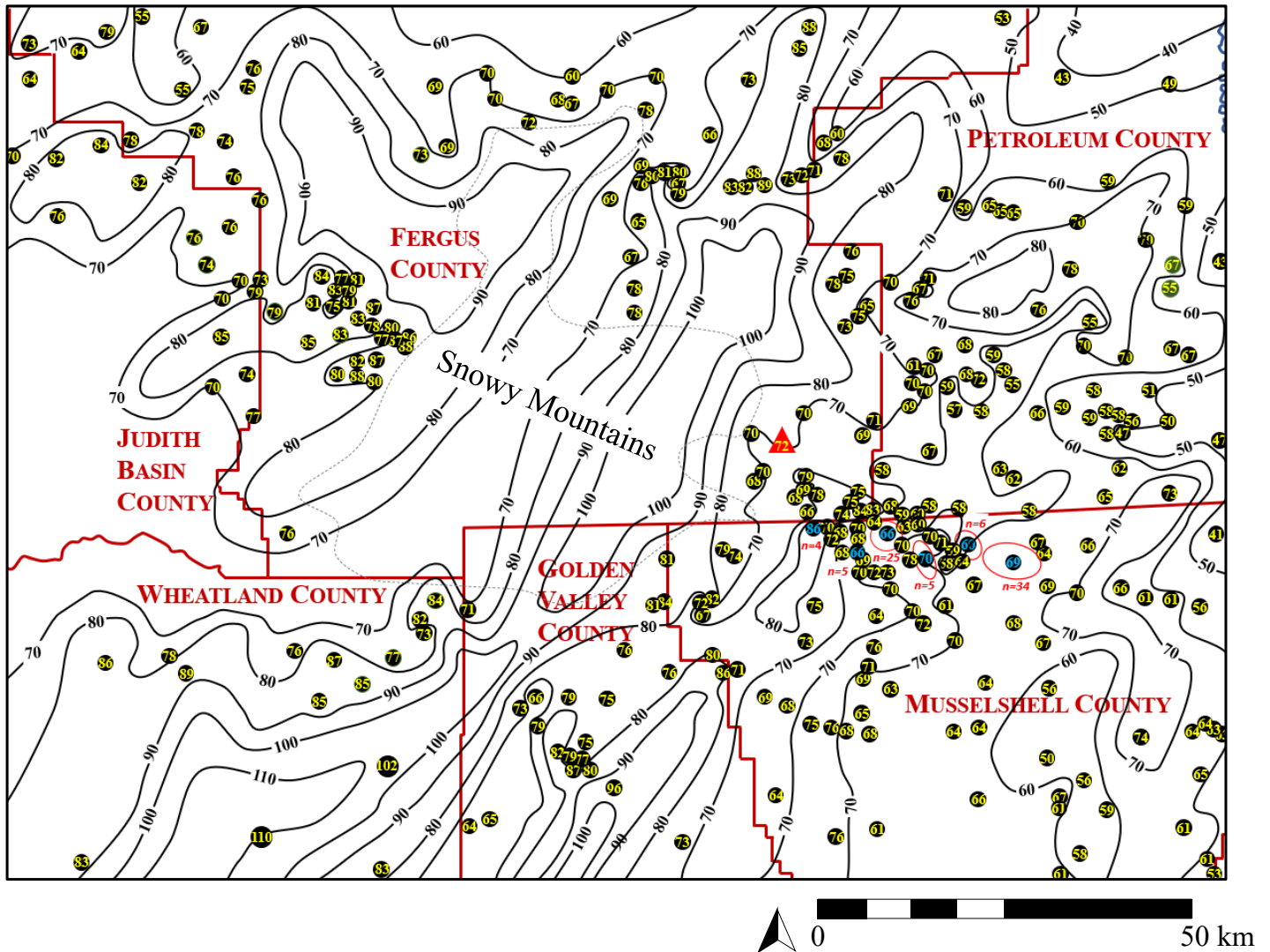


Figure 7. Morrison Formation isopach map for central Montana. Formation thickness was derived from 393 well logs from six counties. The median formation thickness in central Montana is 71 m. Each black dot represents a well location, and the yellow value is the formation thickness in meters. Where well locations cluster too close to post values, an average thickness was calculated and posted in the center of the well cluster (blue values). *N* equals the number of wells in the cluster. The red triangle is the location of the Spindletop dome field area. The thin gray dashed line is the outline of the Snowy Mountains. The isopach contours are thickest in the southwest and thin in the northeast. The data indicate a broad fluvial system prograded northeastward across central Montana.

northern Tobacco Root Mountains in southwestern Montana. They locally divided the formation based on the architectural geometry of lithologic units and siltstone:mudstone ratios on a low-energy terminal fan.

The formation was investigated in the Grass Range region with eight composite stratigraphic sections measured along the southwestern limb of Spindletop dome, where the formation is exposed (figure 10). The upper 20

m of the formation dip southward and are often covered by large, displaced blocks of the Kootenai basal sandstone. In places, the Kootenai basal sandstone blocks form a deflation surface and should not be interpreted as in situ. Normal faulting in and around the anticline makes obtaining accurate stratigraphic measurements difficult. The stratigraphic field sections shown on figure 10 provide a general overview of the formation.

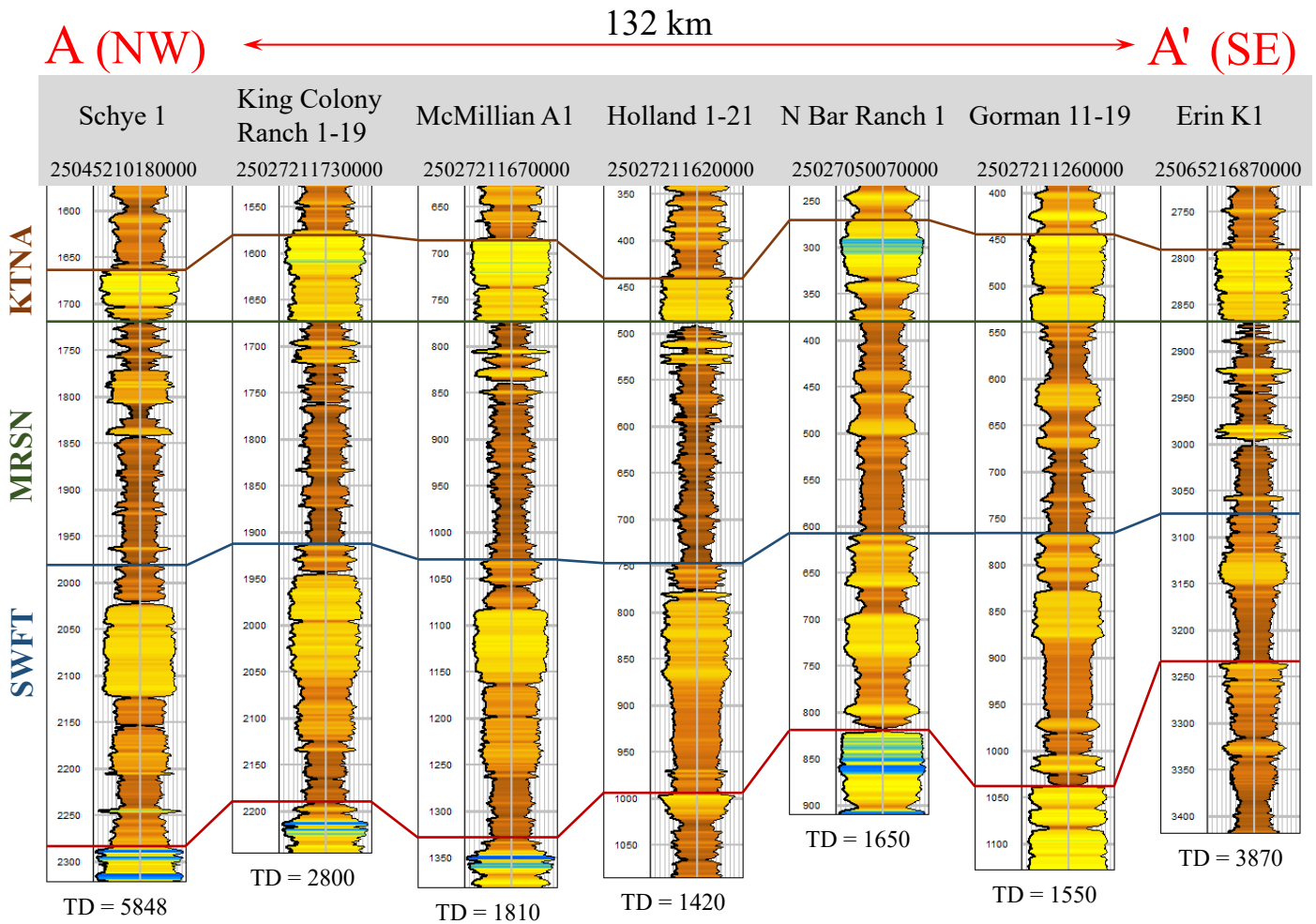


Figure 8. A seven-well log cross section (A-A'; see figure 1 for the line of section) that extends from central Judith Basin County across Fergus County to the southeast. The cross section passes just south of the field study area and into northcentral Musselshell County. The cross section is flattened on the top of the Morrison Formation. The implied lithologies are derived from the mirrored gamma-ray (GR) curve scaled 0 to 150° API. The thickness of the Morrison Formation is consistent across Fergus County (132 km). The displayed GR curves illustrate that the formation has a low sandstone:mudstone ratio. Log total depths (TD) are measured in feet. Formation abbreviations are as follows: Swift (SWFT), Morrison (MRSN), and Kootenai (KTNA).

Based on the field observations and measurements, no definable formation division is recommended.

The regional well-log data were also reviewed to provide a broader scope to determine if the formation could be divided into members. The regional well-log data shows a coarsening upward sequence in the type well log. A potential subdivision (dashed line on figure 5) may be extrapolated on the log curves locally; however, the marker does not extend across central Montana (figures 8 and 9). With no discernible lithologic

changes in the formation and the lack of field or correlative log markers, the formation cannot be divided into members.

## MORRISON FORMATION SEDIMENTOLOGY AND GEOCHEMISTRY

### Mudstone Sedimentology and Geochemistry

In the Grass Range area of Montana, the Morrison Formation is a mudstone-dominated section with thin

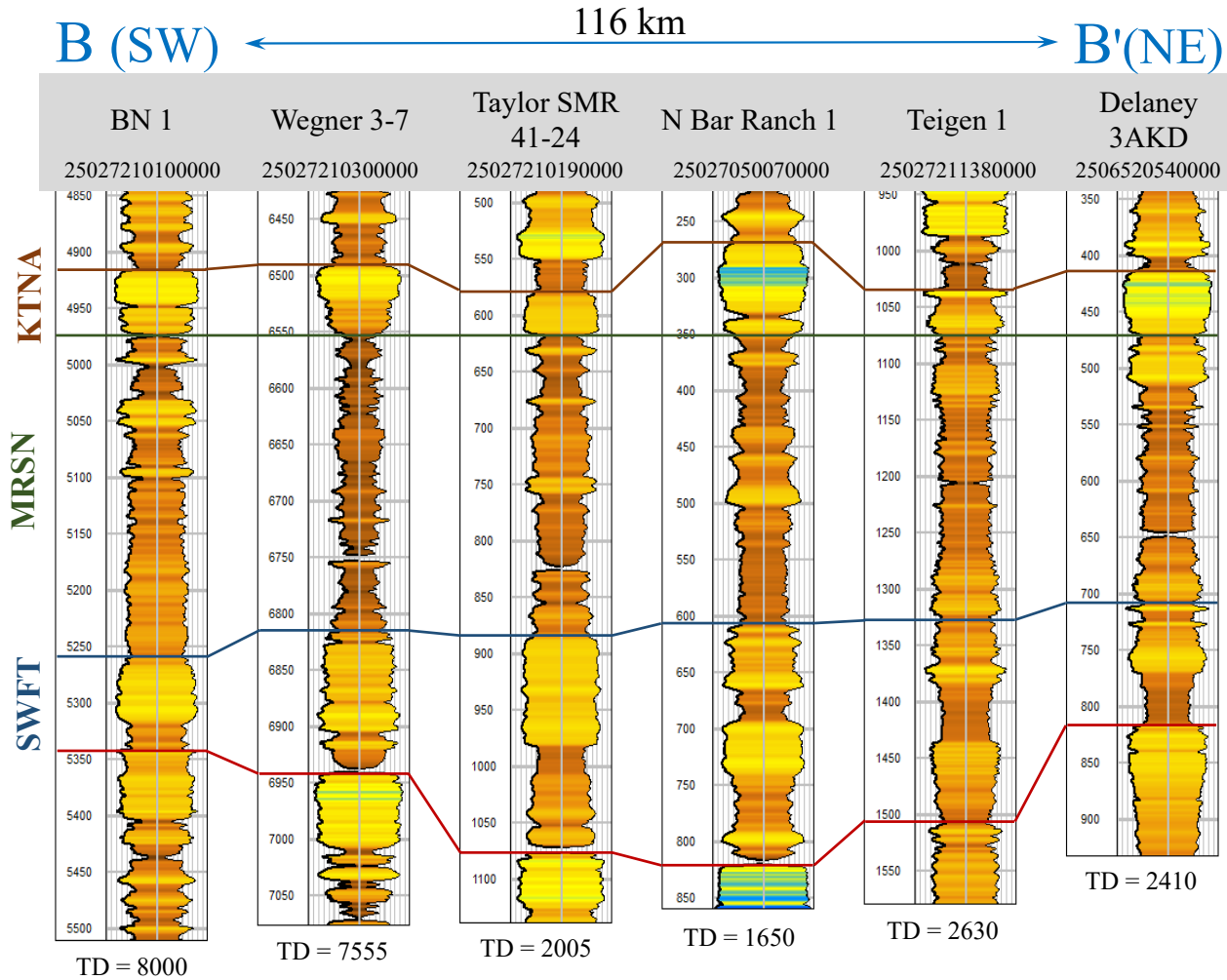


Figure 9. A six-well log cross section (B-B'; see figure 1 for the line of section) that traverses southeastern Fergus County. It extends from western Petroleum County through the field study area in southeastern Fergus County into northwestern Musselshell, northern Golden Valley, and northeastern Wheatland Counties. The cross section is flattened on the top of the Morrison Formation. The implied lithologies are derived from the mirrored gamma-ray curve scaled 0 to 150° API. The thickness of the Morrison Formation is consistent along the five-county transect of 116 km. The displayed GR curves demonstrate that the formation has a low sandstone:mudstone ratio. Log total depths (TD) are measured in feet. Formation abbreviations are as follows: Swift (SWFT), Morrison (MRSN), and Kootenai (KTNA).

sandstone and limestone beds. The sandstone:mudstone ratio from stratigraphic field measurements is 9%. The regional well-log data ( $n = 205$ ) specifies a higher average sandstone:mudstone ratio of 25%.

The base of the Morrison Formation in the Lewistown area is defined by a mudstone bed (Calvert, 1909; Freeman, 1919) that extends from the top of the Swift Formation to the first sandstone or limestone bed of the Morrison Formation. Along the southern flank of Spindletop dome and elsewhere in the research area,

a reddish illitic mudstone bed is also present. The reddish illitic mudstone bed extends into the Morrison Formation from the top of the Swift Formation to 15 m. This formation section generally lacks sandstone beds, with only a few narrow, thin-bedded siltstone beds observed. At the top of the reddish mudstone bed is a sharp, distinct color change to variegated mudstone beds of green, gray, and yellow hues interbedded with thin limestone and sandstone beds (figure 11). Additional reddish mudstone beds occur in the variegated

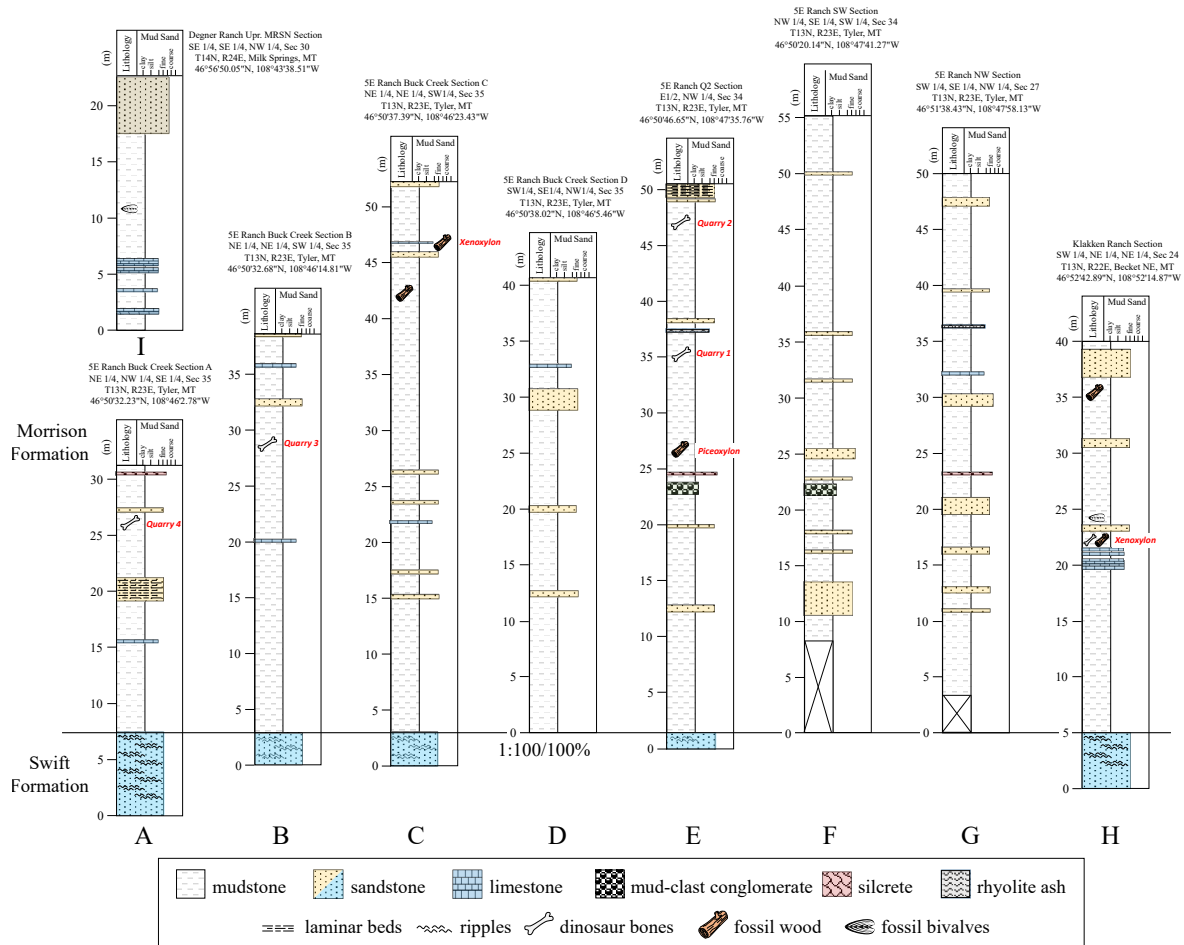


Figure 10. Seven partial stratigraphic sections (A through G) were measured along the southern limb of the Spindletop dome (see figure 1C) where the majority of the Morrison Formation is exposed. The upper 20 m of the formation are often covered by large allochthonous blocks of overlying Kootenai Formation. Partial stratigraphic sections H and I were measured at additional locations. The stratigraphic sections provide a general overview of the sedimentation in central Montana. Most mudstone and sandstone samples for XRD and XRF were acquired from these sections.

units, but these beds are usually localized and less than a few meters thick.

A noticeable color and clay mineralogy change from reddish illitic mudstones to variegated smectitic mudstones was one of three marker beds first described by Peterson and Turner (1993) in the Morrison Formation of the Western Interior. The “clay change” usually occurs in the lower part of the Brushy Basin Member of the Morrison Formation. This change in clay mineralogy has been used as a local and regional marker to place dinosaur quarries in a stratigraphic order within the formation (Peterson and Turner, 1993; Turner and Peterson, 1999; Richmond and Stadtman, 1996; Litwin and others, 1998; Richmond and Morris, 1998;

Schudack and others, 1998; Turner and Peterson, 1999) and correlation of depositional facies (Demko and others, 2004). However, Trujillo (2006) recommends that the Morrison Formation “clay change” should not be used as a regional correlative tool because clay mineralogy varies laterally and vertically.

X-ray diffraction and X-ray fluorescence analyses were completed on mudstone samples for clay identification, mineral, elemental, and rare earth elements (REE). The normalized average clay composition of the formation mudstones ( $n = 7$ ) is illite (38%), goethite (28%), kaolinite (26%), and smectite (8%). The XRF data indicated no mineralogical change from illite to smectite at the color change. The Morrison Formation





Figure 11. The mudstone color change that is prevalent in the study area between the “lower” and “upper” Morrison depositional facies. There is no “clay change” (i.e., illite/smectite) as has been observed in the Morrison Formation on the Colorado Plateau. This color change can be observed along Highway 87 south of Grass Range, Montana, and represents a change in the depositional facies and climate. Meter scale.

“clay change” of the Colorado Plateau does not extend into central Montana (Turner and Peterson, 1999; this study).

The major minerals in the formation of mudstones are quartz, illite, goethite, kaolinite, and smectite, with minor percentages of orthoclase, calcite, dolomite, and pyrite (figure 12A). The mudstone’s primary elements are silica, calcium, iron, aluminum, and potassium, with minor percentages of sodium, titanium, sulfur, manganese, and phosphorus (figure 12B). The alkaline earth and transitional metals are barium, strontium, chromium, zirconium, nickel, rubidium, zinc, and vanadium, with minor ppm of cobalt, copper, molybdenum, gallium, niobium, lead, thorium, arsenic, and uranium. Yttrium is the only rare earth element present (figure 12C).

## Sandstone Sedimentology and Geochemistry

The sandstone beds are characteristically thin-bedded, flat-bottomed, isolated single-bodied units. Sandstone bed vertical aggradation is uncommon. The average thickness of 68 sandstone beds is 94 cm, with a median thickness of 50 cm. Bedforms are usually absent, but some beds display planar or ripple lamina-

tions. Trough cross-bedding and lateral accretion from point bar migration were observed in only a few sandstone beds. Twenty-four sandstone bodies were measured to determine width:thickness ratios. The average sandstone body width:thickness ratio is 13.0.

Morrison Formation sandstones are angular to subangular (0.87–1.98), moderately well to very well sorted (0.50–0.25), very fine to fine-grained (3.48–2.03  $\Phi$ ) quartz arenites ( $n = 22$ ). Grains are cemented with sparry calcite and have low matrix percentages ( $< 10$ ) (figures 4E and 4F). The grain composition of the Morrison sandstones is mainly monocrystalline quartz with low percentages of polycrystalline and microcrystalline quartz. Sutured composite quartz grains are common in the sandstones suggesting a sedimentary quartzite source. The quartz-rich sandstone mineralogy indicates a recycled orogen provenance for the Morrison sandstones (see Dickinson and Suczek, 1979). To differentiate Morrison sandstones from the underlying Swift and overlying Kootenai sandstones, percentages of monocrystalline, polycrystalline, and microcrystalline quartz grains can be used (figure 13).

X-ray fluorescence analysis was completed on sandstones from the Swift ( $n = 3$ ), Morrison ( $n = 11$ ), and Kootenai ( $n = 1$ ) Formations for elemental composition. The sandstone samples are in stratigraphic order. All the sandstones are composed of varying percentages of silicon, calcium, iron, and aluminum with minor proportions of potassium, sodium, titanium sulfur, manganese, and phosphorus (figure 14A). The Morrison sandstones generally have higher percentages of iron and magnesium than the other formational sandstones. The sandstone’s alkaline earth and transitional metals are barium, strontium, chromium, zirconium, vanadium, and copper, with minor ppm of rubidium, zinc, cobalt, molybdenum, gallium, niobium, lead, thorium, arsenic, and the rare earth element yttrium (figure 14B). Uranium, if present, is undetectable. The XRF confirms that the sandstones are quartz arenites.

## Limestone Sedimentology

Thin ( $< 20$  cm) micrite beds are scattered throughout the Morrison section, and most of the beds appear to be laterally limited (figure 10). In the lower part of

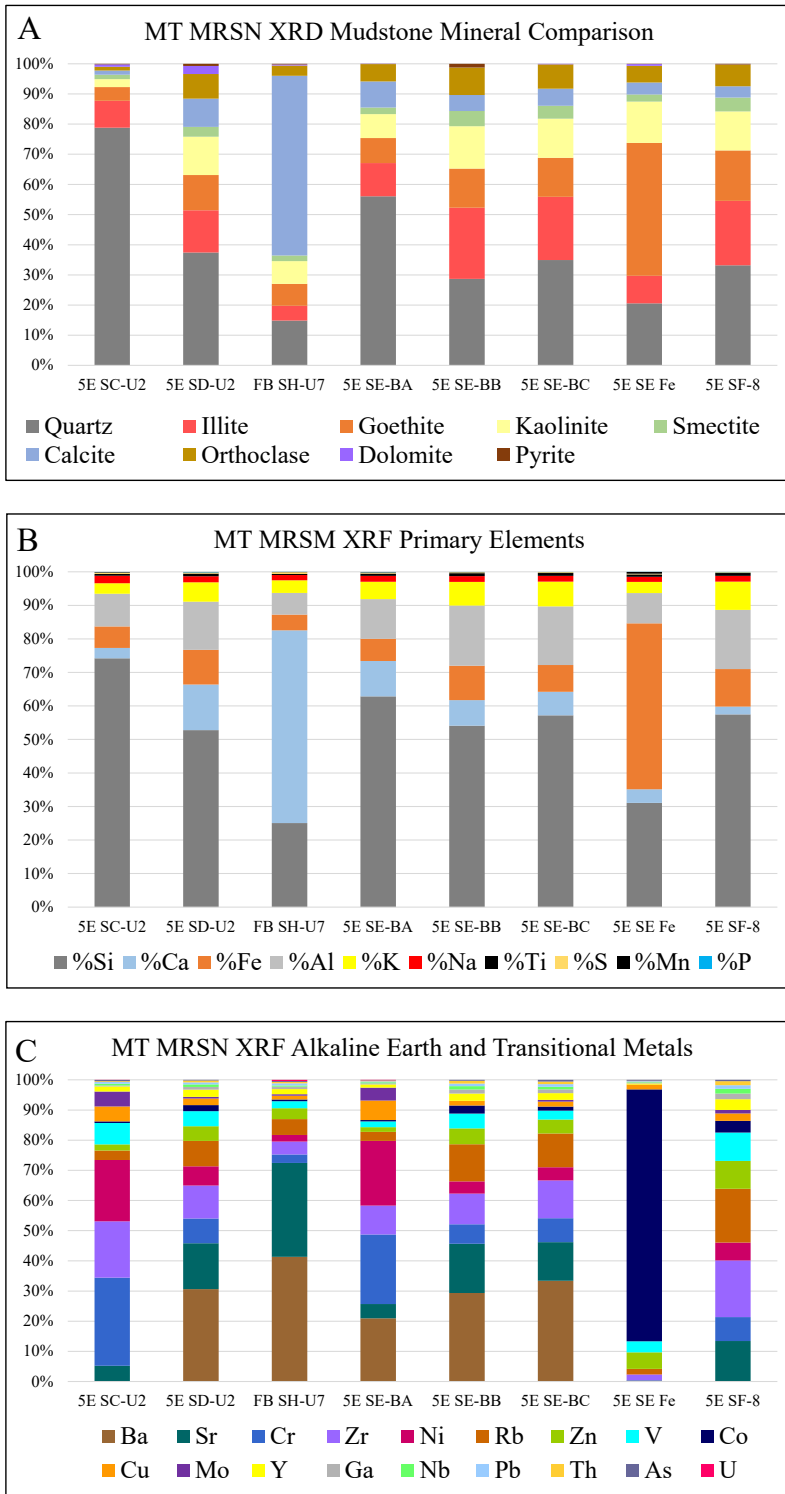


Figure 12. Graphs of X-ray diffraction (XRD) and X-ray fluorescence (XRF) analyses of mudstone samples for mineral composition, primary elements, and alkaline and transitional metals. Two mudstone samples (5E section C and section D are from the lower distal floodplain facies (less than 15 m) above the Swift Formation. Sample FB LM is stratigraphically about 20 m above the Swift Formation. Samples 5E section E-A, B, C, and Fe are from Quarry 2 stratigraphically at 47 m above the Swift Formation. Sample 5E SE-Fe is a goethite concretion found in the quarry. Sample section 5E F-8 is stratigraphically 55 m above the Swift Formation. (A) XRD analyses of several mudstones from the study area indicate that the mudstones are composed of illite, goethite, and kaolinite, with minor percentages of smectite. The illite and goethite indicate intense weathering and high organic content. (B) XRF shows the percentages of the primary elements for the formation. (C) XRF graph that displays the distribution of alkaline earth and transitional metals for the formation. Element abbreviations are as follows: silica (Si), calcium (Ca), iron (Fe), aluminum (Al), and potassium (K), with minor percentages of sodium (Na), titanium (Ti), sulfur (S), manganese (Mn), and phosphorous (P). The alkaline earth and transitional metals are barium (Ba), strontium (Sr), chromium (Cr), zirconium (Zr), nickel (Ni), rubidium (Rb), zinc (Zn), vanadium (V), with minor ppm of cobalt (Co), copper (Cu), molybdenum (Mo), gallium (Ga), niobium (Nb), lead (Pb), thorium (Th), arsenic (As), uranium (U), and yttrium (Y).

the formation, 14.5 m above the Swift Formation, is a 1.5-m-thick micrite bed with thinly interbedded mudstones (20 cm). The micrite bed may have an area larger than approximately 5 km<sup>2</sup>, but exposures are limited (stratigraphic section H on figure 10). The micrite

beds contain unpaired fossil ostracods and charophyte gyrogonites (Johnson-Carroll, 2014). The disarticulated bone material tentatively assigned to the diplodocid *Suuwassea* was encased in the top of the uppermost micrite bed.

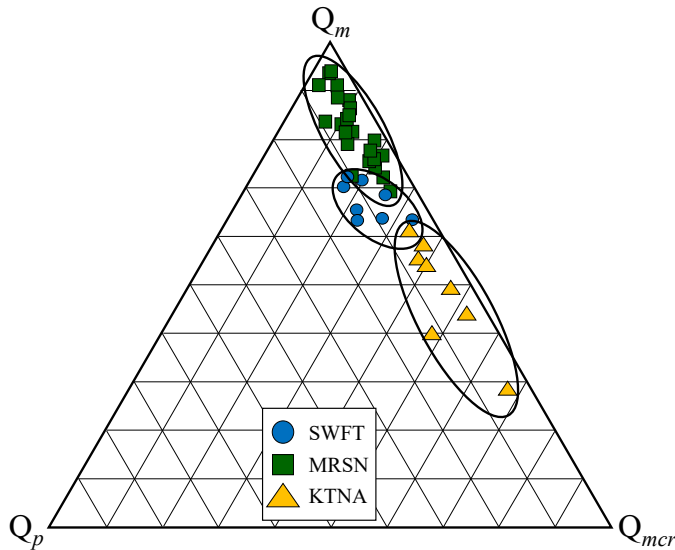


Figure 13. Tertiary diagram displaying the three typical petrographic quartz grain morphologies. The percentages of monocrystalline ( $Q_m$ ), polycrystalline ( $Q_p$ ), and microcrystalline quartz ( $Q_{mcr}$ ) grains can be used to differentiate the Morrison Formation (MRSN) from the underlying Swift (SWFT) and overlying Kootenai (KTNA) sandstones. This change in quartz grain morphology also suggests a change in provenance for each formation.

One hundred and seven small (< 3 m diameter) carbonate buildups were discovered in the Morrison Formation of central Montana (Richmond and others, 2021b). The buildups are distributed stratigraphically between 40 and 52 m above the Swift Formation. The mound springs were produced by subartesian groundwater moving up fractures to the surface. Bulk rock negative  $\delta^{18}\text{O}$  and  $\delta^{13}\text{C}$  values demonstrate the buildups were produced by meteoric waters in a continental setting, with the groundwater having a short residence time in the subsurface, indicating that the region experienced extended periods of increased precipitation (Richmond and others, 2021b; figure 15).

Button Butte is a prominent Laramide uplift 10 km southeast of Grass Range, Montana. Southwest of Button Butte (1.4 km) there are several thin (20 to 50 cm) micrite beds in the uppermost Morrison section. The beds are stratigraphically located 56.6 m above the Swift Formation. The lateral extent is unknown as the outcrop exposure is limited in stratigraphic section I on figure 10.

## Rhyolitic Ash Bed

Stratigraphically 38 m above the Swift Formation is a 20-cm-thick, laterally extensive, coarse-grained, tuffaceous, rhyolitic ash bed (figure 16A). This is the first discovery of an in situ Upper Jurassic-aged ash in central Montana. The majority of magmatism in Montana occurred during the Late Cretaceous and the Paleogene Epochs. Intrusive complexes dominated the Late Cretaceous followed by volcanism during the Paleogene (Scarberry and others, 2020).

The weathered ash bed surface exhibits dissolution pores with the primary pores ranging from macro- to micropore sizes (figure 16B). One hundred meso- and macropore diameters were measured from hand samples. The mean meso/macropore diameter is 4.5 mm with the largest macropore diameter observed measuring 26 mm. Three hundred micropore diameters were measured from a thin section indicating the micropores are very fine grained (3.89  $\Phi$ ). In the fine ash, quartz grains are uncommon. In unweathered rock, the pores are filled with gray-green clay. The ash matrix and the pore material were analyzed with XRF to determine the geochemistry. The XRF indicates that the ash is very silica-rich and therefore is classified as rhyolitic ash. XRF was also performed on two Yellowstone rhyolitic ashes for comparison. Although there is variability in the Morrison ash, its chemical makeup resembles the ashes from the Yellowstone caldera (figure 17). The pore material was altered to a mixture consisting of silica and aluminum-rich clay. In the thin section, the pore material is coarser grained than the matrix with abundant quartz grains; therefore, the pore material is interpreted to have been lapilli, as opposed to an ash aggregate (figure 16C).

## MORRISON FORMATION DEPOSITIONAL FACIES

### Historical Review

The early researchers of the Morrison Formation in Montana (Calvert, 1909; Fisher, 1909, Freeman, 1919; Lupton and Lee, 1921; Dekalb, 1922; Reeves, 1927; Gardner and others, 1945, 1946; Gardner, 1950, 1959; Towse, 1954; Francis, 1956, 1957; Hadley, 1956; Vine,

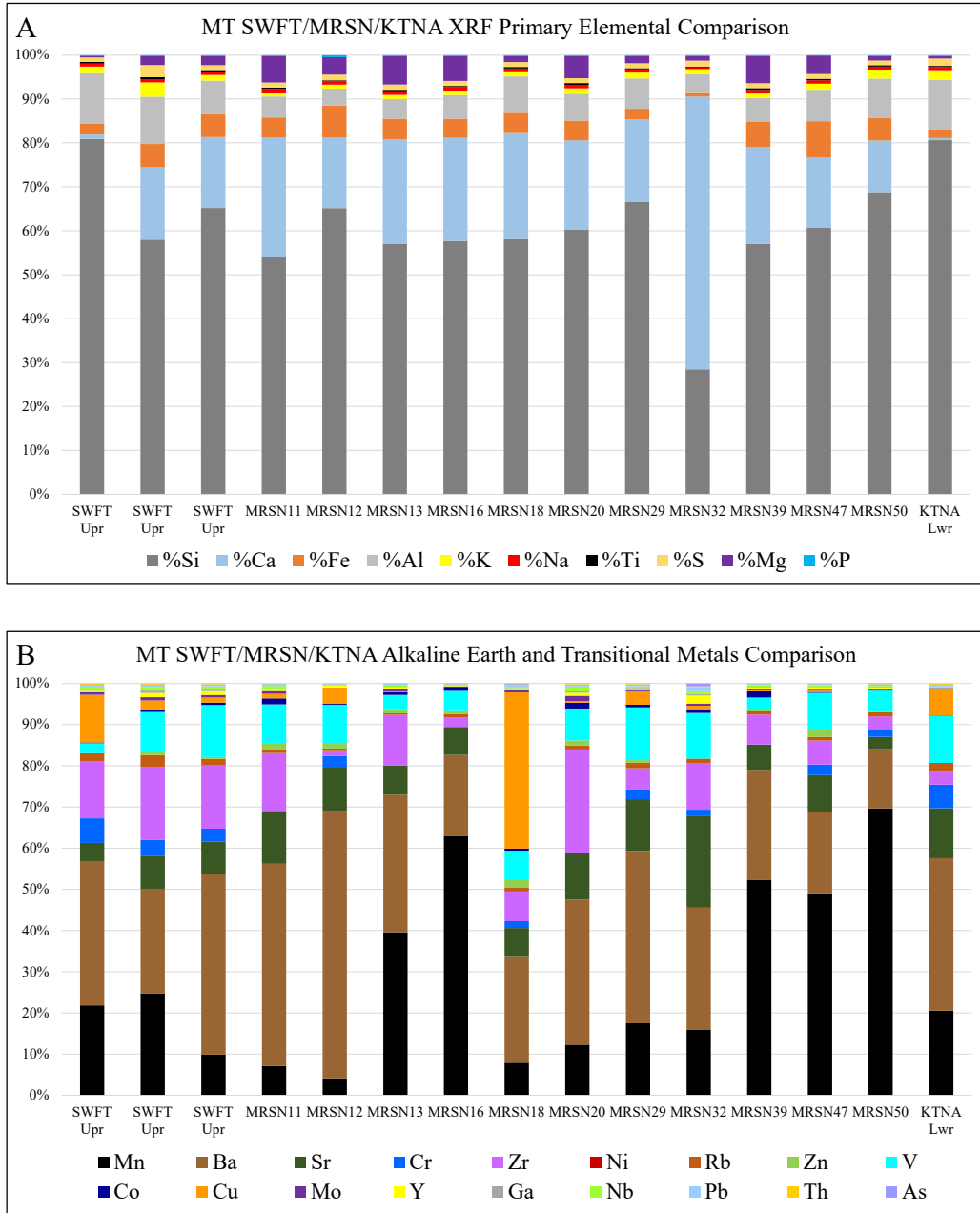


Figure 14. X-ray fluorescence (XRF) comparison of the Swift (SWFT), Morrison (MRSN), and Kootenai (KTNA) sandstones. The percentages of the primary elements were derived from the XRF (A), whereas the percentages for the alkaline and transitional metals (B) were normalized from ppm to show the relative abundance of the elements present in the sandstones. The Swift sandstones are from the upper part of the formation. The Morrison sandstones are labeled by their stratigraphic position above the Swift Formation (example: MRSN11-11 m above the Swift). The primary elements, alkaline, and transitional metals, are likely related to the availability and solubilities of elements from the soil and groundwater from the decomposition of organic matter that subsequently became incorporated into the sandstone bodies. The elements suggest that the climate was humid and warm with high plant productivity. Element abbreviations are as follows: silica (Si), calcium (Ca), iron (Fe), aluminum (Al), and potassium (K), with minor percentages of sodium (Na), titanium (Ti), sulfur (S), manganese (Mn), and phosphorous (P). The alkaline earth and transitional metals are barium (Ba), strontium (Sr), chromium (Cr), zirconium (Zr), nickel (Ni), rubidium (Rb), zinc (Zn), vanadium (V), with minor ppm of cobalt (Co), copper (Cu), molybdenum (Mo), gallium (Ga), niobium (Nb), lead (Pb), thorium (Th), arsenic (As), uranium (U), and yttrium (Y).



Figure 15. A typical carbonate mound spring buildup. This particular mound spring encased a partial fossil log of *Circoporylon*. For further information about the mound springs refer to Richmond and others (2021b). 50 cm scale.

1956; Knechtel, 1959; Moritz, 1960; Christie, 1961; McMannis, 1965; Norwood, 1965; Ballard, 1966; Harris, 1966; Silverman and Harris, 1967; Fraser and others, 1969) provided stratigraphic measurements and lithologic characteristics; however, they did not postulate on the depositional facies but only stated that the formation was a nonmarine or freshwater deposit. Moritz (1951) was the first to propose that after the retreat of the Sundance sea, southwest Montana consisted of a low-gradient plain with fluvial deposits and ephemeral lakes. Hadley and Milner (1953) proposed that the formation was “lagoonal in character.” Peterson (1966) proposed that during Morrison’s time, a large lake occupied the Montana trough during a “moist” climate. Silverman and Harris (1966) agreed with Peterson’s (1966) lake hypothesis but stated that the upper Morrison consisted of lacustrine, floodplain, and fluvial channel deposition. Harris (1968) stated the formation is comprised of mudstone beds interbedded with freshwater lacustrine limestone and fluvial sandstone beds. Walker (1974) reviewed the formation in the Great Falls area and proposed a lacustrine and fluvial depositional model. A study of the sedimentology of the differing lithofacies and sandstone body architecture in the northern Beartooth and Gallatin Ranges determined the formation was deposited on an anastomosing floodplain (Cooley, 1993; Cooley and Schmitt, 1998). A review of the differing lithofacies of the formation north-northwest of Dillon, Montana, Smith and others (2006) concluded that the depositional facies were the product of a mud-dominated fluvial system of a low-gradient floodplain.

### Lower Distal Floodplain Facies

There does not appear to be a regional stratigraphic marker to subdivide the formation into members; however, locally, there is a distinct and abrupt change in the depositional facies. Locally, a thick, laterally extensive reddish illitic mudstone bed (figure 11) rests conformably on the sandstone beds of the upper Swift tidal para-sequence. Isolated small siltstone beds are uncommon. The siltstone/sandstone beds are generally less than 20 cm thick with a minimal limited lateral extent ( $< 1$  m). The siltstones are angular (0.58), moderately sorted (0.61), coarse-grained (4.59  $\Phi$ ), matrix-supported siltstones ( $n = 2$ ; figure 4G). The sandstones are angular (0.52), well sorted (0.50), fine-grained (2.95  $\Phi$ ), quartz arenites ( $n = 1$ ). No fossils have been found in the lower unit. The facies association with the Swift uppermost tidal flat facies (Richmond, 2022) designates that the lower reddish mudstone bed represents a well-drained distal floodplain with its associated very small distributive fluvial channels. No micrite beds were observed associated with the facies.

### Upper Fluvial Depositional Facies

The upper depositional facies is also a mudstone-dominated section ( $\geq 75\%$ ) with small sandstone bodies that have an average width:thickness ratio of 13 ( $n = 24$ ) and thin, flat-bottomed sandstone beds ( $n = 68$ ). The beds are composed of subangular, well sorted, very fine to fine-grained sandstones. The small sandstone beds that display channel geomorphology have a low width:thickness ratio and sometimes display lat-

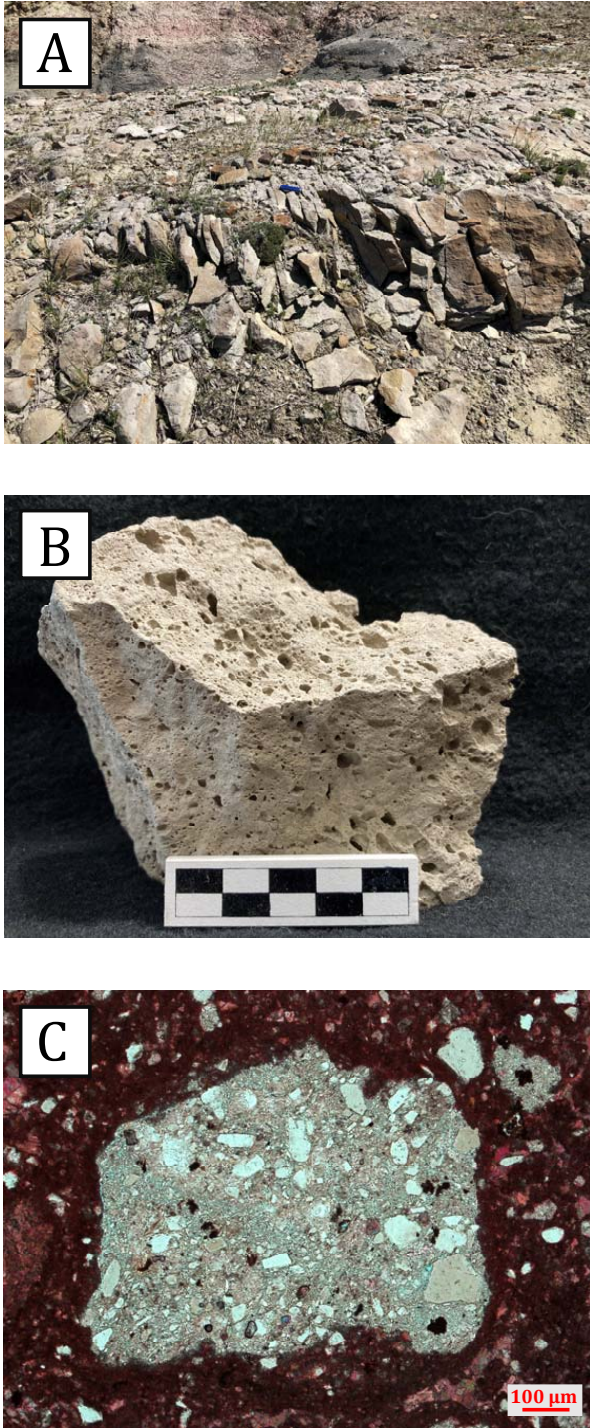


Figure 16. (A) Field outcrop of a 20-cm-thick, laterally extensive, coarse-grained, tuffaceous, rhyolitic ash bed stratigraphically 38 m above the Swift Formation. (B) A hand sample of the rhyolite ash. The meso and micropores from the weathered lapilli are clearly discernible. 5-cm scale. (C) Photomicrograph of a lapilli clast surrounded by a fine ash groundmass. Crossed Nichols.

eral accretion (figure 18). The beds have abrupt lithofacies transitions and are composed of finer-grained sediments interpreted to represent anastomosing fluvial channels (Smith and Putman, 1980; Smith and Smith, 1980; Rust, 1981; Morris and Richmond, 1992; Richmond and others, 2020). Anastomosing (distributive) sandstone channels have width:thickness ratios of less than 40 (Gibling, 2006) and are relatively narrow and deep, with fine-grained sand carried along as bedload in the channel thalweg. Channel fills consist of finer-grained sediments (i.e., silt or mud). Trough cross-bedding is uncommon. The flat-bottomed, single- and multistory sandstone beds are interpreted to be crevasse splays. Herein, flood and crevasse splays are differentiated. During normal flood stages, water tops the channel's levees, depositing silt- and clay-sized particles onto the floodplain (Fisher and others, 2008; Burns and others, 2019). This repeated flooding results in floodplain aggradation (Shen and others, 2015). In contrast, a crevasse splay occurs when the levee wall is breached, cutting down to the channel bottom to release sand-sized sediment onto the floodplain. Morrison Formation crevasse splay sandstone deposits are flat-bottomed, thin (0.9 m average), usually structureless sandstone beds (Richmond and others, 2020). With a few exceptions, the thin, laterally limited micrite beds scattered throughout the section represent interfluvial lakes or ponds (flood ponds). Lacustrine and palustrine deposition is commonly recorded by mudstone deposition (Richmond and others, 2017; Hunt and Richmond, 2018; Richmond and Murphy, 2020).

The depositional model of anastomosing fluvial channels with associated flood and crevasse splay and interfluvial lacustrine micrite and mudstone deposits in central Montana agrees with previous depositional interpretations for the formation of western Montana (Cooley, 1993; Cooley and Schmitt, 1998; Smith and others, 2006). Additionally, the fluvial channel geomorphology, sedimentology, and floodplain facies are similar to those of the Brushy Basin Member of the Morrison Formation on the Colorado Plateau (Kantor, 1995; Richmond and Morris, 1996) and the Kenton Member of the Morrison Formation of Oklahoma (Richmond and others, 2020).

The distributive fluvial system model has been used

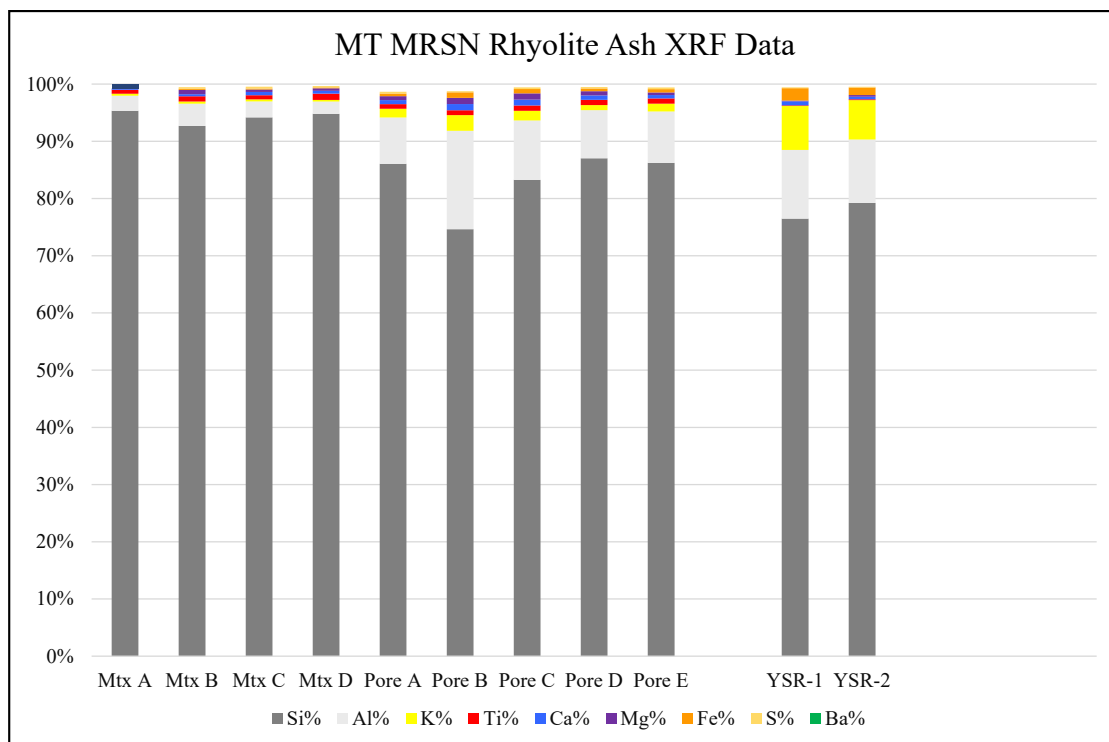


Figure 17. X-ray fluorescence analyses of the Morrison ash bed. The high silica percentages of the ash matrix (Mtx A through D) indicate that the ash is rhyolitic. The XRF of the lapilli (Pore A through E) indicates it altered to a high silica and aluminum clay. Two rhyolites from the Yellowstone basin (YSR-1 and YSR-2) as shown for comparison. The nine mineral percentages represent 99% of the rock. Element abbreviations are as follows: silica (Si), aluminum (Al), potassium (K), titanium (Ti), calcium (Ca), magnesium (Mg), iron (Fe), sulfur (S), and barium (Ba).

to characterize the deposition of the Salt Wash and Brushy Basin Members of the Colorado Plateau and the Kenton Member of Oklahoma (Owen, 2014; Owen and others, 2015; Richmond and others, 2020). The northeastward thinning of the Morrison Formation (figure 7) and the interpreted depositional model support the northeastward progradation of a broad fluvial system across central Montana. Furthermore, the uniform formation thickness across central Montana implies that numerous fluvial channels migrated across the broad, flat floodplain providing fine-grained sediment across the region.

## DISCUSSION: MORRISON PALEOCLIMATE PROXIES

### Morrison Basin Paleoclimatic Overview

Based on climate models and lithologic proxies,

many researchers have proposed the Morrison foreland basin experienced a semiarid to arid zonal climate (Parrish and others, 1982, 2004; Parrish and Peterson, 1988; Demko and Parrish, 1998; Turner and Fishman, 1991; Valdes and Sellwood, 1992). To support the giant herbivorous dinosaurs which roamed the Morrison basin, some researchers have proposed that there were riparian environments that supported abundant plant life (Peterson and Turner, 1987). By the Late Jurassic, North America's northward movement fragmented the Triassic monsoonal climate pattern resulting in a low-pressure cell over the continent (Parrish and Peterson, 1988). Modeled temperatures for western North America during the Late Jurassic ranged from 5°C (winter) to greater than 36°C (summer) and were about 5°C warmer than at present (Demko and Parrish, 1998). Temperature independently does not account for the aridity of western North America during the Late Jurassic. The aridity was likely generated by several factors,

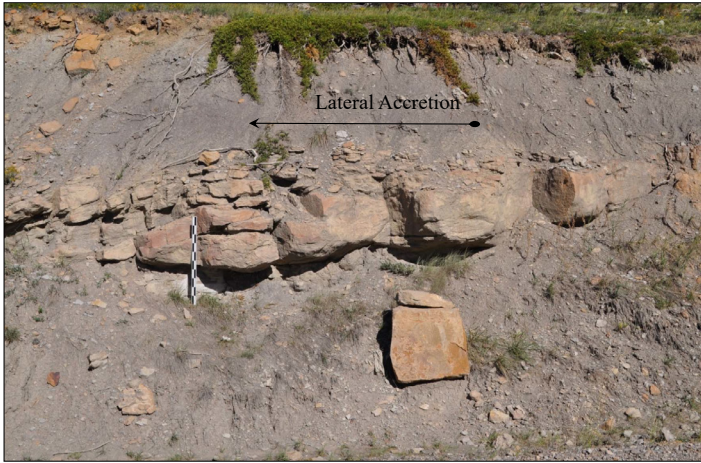


Figure 18. An example of an anastomosing fluvial channel bed in the Morrison Formation. The lateral accretion direction is to the north. Typically, the small fluvial channel beds are isolated in a mudstone-dominated section. The sandstone bed is stratigraphically 34 m above the Swift Formation. The outcrop is exposed along the Tyler Cut Road, southwest of Grass Range, Montana. Meter scale.

including the latitudinal position in the subtropical dry belt, the Sevier orogenic belt acting as a rain shadow (Demko and Parrish, 1998), and oceanic upwelling driven by coastal wind patterns, which would have increased the aridity of western North America (Parrish and Peterson, 1988). Using eolian lithologic units from the Tidwell, Salt Wash, Bluff Sandstone, Junction Creek, and Recapture Members of the Morrison Formation, a westerly wind direction was ascertained for the Late Jurassic of North America (Parrish and Peterson, 1988; Peterson, 1988). These eolian units of the Morrison are stratigraphically in the lower part of the formation (Demko and Parrish, 1998). A zonal climate model by Parrish and others (1982) predicted low rainfall patterns for much of the Morrison basin during the Volgian Regional Stage (Tithonian). They also mapped evaporates and coals for the same stage, and the spatial representation for these proxies corresponds to a Tithonian zonal climate. Further geologic evidence for a dry climate is the large saline lake, Lake T'ood'ichi, demarcated by diagenetic zeolites and feldspars, indicating the lake underwent repeated wetting and drying under arid conditions punctuated by episodic rainfall (Turner and Fishman, 1991). Richmond and Morris (1998) reported

similar findings at the Dry Mesa Dinosaur Quarry. The quarry is located on the northeastern margin of Lake T'ood'ichi and records an extreme drought (Phase 3; Shipman, 1975) in which 30 genera of vertebrates, including dinosaurs, pterosaurs, crocodiles, lungfish, and mammals, died at a local waterhole. Following decomposition and disarticulation, their bones were transported for a short distance by a catastrophic flash flood and were buried.

Additional evidence for drier climatic intervals is the presence of evaporite-associated chert beds (Magadi-type cherts). Evaporite-associated chert beds have been reported from the Morrison Formation in Wyoming (Surdam and others, 1972), Colorado (Dunagan and others, 1997), and Oklahoma (Richmond and others, 2019a, 2020). These evaporite-associated cherts form in a shallow acidic ( $\text{pH} > 9$ ) phreatic zone as a result of the silicification of sulfate evaporites (anhydrite). The antecedent lacustrine evaporites designate prolonged periods of increased evaporation due to increased temperature or decreased precipitation. Gypsum mineralization signifies a mean annual precipitation of less than 350 mm/year (Gu and others, 2015).

In contrast, other lithologic evidence supports the presence of perennial fluvial, pluvial, and lacustrine facies in the Morrison basin (Lockley and others, 1984, 1986; Dunagan, 1999; Dunagan and Turner, 2004; Gorman, 2007; Gorman and others, 2008; Richmond and others, 2020). Several paleolakes have lacustrine ooid facies (Lockley and others, 1984; 1986). Ooids can take over a thousand years to form (Neese and Pigott, 1987), suggesting a long-term presence for these paleolakes. The first tufa deposits for the Morrison Formation have been identified in central Montana and are indicative of a high groundwater table (Richmond and others, 2021b). There is also an indication of ephemeral deposition, particularly from fluvial and pluvial deposits signifying seasonal or episodic precipitation was sufficient for fluvial deposition and the wetting of ponds (Richmond and Morris, 1996; Richmond and others, 2020). Dodson and others (1980) suggested a strongly seasonal climate based on dinosaurian fauna and taphonomy. However, some dinosaurs are assumed to have been migratory (Bronzo and others, 2017). Therefore, their presence or absence from a region should not be used as



evidence to infer paleoclimate. The presence of aquatic vertebrates, e.g., crocodiles (Dunagan, 1999; Connelly, 2002; Hunt and Richmond, 2018), turtles (Gaffney, 1979; Hunt and Richmond, 2018), lungfish (Kirkland, 1987), boney fish (Small and others, 2007, Gorman and others, 2008), and amphibians (Hecht and Ester, 1960) are generally associated with their aquatic environment and indicate perennial lakes and rivers were present in the Morrison basin (Gorman and others, 2008; Richmond and others, 2020). Aquatic invertebrates have specific environments in which they live (Evanoff and others, 1998; Schudack and others, 1998; Good, 2004; Richmond and others, 2017) and usually require clean perennial lakes and rivers to survive. Aquatic invertebrates are present throughout the Morrison basin (Evanoff and others, 1998).

Horsetails, ferns, cycads, and various large gymnosperms indicate sufficient precipitation for growth. According to Tidwell (1990), the abundance of plant fossils in the formation indicates a humid, tropical climate. A newly described fossil wood, *Agathoxylon hoodi*, from the Salt Wash Member of the Morrison Formation in eastern Utah infers a warm equable climate for the eastern basin lowlands (Gee and others, 2019; Sprinkel and others, 2019). Three fossil wood genera were newly discovered in close proximity to one another in the Boise Member of the Morrison Formation in western Oklahoma. The occurrence of three fossil wood genera, *Xenoxylon meisteri*, *Cupressinoxylon*, and *Agathoxylon*, in the same stratigraphic horizon, indicates a period of increased precipitation at the southern basin periphery during deposition of the Boise Member (Richmond and others, 2018, 2020).

Different regions of the Morrison Formation have been explored for palynology (Newman, 1972; Tschudy and others, 1980, 1988; Hotton, 1986; Litwin and others, 1998; Baghai-Riding and Hotton, 2009, 2011; Hotton and Baghai-Riding, 2010, 2016; Baghai-Riding and others, 2013, 2014, 2015, 2018) The majority of the data indicates arid climatic conditions for the formation with wetter conditions in the more northern part of the foreland basin. Demko and Parrish (1998) suggested plants only represent a small spatial and stratigraphic part of the formation and are inconsequential to the overall climatic interpretation.

Climatic proxies require a stratigraphic and areal position, and although there were intervals and regions where the formation was wetter, overall, the Morrison of the southern states and Colorado Plateau is considered semiarid to arid (column A on figure 19). In the following sections, climate proxies will be addressed in order of lithologic proxies, faunal and floral proxies, and will be, where applicable, presented in stratigraphic order. Each proxy will be first described and then followed by its climatic interpretation.

## LITHOLOGIC CLIMATIC PROXIES

### Sandstone Geochemistry

Sandstone geochemistry is a compilation of sandstone mineralogy, groundwater chemistry, and diagenetic fluids. The sandstones are quartz arenites with low percentages of the interparticle matrix, and there is no evidence of diagenetic overprinting on the sandstones. The primary elemental percentages are derived from the sandstone's composition (see figure 14A). The alkaline earth metal barium and the transitional metal manganese together typically make up more than 50% of the alkaline earth and transitional metal elements (see figure 14B). The high percentages of these two elements may be related to the availability and solubilities of these elements from the soil and groundwater as byproducts of the decomposition of organic matter. Therefore, the mobilization pathways of these elements are evaluated.

The accumulation of organic materials is chiefly a function of the annual litterfall minus decomposition. The most sizable proportion of allochthonous organic matter is from foliage, seeds, branches, and bark. The main litterfall contribution is from the overstory, with understory plants supplying about 10% (Binkley and Fisher, 2019). Storms can accelerate litterfall volumes, whereas elevated temperatures and soil moisture can hasten decomposition rates. Conversely, ground fires can consume organic materials. Annual litter production can be related to latitude. During the Late Jurassic, central Montana was at a paleolatitude of 50° north (Richmond and others, 2019d). Most modern conifer forests have an annual litterfall of 1975 to 5900 kg/hectare/year (Binkley and Fisher, 2019); however, a temper-

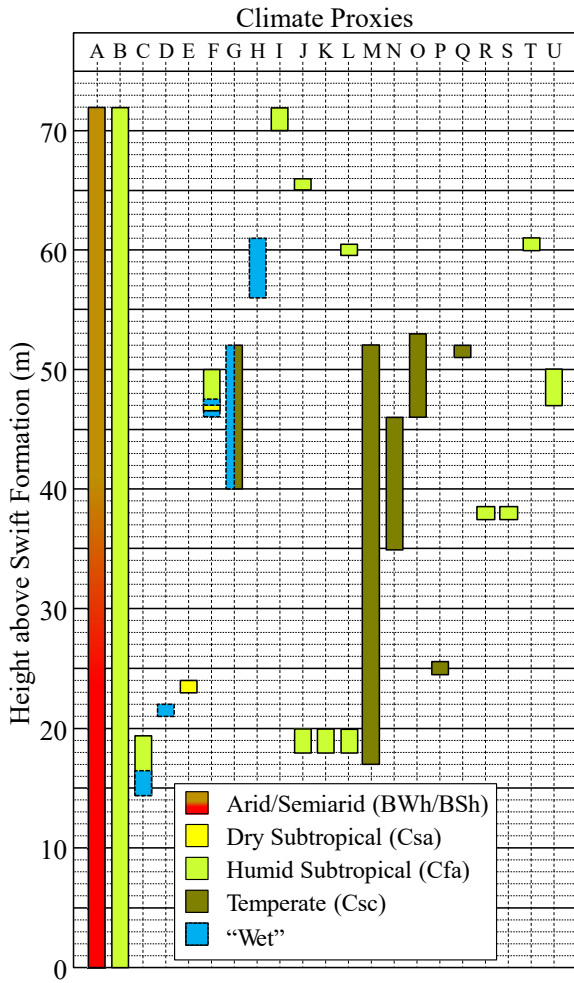


Figure 19. Summary of the central Montana Morrison climate proxies displayed in stratigraphic position with their interpreted ranges. The colors and climate categories follow the Köppen-Geiger climate classification system (Beck and others, 2018). The climate codes are BWh/BSh: B (arid), W (desert), h (hot); B (arid), S (steppe), h (hot); Cfa: C (temperate), f (fully humid), a (hot summer); Csa: C (temperate), s (dry summer), a (hot summer); Csc: C (temperate), s (dry summer), a (cold summer). Whereas “wet” signifies that there was sufficient precipitation for the formation of local lakes and flooding of rivers. To associate the climate codes to modern locations, the BWh/BSh climate is analogous to the deserts of the southwestern U.S. and northwestern Mexico; the Cfa climate is comparable to the climate of Houston, Texas, and the coastal states; and the Csc climate is similar to the climate of the Mediterranean where summers are cool and the majority of precipitation is received during the winter months. The overall climatic interpretation for the Morrison Formation of the Colorado Plateau is provided in column A. Sandstone and mudstone geochemistry proxies are combined in column B.

ate forest at 50° north latitude generates 3700 kg/hectare/year (Bray and Gorham, 1964).

The rate of organic decay depends on the interaction of physical factors, water chemistry, and biological agents. Decomposition can be rapid, with turnover rates varying between 1 to 3 years for cool temperate climates (Binkley and Fisher, 2019). Litterfall on the forest floor is fragmented by arthropod and annelid decomposers, then consumed by rotifers and pervasive microbes. The top organic soil layer comprises undecomposed litter that overlies the fermentation layer, where decomposition occurs. This layer overlies the humus layer, where decay is nearly complete.

In boreal forests nutrient turnover is slow. Potassium and sodium are quickly leached from the soil. Nitrogen, phosphorus, sulfur, and magnesium are released into the soil after a long period. Iron, zinc, and copper are left in the accumulated litter material (Staaf, 1980).

Barium and manganese are related to vegetative cycling. Barium concentrations are controlled by soil acidity but also by the concentration of sulfates (Guyette and Cutter, 1994; Jennings and others, 2015). According to Jennings and others (2015), barite formation occurs in exposed wetland, lacustrine, and coastal plain environments. Wetlands contain sulfate-reducing microorganisms resulting in a high sulfate reduction rate (Pester and others, 2012). Sulfate-reducing microorganisms may limit the sulfate concentration in groundwater and lower the soil’s barium concentration.

Manganese is an essential plant nutrient in the bole wood and foliage (Guyette and Cutter, 1994). The subsurface geology controls soil manganese concentrations and increases vegetation cycling (Richardson, 2017). The soil pH controls its solubility and concentrations, with more acidic soils greatly influencing potencies (Guyette and Cutter, 1994). Soils in wet climates are typically acidic, whereas in dry climates, the soils are alkaline (Richmond and others, 2021b; Slessarev and others, 2016). The high mobilization of manganese and barium demonstrates the presence of acid soils, which are indicative of a wetter climate.

Interestingly, a lower Morrison splay sandstone bed stratigraphically 18 m (sample MRSN18 on figure 14B) above the Swift Formation and 1.5 m above a lacustrine limestone bed has a high percentage of copper. Copper

is an essential element for plant growth, and soils naturally contain copper ranging from 2 to 100 ppm and averaging about 30 ppm. This sandstone has greater than 900 ppm copper (figure 14B). Acidic soils are more likely to be deficient in copper, but a higher pH with humid and wet climatic conditions supports copper concentrations in soils (Ballabio and others, 2018). The more alkaline pH may be due to its stratigraphic proximity to the lacustrine limestone and not a drier climate.

The sandstone alkaline earth and transition metals concentrations suggest a wet environment with associated high plant productivity. Vegetation decomposition leached minerals into the soil and groundwater and subsequently into the fluvial channels to become incorporated into the sandstone bodies. The sandstone geochemistry suggests a humid subtropical climate was pervasive during the deposition of the upper fluvial depositional facies (column B on figure 19).

### **Mudstone Geochemistry**

The distinct clay mineral type and abundance in any deposit depend upon three major factors: provenance, transformation, and neof ormation. Clay minerals can be a reliable indicator of provenance and depositional environments (Chaudhri and Singh, 2012). Illite is the allogenic product of weathering feldspathic and micaceous crystalline rocks under cool/temperate and dry conditions (Chaudhri and Singh, 2012; Raigemborn and others, 2014). Kaolinite is the byproduct of in situ weathering of feldspars, micas, smectite, and other volcanic material under warm and mesic conditions (Singer, 1980, 1984; Raigemborn and others, 2014). In addition to the three principal clays of the Morrison Formation, mudstones of the formation in central Montana also have significant percentages of goethite (figure 12A). The two most common pedogenic Fe-oxides in soils are hematite and goethite. Hematite formation is facilitated by alternating wet (less than 350 mm/year; Wu and others, 2018) and dry environmental conditions under warm to hot temperatures (Zhao and others, 2017). The presence of hematite contributes a predominantly reddish hue to soils. In contrast, goethite is formed under continuously wet conditions under a wide range of temperatures and gives a yellowish reflec-

to the soil (Zhao and others, 2017; Wu and others, 2018).

The mudstone strata of the well-drained distal floodplain depositional facies (< 15 m) are locally a deep reddish color (figure 11). In contrast, the upper fluvial depositional facies are variegated with hues of green, gray, yellow, and red (figure 11). Stratigraphically percentages of goethite tend to increase higher in the upper fluvial section (figure 12A). The mudstone color change from red to variegated hues may signify a climatic change from alternating wet and dry to continuously wet conditions. Soils with a high organic content tend to favor goethite formation over hematite.

Analysis of channel geomorphology and channel fill can determine the climatic regime under which the anastomosing fluvial systems were deposited; however, the associated floodplain facies give the strongest signal. In mesic regions, interfluvial sediments consist of lacustrine and palustrine deposits; coals are often present (Smith and Smith, 1980; North and others, 2007). In arid environments, there is a general absence of levees. As a result, crevasse avulsions, lacustrine, palustrine, and organic deposits are primarily absent from the floodplain (Rust, 1981; Nanson and others, 1986; North and others, 2007). In central Montana, Morrison interfluvial sediments comprise crevasse and flood splay deposits, lacustrine, palustrine, and organic-rich deposits.

X-ray fluorescence data of the mudstones (B paleosol horizons) can be used to calculate the chemical index of alteration minus potassium (CIA-K) and the calcium and magnesium weathering index (CALMAG). These values have been used to estimate mean annual precipitation (MAP) for the Morrison Formation in North America (Myers, 2009; Myers and others, 2012b, 2014) and the Lourinhã Formation in Portugal (Myers, 2009; Myers and others, 2012a). The estimated mean annual rainfall for northern Wyoming and southern Montana was greater than 1200 mm/year (Myers and others, 2012b, 2014). The central Montana CIA-K values range from 57 to 86, averaging 73. The calculations provide a CIA-K MAP estimate between 759 to 1270 mm/year with an average of 999 mm/year. The CALMAG values range from 53 to 91, averaging 74. The CALMAG calculations yield MAP estimates between 775 to 1625 mm/year with an average of 1234 mm/year (table 1).

Table 1. Ten mudstone samples were used for CIA-K mean annual precipitation and CALMAG mean annual precipitation. The samples MRSN MM 36 and 38 are from Highway 87 and mile markers 36 and 38, respectively. These samples are interpreted to be from the Morrison lower distal floodplain facies. Sample MRSN KLKN BV is from the bivalve location off Tyler Cut Road. The other samples are from the measured stratigraphic sections shown on figure 10. Each measurement is provided stratigraphically in meters above the Swift Formation. Data from the formation displays a high average precipitation for the region.

Sample	Strat. (m)	Al <sub>2</sub> O <sub>3</sub> (wt%)	CaO (wt%)	MgO (wt%)	Na <sub>2</sub> O (wt%)	CIA-K	CIA-K MAP (mm yr-1)	CALMAG	CALMAG MAP (mm yr-1)
MRSN MM36	< 15*	16	0.78	1.45	0.36	91.69	1270.39	86.3	1522.26
MRSN MM38	< 15*	11.94	8.97	1.46	0.26	56.39	766.72	53.36	774.88
MRSN 5E Sec C	13.5	7.61	1.78	-0.02	1.24	71.54	982.87	81.15	1405.49
MRSN 5E Sec D	16	11.76	8.25	0.14	1.05	55.87	759.33	58.39	889
MRSN KLKN BV	19	14.5	4.99	1.65	0.34	73.13	1005.52	68.6	1120.69
MRSN 5E Sec B	28	15.85	1.42	1.63	0.28	90.32	1250.77	83.87	1467.24
MRSN 5E Sec E	47	9.85	6.5	-0.04	1.05	56.6	769.78	60.39	934.48
MRSN 5E Sec E	47.5	14.9	4.68	0.22	1	72.4	995.14	75.25	1271.56
MRSN 5E Sec E	48.5	14.45	4.29	-0.16	1.04	73.07	1004.68	77.77	1328.86
MRSN 5E Sec F	55	14.86	1.45	0.51	1.02	85.77	1185.86	90.84	1625.32
Average						72.68	999.11	73.59	1233.98

A review of the stratigraphic position of the samples in table 1 shows that the mean annual precipitation was not constant throughout the section. However, the average CIA-K MAP (999 mm/year) and CALMAG MAP (1234 mm/year) correlate with the estimates for the region derived by Myers and others (2014). Mudstone geochemistry, interfluvial sedimentation, and CALMAG data show a predominantly humid subtropical climate for the formation (column B on figure 19).

### Micrite and Mudstone Beds

West of Spindletop dome along the Tyler Cut Road, stratigraphically at 14.5 m, is a 6-m-thick section of interbedded micrite and mudstone beds (Johnson-Carroll, 2014). Some micrite beds are fossiliferous, containing small bivalves, ostracods, and charophyte gyrogonites, whereas others appear unfossiliferous (Johnson-Carroll, 2014). The lateral extent of the micritic section is unknown due to the lack of outcrop exposures but is estimated to be at least 10 km<sup>2</sup>. The micrite and mudstone section represents shallow lacustrine and subsequent palustrine depositional facies. Also associated with these beds are the vertebrate fossils (?*Suuwassea*,

and an identified ornithomimid dinosaur) and the fossil wood, *Xenoxylon meisteri*.

Above the lacustrine/palustrine facies at 19 m is a greenish illitic mudstone bed. The mudstone bed contains abundant invertebrate fossils. The mudstone bed, with its numerous invertebrate fossils, is interpreted to be a flood splay deposit that transported the fossils (Richmond and others, 2017). The invertebrate fossils and their paleoclimatic interpretation will be discussed below. The lacustrine/palustrine depositional facies recorded the transition from shallow ponds to wetlands and a fluvial floodplain documenting a flooding event. The facies transition may be due to sediment infilling of the lake or as a response to a drier paleoclimatic trend. The presence of a small lake, associated wetlands, and splay events indicate high precipitation during the deposition of these strata (column C on figure 19).

### Mud-Clast Conglomerate Bed

Southwest of Quarry 2 is a meter-thick, mud-clast conglomerate bedset stratigraphically 21 m above the Swift Formation (see stratigraphic columns E and F on figure 10). The bedset is divided into numerous beds



Figure 20. The outcrop of a crevasse splay mud-clast conglomerate bed. The meter-thick bed is stratigraphically 21.5 m above the Swift Formation (stratigraphic column F on figure 10). The collated layers show numerous repeated splay flooding on the proximal facies. 40 cm ruler for scale.

of rip-up conglomerate, fine-grained sandstone, and mudstone (figure 20). The bedset represents a proximal crevasse splay deposit produced from multiple flooding events. No correlative fluvial channel has been recognized. The repeated flooding indicates high, possibly seasonal, precipitation (column D on figure 19).

### **Silcrete Bed**

A reddish illitic mudstone bed is capped by a 20-cm thick, laterally extensive, silcrete bed. The silcrete bed is stratigraphically 23 m above the Swift Formation. The parent rock is a subangular (1.34), moderately well sorted (0.60), very fine grained (3.95  $\Phi$ ) quartz arenite.

In a hand sample cross section, the silcrete exhibits angular and subangular blocky microstructures resulting in ped blocks and nodules that range in size up to 20 mm (figures 21A and 21B). In the thin section, the microstructure matrix is light and dark (figures 21C and 21D). Figure 21C shows an annealed fracture, whereas figures 21D and 21E display fractures filled with organic-rich sediments. Additional interesting features observed in the thin section are concentric rings (figure 21F) interpreted to be the initial stages of concentric nodule formation. The silcrete ped block (figure 21A,

site 1) and the microstructure matrix (figure 21A, site 2) were analyzed by XRF. Both the ped block and microstructure matrix have high percentages of silica. However, the moderate reddish-orange matrix (figure 21A, site 2) has higher percentages of aluminum, titanium, calcium, and iron (figure 22).

Silcretes form in the phreatic zone associated with soil formation and require stable geological conditions for an extended time (Milnes and Thiry, 1992). Silcrete customarily forms in arid or semi-arid climates according to numerous Cenozoic studies of silcretes in southern Africa, Australia, and elsewhere (Summerfield, 1983; Trewin and Fayers, 2005). However, silcretes also form where there is an abundance of water and organic acids. The water, which may be seasonal, is required to migrate organic acids and mobilize silica. The organic acids, formed by copious plant life, enhance quartz dissolution but not its solubility (Taylor and Eggleton, 2017). In topographically low areas, near fluvial systems or lakes with slow-flowing or stagnant water and abundant plants, organic-rich water produces the acidic reducing conditions for silica dissolution. Silica-saturated alkaline groundwater ( $\text{pH} \geq 9$ ) precipitates silica, especially when mixing with a lower pH surface water. These added ions will facilitate the silica precipitation if aluminum, iron, magnesium, or sodium chloride ions are also present (Trewin and Fayers, 2005; Taylor and Eggleton, 2017).

Metallic oxides, such as aluminum, titanium, and iron, are most common where the climate is warm and wet but unusual at higher elevations and cool temperate zones (Ségalen, 1971). Titanium comprises about 0.57% of the Earth's crust. Therefore, a concentrated titanium weight percent in silcretes is typical. Australian silcretes have an average weight percentage of 1% (Taylor and Eggleton, 2017). The Montana Morrison silcrete samples have high concentrations of titanium at 1.4% and 5.5%. Titanium is mobile in weathering environments with a pH less than 4, but between a pH of 4.7 and 6.7 (figure 22), titanium hydroxyls tend to be absorbed in silica because silica and titanium have opposite charges over this pH range. A highly acidic environment in which titanium is soluble and incorporated into silcrete suggests abundant vegetation and a mesic to subtropical climate (Summerfield, 1983).

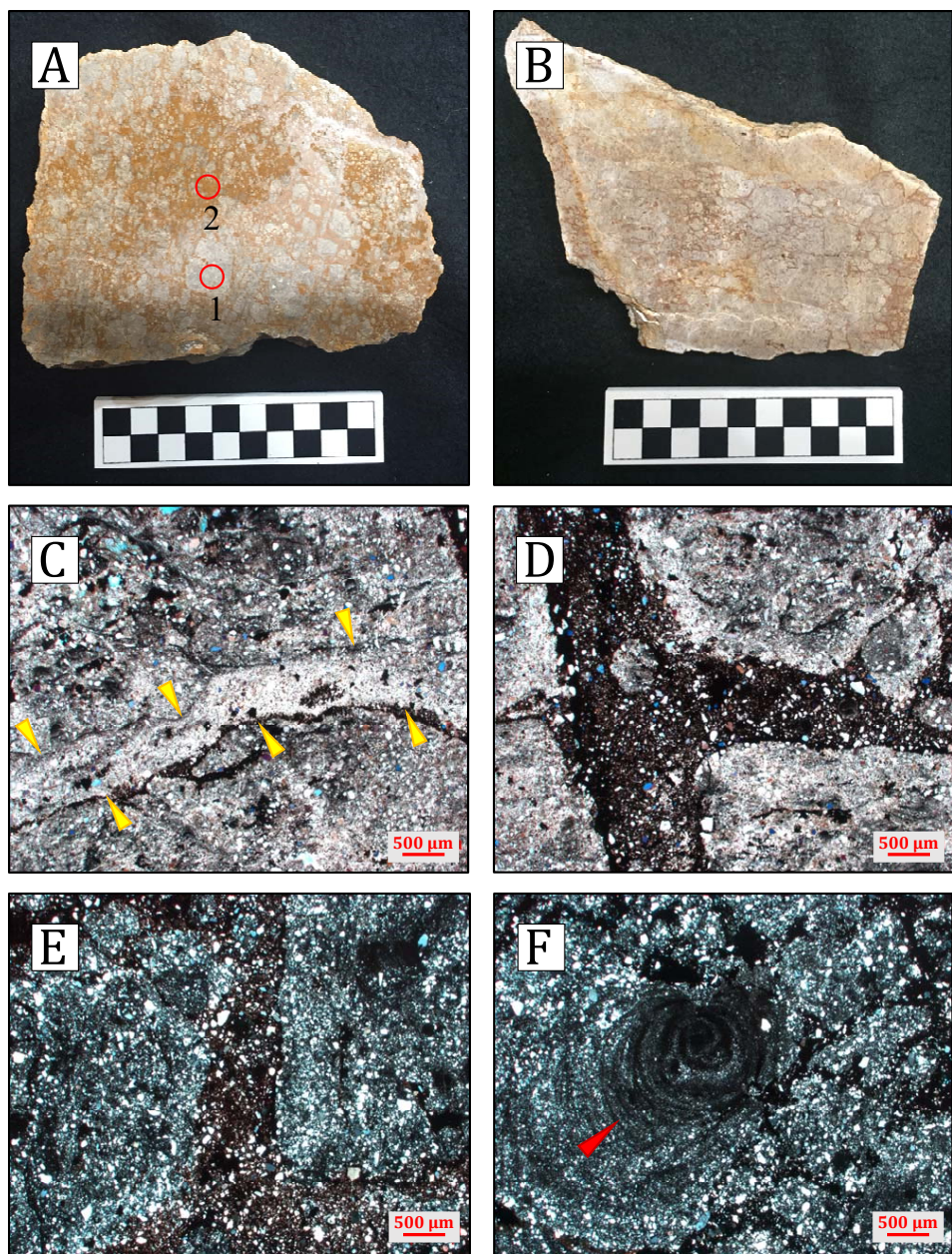


Figure 21. Two different silcrete hand samples (A and B) from a 20-cm thick silcrete layer that is exposed 0.85 km west of quarry 2. The layer is stratigraphically 23 m above the Swift Formation (figure 10 column E). Samples (A) and (B) show the angular and sub-angular blocky microstructures, resulting in ped blocks and nodules ranging up to 20 mm. Sample A shows the two sites (red circles labeled 1 and 2) where XRF analyses were performed. (C) A microstructure that has been annealed with light-grained sediments (border outlined by yellow arrows, sample A). (D) A microstructure that has been filled with dark organic sediments (sample A). (E) An additional microstructure filled with dark organic sediments (crossed Nichols; sample A). In the examples, the edges of the ped blocks can clearly be observed. (F) The swirl pattern (red arrow) is interpreted to be the initial stages of a concentric nodule (crossed Nichols; sample B). These concentric nodules were observed in both thin sections. The microstructures with the blocky peds and the concentric nodules of the silcrete indicate several prolonged dry periods followed by wet intervals.

Blocky microstructures often form by contraction from sediment desiccation (Stoops and others, 2010). Vertisols repeatedly crack and swell in response to desiccation and precipitation with successive wet and dry cycles, gradually and progressively reducing the size of the peds from blocky to platy (Kovoda and Mermut, 2010). The width of the microstructures implies long dry periods. However, the large size of the ped blocks indicates that dry/wet cycles were few. The light and dark microstructures (figures 21C, 21D, and 21E) suggest multiple dry cycles followed by cementation. The light microstructure (figure 21C) is likely from the re-

mobilization of quartz from the sandstone. In contrast, the dark microstructure is a subsequent dry/cementation cycle infilled with a high percentage of organic matter (Kovoda and Mermut, 2010). Concentric nodules are common in vertisols and suggest a moist climatic regime with seasonal wet/dry cycles (Kovoda and Mermut, 2010), but the conditions were insufficiently long for the concretion to form fully.

The central Montana Morrison silcrete indicates a minimum of several prolonged dry periods followed by wet intervals. The thinned bedded, fine-grained quartz arenite is interpreted to be a crevasse splay bed. Inor-

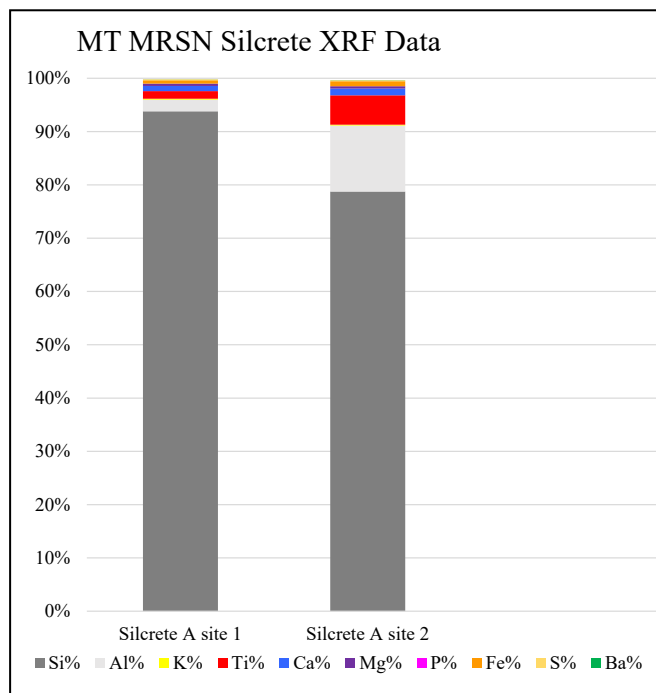


Figure 22. X-ray fluorescence (XRF) analyses of the silcrete. Site 1 (figure 21A) XRF analysis of a ped block, whereas site 2 (figure 21A) was of the moderate reddish-orange microstructure matrix. Both sites display high percentages of silica, aluminum, and titanium. Metal oxides, aluminum, and titanium are common where the climate is warm and wet. Element abbreviations are as follows: silica (Si), aluminum (Al), potassium (K), titanium (Ti), calcium (Ca), magnesium (Mg), iron (Fe), sulfur (S), and barium (Ba).

porated into the upper phreatic zone, it and any overlying soil cracked from a prolonged dry period. Some microstructures were cemented during a subsequent wet interval with the white quartz. A subsequent dry period again produced sand cracks that were infilled with a dark organic, mineral-rich matrix. The matrix chemistry indicates an abundance of vegetation that grew in a typically warm, mesic climate. The formation of the silcrete exhibits a complicated climate record marked by an overall dry period (column E on figure 19).

### Quarry 2 Mudstone and Sandstone Bed Sequence

The stratigraphic sequence at Quarry 2 records a depositional facies transition from a humic pond to a fluvial floodplain capped by distal crevasse splay beds

(figure 23). The lowest exposed bed of the sequence is an indurated yellowish-brown illitic mudstone bed (figure 23, bed A). The subsequent stratum is a 15-cm-thick, reddish illitic mudstone bed (figure 23, bed B). The bonebed is located at the base of a 70-cm-thick, gray illitic mudstone bed stratigraphically 47 m above the Swift Formation (figure 23, bed C). A 140-cm-thick, greenish illitic mudstone bed is overlying the bone bed (figure 23, bed D) and is capped by a 20-cm-thick sandstone bed. This sandstone is a subangular, well sorted (0.35), fine-grained (2.83  $\Phi$ ), quartz arenite (figure 23, bed E). The sandstone bed is overlain by a 20-cm-thick mudstone bed and is capped by numerous stacked, thin-bedded (< 5 cm) sandstone beds totaling 70 cm thick. The sandstones are subangular, moderately sorted (0.50), fine-grained (2.98  $\Phi$ ) quartz arenites.

The XRF analysis of the lowest mudstone bed recorded a high concentration of molybdenum (144 ppm) (figures 12C, column 5E SE-BA). The average background molybdenum concentration for Morrison mudstone beds is 8 ppm. In terrestrial environments, molybdenum is typically enriched in humic or dystrophic lake or pond environments filled with decaying organic material. The overlying reddish mudstone bed likely represents well-drained sediments of the desiccated or infilled underlying humic pond. The overlying gray dinosaur-yielding mudstone bed is interpreted to represent the reoccurrence of the pond. No microvertebrate or invertebrate fauna were found in the bed. Only a few charophyte gyrogonites (*Aclistochara*), freshwater diatoms, and algae (unidentified calcispheres) were recovered (Styles, 2014). Clumped oxygen isotope analysis of the quarry mudstone yielded a paleotemperature of 44° C. The greenish mudstone records the transition to a floodplain depositional facies. The 20-cm-thick sandstone bed represents an isolated distal crevasse splay. Numerous thin (< 5 cm) distal crevasse splay sandstone beds cover the intercalated mudstone bed. Often preserved atop the sandstone beds are very thin laminae (< 1 cm) of banded microbialites formed by cyanobacteria (figure 4H). The sedimentary succession indicates a variable paleoclimate with an overall trend of high precipitation exceeding evaporation with elevated temperatures (Richmond and Murphy, 2020; column F on figure 19).

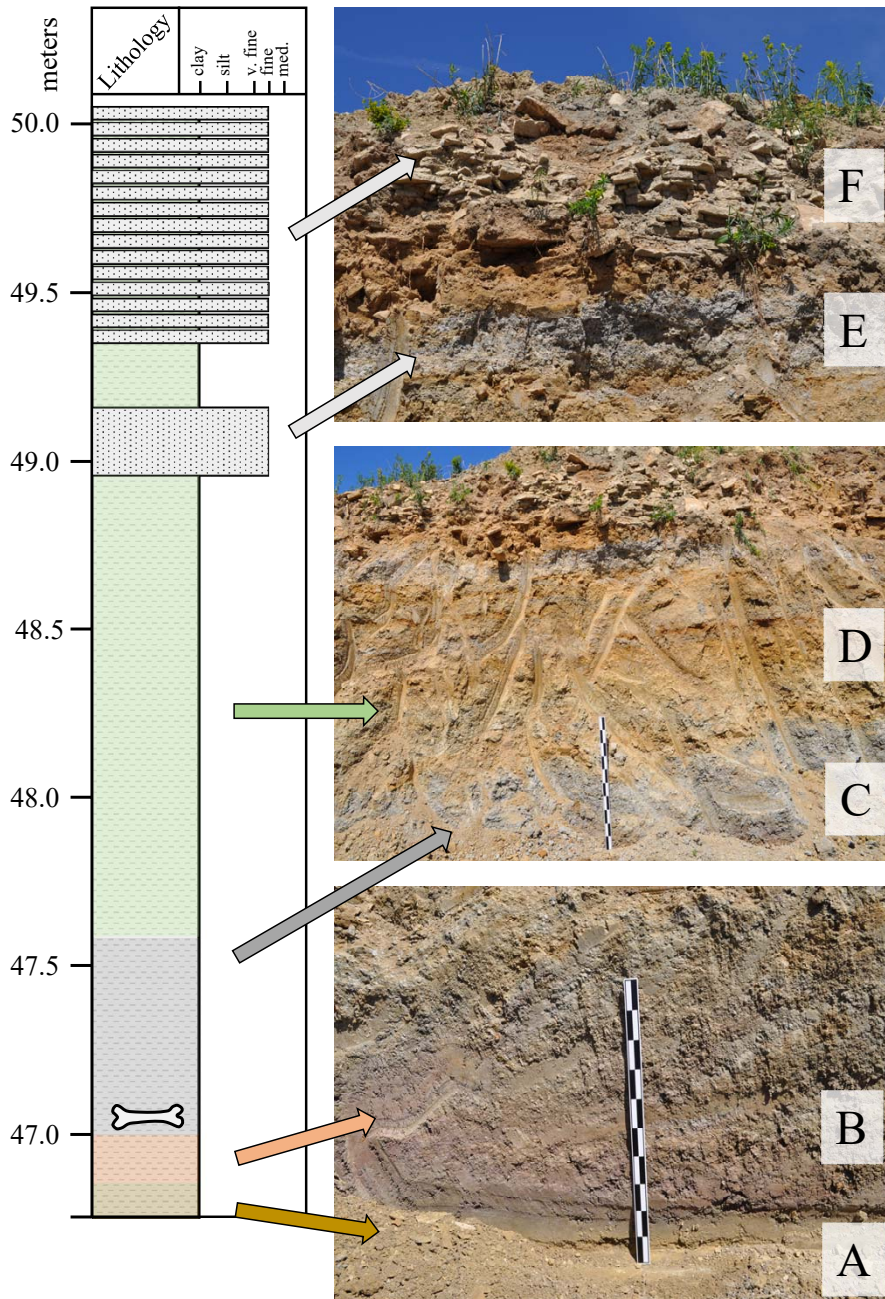


Figure 23. The stratigraphic sequence at Quarry 2 records a depositional facies transition from a humic pond to a fluvial floodplain capped by distal crevasse splay beds. Mudstone bed A represents a humic pond with high concentrations of molybdenum (144 ppm). Mudstone bed B is a 15-cm-thick bed. The bed records the transition from the humic pond to well-drained floodplain sediments. Mudstone bed C is the bone bed. Dinosaur bones were excavated from the base of the 70-cm-thick bed. The gray mudstone bed is interpreted to represent the reoccurrence of the pond. Clumped oxygen isotope analysis of the quarry mudstone yielded a paleotemperature of 44°C. Overlying the bone bed is a 140-cm-thick, greenish illitic mudstone bed (mudstone bed D) capped by a 20-cm-thick sandstone bed (sandstone bed E). The sandstone is a subangular, well sorted (0.35), fine-grained (2.83  $\Phi$ ) quartz arenite. Between sandstone beds E and F, there is a 20-cm-thick mudstone bed. The capping sandstone unit is comprised of numerous stacked thin sandstone beds. The sandstones are subangular, moderately sorted (0.50), fine-grained (2.98  $\Phi$ ) quartz arenites. The thin beds are interpreted to be a sequence of distal splay beds indicating repeated crevasse splay flood events. The sedimentary succession specifies a variable paleoclimate with an overall trend of high precipitation exceeding evaporation with elevated temperatures.

### Carbonate Mound Springs

One hundred and seven small carbonate buildups were discovered in the Morrison Formation of central Montana. They are interpreted to be subartesian freshwater mound springs and occur stratigraphically between 40 and 52 m above the Swift Formation (Richmond and others, 2021b). These are the first tufa mounds recorded for the Morrison Formation and are

North America's second oldest tufa deposits (Richmond and others, 2021b). The mound springs indicate long durations of groundwater discharge at the surface. The mound springs' oxygen and carbon isotopic data indicate they are ambient water-temperature tufa mounds. The  $\delta^{18}\text{O}$  data matches the expected paleolatitude of the region. The  $\delta^{13}\text{C}$  data indicates a short residence time for the groundwater in the subsurface.

Interestingly, variation in the data sets provides



additional insights into the paleoclimate. A few more negative  $\delta^{18}\text{O}$  values infer there may have been precipitation input from northern storms from the retreating Sundance sea. A cluster of more negative  $\delta^{13}\text{C}$  values also implies drier periods. This resulted in a longer subsurface residence time allowing groundwater to interact with plant carbon. The average annual temperatures most favorable to tufa formation and growth are between 5° and 15° C (Pentecost, 1991; Ibarra and others, 2014). Therefore, the mound springs' occurrences in central Montana indicate a regular high precipitation rate with cool paleotemperatures (Richmond and others, 2021b; column G on figure 19).

### **Micrite and Mudstone Beds (Upper Section)**

Southwest of Button Butte is a laterally limited outcrop of the uppermost Morrison Formation stratigraphic section. The exposed outcrop begins at 55 m above the Swift Formation and extends to the basal Kootenai Sandstone bed (72 m). The uppermost section is dominated by mudstone; however, four micrite beds are in the section's lower part. The lowest micrite bed is stratigraphically at 56.6 m, and the uppermost bed is at 60.7 m. The 20- to 50-cm-thick micritic beds are separated by 1.5 m of mudstone beds. The micrite beds indicate the presence of shallow ponds or lakes of unknown size. The intercalated mudstone and micrite beds suggest dry intervals followed by periods of increased precipitation (column H on figure 19).

### **Morrison Formation Coal Strata**

High volatile bituminous coal beds are known from the uppermost stratigraphic section of the Morrison Formation of central Montana (Daniel and others, 1992). Overlying the coal strata is the K-1 unconformity and basal Kootenai sandstone bed (Harris, 1966; Daniel and others, 1992). However, in the early days of exploration, researchers interpreted the coal beds to be part of the "Kootanie" Series, a name proposed by Dr. George M. Dawson in 1885 for the Indian tribe that had previously hunted the region (Fisher, 1908; Knowlton, 1908). Geologists of the Transcontinental Survey and the Yellowstone and Missouri River exploration party in 1860 first reported on the coal beds of central Montana

(Hayden, 1869). Fisher (1909) lists a comprehensive literature review of the pre-1909 publications. Newberry (1888) briefly mentioned "Kootanie" age (Lower Cretaceous) coals at the Falls of the Missouri River (i.e., Great Falls, Montana). Newberry (1891) later reviewed the fossil flora from the coal beds of Sand Coulee and Belt Creek, Montana, saying that coal miners had reported fern impressions in the coal. Based on the coal plant fossils and their comparison to other formations, Newberry maintained that the coal was of Lower Cretaceous age. Fontaine (1893) reviewed a small collection of plants preserved from the coals and said that the sample consisted of fossil plants from the families of Polypodiaceae, Equisetaceae, Cycadaceae, and Coniferae. Knowlton (1908) completed a more in-depth fossil plant review from the coals and added the family Ginkgoaceae to the then-known fossil plant varieties.

The first geological evaluation of the Great Falls coal was performed by Weed (1892), who measured the coal beds as more than 3 m thick and intercalated with thin shale beds. The coal beds are overlain by a prominent sandstone ledge that measures up to 15 m thick (i.e., Kootenai basal sandstone bed). Fisher (1907) erroneously placed the coal-bearing strata in the overlying Kootenai Formation and reported that the coal beds were 18 m above the base of the formation. The following year, Fisher (1908) suggested that the central Montana coal strata correlated to other coal beds to Cretaceous-aged coal strata around Montana and the Cloverly Formation of the Bighorn Basin. Fisher (1909) described the general geology of the Great Falls area, including the coal beds, whereas Calvert (1909) explained similar parameters for the Lewistown area and its coal field. Since then, several papers have further discussed the geology and economic importance of the coal (Harris, 1966, 1968; Silverman and Harris, 1966, 1967).

Although the coal's fossil plants, stratigraphy, and economic aspects have been evaluated, the depositional facies that produced the coal still needs to be sufficiently explored. Daniel and others (1992) propose that the Morrison coals formed in situ in flooded swamps composed of ginkgophytes and other plant materials. Based on the abundant layers of fusain, Daniel and others (1992) also suggested that the marshes occasionally burned and were later followed by clay-rich sediment

deposition. Although a large-scale depositional model has yet been proposed for the Morrison coal strata, the freshwater coal swamps likely formed on the prograding fluvial plain. Interestingly, the Upper Jurassic-Lower Cretaceous coal strata of the Kootenay Formation of the southern Canadian Rocky Mountains were formed by deltaic accretion of coastal marshes that developed on a prograding coastal plain (Jansa, 1972).

Coals require abundant plant growth from high precipitation, poor drainage on low gradient topography, or changes in the eustatic sea level (Parrish and others, 1982). Based on the previously described lithologic proxies, the Morrison coal beds were likely formed in an environment with high precipitation and/or poor drainage. The presence of abundant plants to generate greater than meter-thick coal beds indicate climatic conditions were suitable for copious plant growth for long durations. However, the presence of fusain and clay-rich interbeds suggest that unfavorable climatic conditions were sufficiently long to dry the swamps and enable fires to burn them (i.e., droughts; column I on figure 19).

## BIOLOGIC CLIMATIC PROXIES

Modern terrestrial fauna and flora are assembled by climatic zones in which they reside. The preferred climatic zone and their biological characteristics have been used repeatedly to develop paleoclimatic interpretations.

### Vertebrate Proxies

Currently, the dinosaurs discovered in the research area include *Hesperosaurus* (Saitta, 2015; Maidment and others, 2016, 2018), *Camarasaurus* (Woodruff and Foster, 2017), *?Haplocanthosaurus*, *?Camptosaurus*, *Allosaurus* (identified from shed teeth in Quarry 2), and *?Suuwassea*. Dinosaurs are suggested to have elevated metabolic rates more akin to living endotherms. Therefore, their fossil record and bone growth are not as reliable proxies for climatic changes as those of other organisms. Semiaquatic vertebrates, including crocodiles and turtles, have bone tissue that does show environmental sensitivity. Connely's (2006) unpublished report stated that fossil turtle, crocodile, and possibly amphib-

ian material was recovered from the bivalve splay mudstone bed, but this material has not been located. No additional environmentally sensitive fossil vertebrates have been reported.

## Invertebrate Proxies

### Bivalvia

A gray-green fossiliferous mudstone bed stratigraphically 19 m above the Swift Formation (column H on figure 10), is interpreted to be a flood splay deposit because of the diversity and concentration of fossil material (Richmond and others, 2017). The bed contains seven genera of bivalves, including *Unio felchi*, *U. mammillaris*, *U. nucalis*, *U. stewardi*, *U. toxonotus*, *Vetulonaia whitei*, and *V. mayoworthensis* (figure 24A). Thick- and thin-shelled ecophenotypes are represented, indicating lotic and lentic environments. Gastropods (*Viviparus* and *Tropidina*), ostracods (*Alicenula*, *Candona*, *?Cetacella*, and *Theriosynoecum*), and charophytes (*Aclistochara*, *Mesochara*, and *Porochara*) are also represented. Fish bones and piscivorous teeth were also recovered (Richmond and others, 2017).

The *Unio* and *Vetulonaia* specimens are the largest recorded sizes for the Morrison Formation (> 13 cm). This indicates a long-lived salubrious perennial clear freshwater environment. Ten shells were thin-sectioned to observe the growth bands. Thin closure lines demarcate the various growth bands. Interestingly, the observed bandwidths correlate among the specimens. This infers the community response is likely linked to environmental disruptions. Shell closure recorded by the thin bands represents short periods of adverse conditions due to turbidity from seasonal storms or eutrophication. The paleoclimate, as recorded by the bivalves, showed negligible seasonal variation but was punctuated by occasional storms (column J on figure 19).

A single thick-shelled bivalve, *V. mayoworthensis*, was found in a green-gray mudstone bed at 65.7 m. The genus is interpreted to inhabit lentic environments and was likely deposited onto the floodplain by a flood splay. The bivalve indicates the presence of a lentic freshwater body nearby (stratigraphic column I on figure 10 and column J on figure 19).

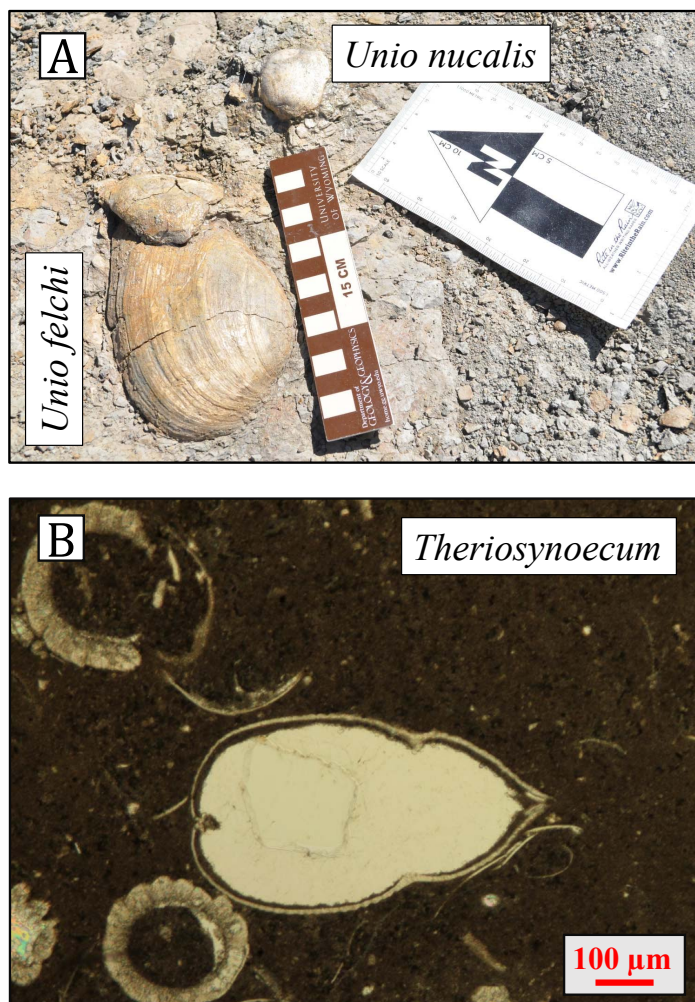


Figure 24. (A) A green illitic mudstone flood splay bed at 19 m consisting of seven genera of Jurassic freshwater bivalves, including *Unio felchi*, *U. mammillaris*, *U. nucalis*, *U. stewardi*, *U. toxonotus*, *Vetulonaia whitei*, *V. mayoworthensis*. *Unio felchi* and *U. nucalis* displayed in situ. Additionally, the bed contained gastropods (*Viviparus*, *Tropidina*), ostracods (*Alicenula*, *Candona*, *?Cetacella*, *Theriosynoecum*), and charophytes (*Aclistochara*, *Mesochara*, *Porochara*). Fish bones and piscivorous fish teeth were also recovered. The presence of the numerous invertebrate genera indicates a long-lived salubrious perennial clear freshwater environment. (B) A magnificently preserved female *Theriosynoecum* showing the anterior and posterior duplicatures from a micritic bed stratigraphically 60.5 m above the Swift Formation. The presence of the ostracod taxa indicates perennial freshwater bodies with no seasonal drying.

### Gastropoda

The fossiliferous flood splay bed at 19 m also con-

tained the prosobranch gastropod genera *Viviparus* and *Tropidina* (Richmond and others, 2017). Prosobranchs of the Morrison Formation are interpreted to have lived in perennial well-oxygenated lentic environments (Evanoff and others, 1998). Neither gastropod genera have any biostratigraphic significance for the Morrison (Evanoff and others, 1998). The depositional environment inferred from the gastropods correlates with that designated by the bivalve genera (column K on figure 19).

### Ostracoda

Ostracods are abundant in the calcareous shales and limestones of the Morrison Formation in central Montana (Peck, 1956, 1957, 1959). Unidentified ostracods are present in the lacustrine/palustrine micrite beds (Johnson-Carroll, 2014) of the paleolake at 13 m. The gray-green illitic fossiliferous bed at 19 m contains the ostracod genera *Alicenula*, *Candona*, *?Cetacella*, and *Theriosynoecum* (Richmond and others, 2017). Near Button Butte there is a 5-m exposure of four interbedded micrite and mudstone beds (column I on figure 10). The micrite beds vary from 20 to 50 cm in thickness. A limited outcrop exposure constrains an assessment of the lateral extent. The micrite and mudstone beds represent a shallow paleolake. The uppermost and thickest bed (60.5 m above the Swift Formation) is an ostracodal biomicrite with numerous separated ostracod valves and unidentified charophyte gyrogonites. Fortunately, there are also some exceptionally preserved ostracods. A magnificently preserved ostracod specimen is identified as a female *Theriosynoecum* individual showing preserved anterior and posterior duplicatures (figure 24B). *Theriosynoecum* is a representative Upper Jurassic-Lower Cretaceous genus (Horne, 2002). The ostracod taxa indicate perennial freshwater bodies with no seasonal drying indicating precipitation exceeded evaporation (B. Sames, University of Vienna, written communication, 2021) (column L on figure 19).

## Palaeobotanical Proxies

### Fossil Wood

In contrast to Brown (1946), who stated the Morrison Formation in Montana is “practically barren of plant

fossils throughout most of its sequence;” in the formation research area, fossil wood is abundant throughout the section. The majority of the fossil tracheidoxyls are found between 40 and 60 m above the Swift Formation. Fossil wood preservation varies from extremely well (Richmond and others, 2019d) to poor. To date, five fossil wood genera have been described, including *Xenoxylon* (Richmond and others, 2019d), *Piceoxylon* (Richmond and others, 2019b), *Circoporoxylon* (Richmond and others, 2019c), *Cupressinoxylon* (Richmond and others, 2021a), and *Protocedroxylon* (Richmond and others, 2022). Two wood genera (*Xenoxylon* and *Circoporoxylon*) are associated with or are encased in mound spring deposits (Richmond and others, 2021b). Ten *Xenoxylon* fossil sites have been identified (in stratigraphic order: FB PW1, RR PW1, 5E PW20, 5E PW17, 5E PW18, 5E PW21, 5E PW6, 5E SQRT, 5E PW5, and 5E WTFA; table 2) showing a current stratigraphic range for the genus that extends from approximately 17 to 51 m (column M on figure 19). The numerous discoveries indicate that *Xenoxylon* was an integral part of the Jurassic paleoforest and that the climate in central Montana was suitable for its proliferation. Five *Circoporoxylon* fossil sites have been identified (5E PW16, 5E PW14, 5E TUFA1, 5E TUFA2, and 5E PW13; table 2). The current stratigraphic range of the known *Circoporoxylon* sites is 35 to 46 m (column N on figure 19). Three *Cupressinoxylon* fossil sites have been identified (5E TUFA4, 5E PW33, and 5E CSPW; table 2). The current stratigraphic range of the known *Cupressinoxylon* sites is 46 to 53 m (column O on figure 19). One *Piceoxylon* fossil site has been identified (5E TREE1; table 2) at 25 m (column P on figure 19). One *Protocedroxylon* fossil site has been identified (5E PW4; table 2) at 46 m (column Q on figure 19). The same boreal wood genera have been reported together in the high-latitude boreal forests of the Cretaceous Period of North America (Harland and others, 2007). The Upper Jurassic fossil wood assemblage and in particular *Xenoxylon*, are suggestive of a cool/wet climate (Philippe and Thévenard, 1996; Marynowski and others, 2008; Philippe and others, 2009, 2017; Tian and others, 2016). The occurrence of these five boreal fossil wood genera designates that for the stratigraphic interval from 17 to 53 m, the climate was cool and/or wet (Richmond, 2023).

Table 2. List of currently identified fossil wood genera from the study area with each sample’s stratigraphic position within the formation measured in meters above the Swift Formation. The samples with the associated asterisks show approximate stratigraphic positions.

Sample	Assigned fossil wood genus	Stratigraphic position (m)
MRSN FB PW1	<i>Xenoxylon</i>	17.5*
MRSN RR PW1	<i>Xenoxylon</i>	17.9*
MRSN 5E PW20	<i>Xenoxylon</i>	42.5
MRSN 5E PW17	<i>Xenoxylon</i>	43.2
MRSN 5E PW18	<i>Xenoxylon</i>	43.4
MRSN 5E PW21	<i>Xenoxylon</i>	43.4
MRSN 5E PW6	<i>Xenoxylon</i>	44.1
MRSN 5E SQRT	<i>Xenoxylon</i>	45.4
MRSN 5E PW5	<i>Xenoxylon</i>	45.9
MRSN 5E WTFA	<i>Xenoxylon</i>	51.1
MRSN 5E PW 16	<i>Circoporoxylon</i>	35.0
MRSN 5E PW14	<i>Circoporoxylon</i>	44.4
MRSN 5E TUFA1	<i>Circoporoxylon</i>	45.9
MRSN 5E TUFA2	<i>Circoporoxylon</i>	45.9
MRSN 5E PW13	<i>Circoporoxylon</i>	51.6
MRSN 5E TUFA4	<i>Cupressinoxylon</i>	45.9
MRSN 5E PW 33	<i>Cupressinoxylon</i>	48.0
MRSN 5E CSPW	<i>Cupressinoxylon</i>	53.1
MRSN 5E TREE1	<i>Piceoxylon</i>	25.0
MRSN 5E PW4	<i>Protocedroxylon</i>	45.8

### Macro and Microfossil Flora

Additional Coniferales from the Morrison Formation of central Montana include *Podozamites lanceolatus* (Podocarpaceae), *Pityophyllum lindstromi* (Gnetophyta), *Pityocladus* sp. (Cycadophyta), and *Pagiophyllum* sp. (Brown, 1972). Based on palynology, the families Pinaceae and Podocarpaceae were also present (Hotton and Baghai-Riding, 2010). Subdominant understory woody plants included Cycadales (*Zamites arcticus*), Ginkgoales (*Ginkgoites marginatus*, *Ginkgoites pluripartita*), and Bennettitales (*Cycadolepis* sp., *Nilssonia compacta*, and *Weltrichia* sp.) (Brown, 1972). The groundcover in the Late Jurassic of central Montana was comprised

of fungi, the sphenophyte *Equisetum lateralis*, the pteridophytes *Hausmannia fisheri*, *Coniopteris hymenophylloides*, *Adiantites montanensis*, *Cladophlebis alberta*, *Cladophlebis heterophylla*, and *Cladophlebis virginensis*, and the pteridosperm *Sagenopteris elliptica* (Brown, 1972).

Brown (1972) reexamined previous late 19th-century fossil plant assemblages and collected additional fossil plants from several locations in central Montana. Brown's fossil specimens were from carbonaceous shales of the formation's upper strata. As mentioned, Brown (1972) identified a pteridophyte of the Dicksoniaceae tree fern family. Specimens from the Belt and Lewiston areas of Montana were described as the fern *Coniopteris hymenophylloides*. Dicksoniaceae (*Coniopteris*) first appeared in the Early Jurassic (Seward, 1900; Vakhrameyev, 1964; Wang, 2002) and is found Northern Hemisphere in the Middle Jurassic (Vakhrameyev, 1964; Vaez-Javada, 2018; Xin and others, 2018; Yuan and others, 2018; Zhang and others, 2019), Late Jurassic (Vakhrameyev, 1964; Brown, 1972; Miller, 1987; Ash and Tidwell, 1998), and Lower Cretaceous strata (LaPasha, 1982; LaPasha and Miller, 1985; Miller, 1987). *C. hymenophylloides* is the only member of the Dicksoniaceae family recognized from the Morrison Formation (Ash and Tidwell, 1998) and has only a few occurrences. In addition to the locations in central Montana (Brown, 1972; Miller, 1987), it is also known from the Montezuma Creek locality in southeastern Utah (Ash and Tidwell, 1998), the Temple Park area near Cañon City, Colorado (Gorman and others, 2008), the Turtle Island plant site north of Vernal, Utah (Foster and others, 2003), and the Jurassic Sald Bar site in southeastern Utah (Foster and others, 2022, 2023). Additionally, *C. hymenophylloides* has also been described from the Lower Cretaceous Kootenai Formation of central Montana (LaPasha, 1982; LaPasha and Miller, 1985; Miller, 1987).

The sterile and fertile pinna of *C. hymenophylloides* (figure 25A) (E. Kustatscher, Museum of Nature South Tyrol, written communication, 2021) were recently discovered in a thin carbonaceous shale bed stratigraphically at 38 m in the study area. Foster and others (2023) differentiate between the fertile and sterile pinna, classifying the fertile pinna as *Coniopteris* and the sterile pinna as *Sphenopteris*.

*Coniopteris* is interpreted to be a small to large rhizomatous fern that grew in mesic environments (Deng, 2002). Numerous researchers propose that the paleoecology of the *Coniopteris* signifies a warm and mesic paleoenvironment (Wang, 2002; Vaez-Javada, 2018; Xin and others, 2018; Zhang and others, 2019) (column R on figure 19).

An unidentified pteridophyte was discovered in the same shale bed (figure 25B). Most fern diversity is encountered in mesic and warm environments. An unidentified ginkgophyte was also discovered in the same shale bed (figure 25C). Extant ginkgophytes prefer mesic environments but can tolerate a wide range of soil moistures and temperatures.

### Palynology

The majority of palynological data for the Morrison Formation comes from Utah, Colorado, Arizona, and New Mexico (Tschudy and others, 1980, 1988; Hotton, 1986; Litwin and others, 1998; Baghai-Riding and Hotton, 2009, 2011; Baghai-Riding and others, 2013, 2014, 2015, 2018; Hotton and Baghai-Riding, 2010, 2016). In addition, limited sampling has been done in the more northern parts of the Morrison basin in Wyoming and Montana (Newman, 1972; Litwin and others, 1998; Baghai-Riding and Hotton, 2009, 2011; Hotton and Baghai-Riding 2010; Baghai-Riding and others, 2015). For an overview of the palynology of the Morrison Formation, refer to Litwin and others (1998) and Hotton and Baghai-Riding (2010).

Palynological studies of the Canadian Upper Jurassic Kootenay Formation are interpreted as the northern equivalent of the Morrison Formation in south-central Canada. The formation has numerous coal seams, and these were investigated for pollen in the 20<sup>th</sup> century by Berry (1929), Bell (1956), and Rouse (1959). Newman (1972) was the first to review the palynology of the Morrison Formation in Montana and only sampled one Morrison site. The majority of Newman's paper discussed Cretaceous and Paleogene palynology. Four palynology samples are from a carbonaceous shale bed, 3 m stratigraphically below the Kootenai basal sandstone bed, 0.5 km south of Belt, Montana (Stop 6 of the 1966 Billings Geological Society 17<sup>th</sup> annual field conference,

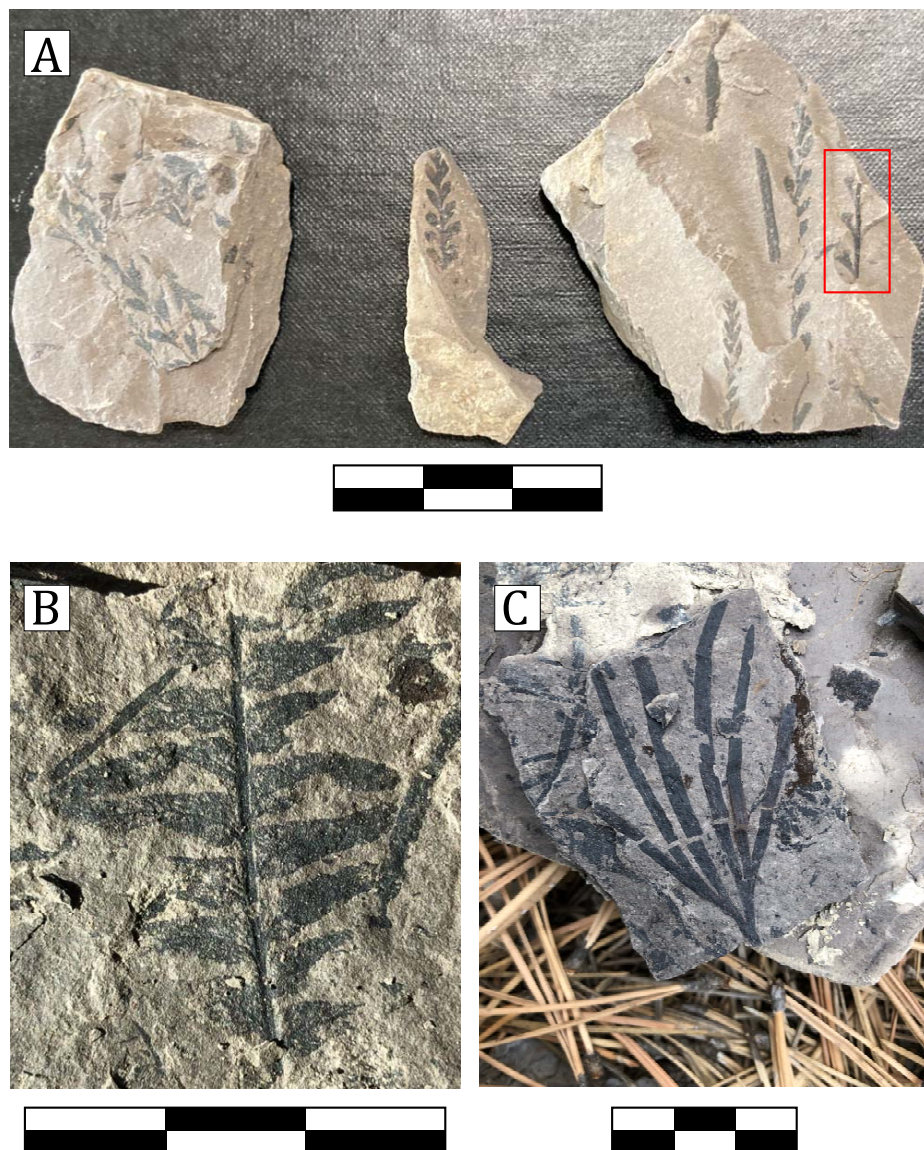


Figure 25. A carbonaceous shale stratigraphically at 38 m above the Swift Formation has compressed plant fossils. A preliminary investigation has yielded the pteridophyte *Coniopteris hymenophylloides*. (A) Photograph of shale fragments that displays both the sterile and fertile pinna (red box) of *C. hymenophylloides*. (B) Photograph displaying an unidentified pteridophyte. (C) Photograph displaying an unidentified ginkgophyte. The pteridophytes and the ginkgophyte suggest a mesic and warm environment. Scale bars are each 3 cm.

p. 36; Newman, 1972). Newman only mentioned four palynological genera: *Callialasporites dampieri*, *Eucommiidites*, *Classopollis*, and *Inapertisporites pseudoreticulatis*. Newman specified that *Eucommiidites* were prevalent and that *Classopollis* were infrequent (table 3).

Litwin and others (1998) sampled the formation west of the Yellowstone River south of Livingston, Montana (samples R4684A, B) and along the eastern flank of Shell Mountain along the West Boulder Road southeast of Livingston (samples R4690A, C, E). Only data from samples R4690A, C, and E were published; however, no stratigraphic information was provided (table 3). Hotton and Baghai-Riding (2010) processed a

sample collected near Belt, Montana; however, they did not publish the data. In the study area, a limited palynological sample was procured from a carbonaceous shale bed stratigraphically 38 m above the Swift Formation (table 3). The mudstone sediments yielded several fossil pollen and spores (table 3). Several carbonaceous shales were also sampled but did not yield viable material, but each contained an abundance of fusain. The Morrison coals from the Five Fingers coal mine near Sand Coulee, Montana were also sampled. Palynomorph recovery was poor due to maceral debris and the degradation of the pollen. Some pollen were tentatively identified to the family and genus level including ?Araucariaceae,

Table 3. Summary of the palynological samples from the Morrison Formation of Montana. The table provides the taxonomical identification, the stratigraphic position above the Swift Formation, and the pollen's preferred moisture and temperature.

Reference	Class	Order	Family	Genus	Species	Position	Moisture	Temperature
Newman, 1972	Pinopsida	Araucariales	Araucariaceae	<i>Callialasporites</i>	<i>dampieri</i>	69 m	wet to mesic	megathermic
	Pinopsida	Cheirolepidiales	Cheirolepidiaceae	<i>Classopollis</i>	sp.	"	dry	megathermic
	Gnetopsida	Erdtmanithecales	Erdtmanithecaeae	<i>Eucommiidites</i>	sp.	"	wet to mesic	eurythermic
	unknown	unknown	unknown	<i>Inapertisporites</i>	<i>pseudoreticulatis</i>	"	Unknown	unknown
Litwin and others, 1998	Pinopsida	Pinales	Podocarpaceae	<i>Pristinuspollenites</i>	<i>microsaccus</i>	Unknown	mesic	megathermic
	Pinopsida	Pinales	Podocarpaceae	<i>Parvisaccites</i>	sp.	"	wet to mesic	megathermic
	Pinopsida	Pinales	Pinaceae	<i>Pityosporites</i>	sp.	"	wet to mesic	mesothermic
	Pinopsida	Pinales	?Pinaceae	<i>Rugubivesiculites</i>	sp.	"	unknown	unknown
	Ginkgoopsida	Caytoniales	Caytoniaceae	<i>Vitreisporites</i>	<i>pallidus</i>	"	wet to mesic	megathermic
	Polypodiopsida	Cyatheaales	Cyatheaaceae	<i>Cyathidites</i>	<i>concausus</i>	"	wet (locally)	eurythermic
	Polypodiopsida	Schizaeales	Schizaeaceae	<i>Concavissimisporites</i>	<i>montuosus</i>	"	wet (locally)	megathermic
	Polypodiopsida	Schizaeales	Schizaeaceae	<i>Concavissimisporites</i>	<i>irroratus</i>	"	wet (locally)	megathermic
	Polypodiopsida	Schizaeales	Anemiaceae	<i>Cicatricosporites</i>	sp.	"	wet (locally)	megathermic
	Polypodiopsida	Osmundales	Osmundaceae	<i>Todisporites</i>	<i>minor</i>	"	wet (locally)	mesothermic
	Polypodiopsida	unknown	unknown	<i>Granulatisporites</i>	<i>dailyi</i>	"	unknown	unknown
	Polypodiopsida	unknown	unknown	<i>Ischyosporites</i>	<i>disjunctus</i>	"	wet (locally)	unknown
	Lycopsida	unknown	Selaginellaceae	<i>Neoraistrickia</i>	sp.	"	wet (locally)	eurythermic
Sphagnopsida	Sphagnales	Sphagnaceae	<i>Stereisporites</i>	sp.	"	wet (locally)	eurythermic	
?Marchantiopsida	unknown	unknown	? <i>Hymenozonotriletes</i>	mesozoicus	"	unknown	unknown	
Present study	Pinopsida	Pinales	Pinaceae	<i>Alisporites</i>	<i>bilateralis</i>	38 m	mesic	eurythermic
	Pinopsida	Cheirolepidiales	Cheirolepidiaceae	<i>Classopollis</i>	sp.	"	dry	megathermic
	Gnetopsida	Erdtmanithecales	Erdtmanithecaeae	<i>Eucommiidites</i>	<i>troedssonii</i>	"	wet to mesic	eurythermic
	Polypodiopsida	Gleicheniales	Dipteridaceae	<i>Dictyophyllidites</i>	sp.	"	wet to subarid	megathermic
unknown	unknown	unknown	<i>Cycadopites</i>	<i>fragilis</i>	"	wide range	eurythermic	

?Osmundaceae, ?*Dictyophyllidites*, ?*Gleicheniidites*, ?*Ischyosporites*, and *Cycadopites* (Hotton, National Museum of Natural History, written communication, 2022).

**Gymnospermae:** *Callialasporites dampieri* (Pinopsida/Araucariales/Araucariaceae). *Callialasporites dampieri* is a conifer pollen with affinities to either Araucariaceae or Podocarpaceae. However, a review of the ultrastructure of the exine designates the pollen genus as Araucariaceae (Batten and Dutta, 1997; Schrank, 2010). *Callialasporites* are present in the Salt Wash and Brushy Basin Members of the Morrison Formation in Utah (Tschudy and others, 1980, 1988; Hotton, 1986). The ecological range of modern Araucaria extends from rainforests to cool temperate forests. Extant Araucaria are generally hygrophytes and megathermic trees (Schrank, 2010; Zhang, 2022).

*Pristinuspollenites microsaccus* (Pinopsida/Pinales/Podocarpaceae). The genus is often found with *Alisporites* and other mesic pollens. Extant Podocarpaceae are common to the Southern Hemisphere in tropical-subtropical climates and mountains, and are generally hygrophytes and megathermic trees (Zhang, 2022).

*Parvisaccites* sp. (Pinopsida/Pinales/Podocarpaceae). Extant Podocarpaceae are common to the Southern Hemisphere in tropical-subtropical climates and mountains, and are generally hygrophytes and megathermic trees (Zhang, 2022).

*Alisporites bilateralis* (Pinopsida/Pinales/Pinaceae; figure 26A). The genus is also present in the Kootenay Formation of British Columbia, Canada (Rouse, 1959). Extant Pinaceae are generally mesophytes and microthermal plants that grow in acidic, wet, or rocky habitats in northern temperate zones (Zhang, 2022).

*Pityosporites* sp. (Pinopsida/Pinales/Pinaceae). The genus is considered a bisaccate gymnosperm pollen with no known affinities (Ludvigson and others, 2010; Zhang, 2022). However, Hotton (National Museum of Natural History, written communication, 2022) believes that the genus is synonymous with *Alisporites*.

*Rugubivesiculites* sp. (Pinopsida/?Pinales/?Podocarpaceae). *Rugubivesiculites* is a bisaccate gymnosperm pollen with uncertain affinities (Falcon-Lang and others, 2003). Extant Podocarpaceae are common to the Southern Hemisphere in tropical-subtropical climates and mountains, and are generally hygrophytes and

megathermic trees (Zhang, 2022).

*Classopollis* sp. (Pinopsida/Cheirolepidiales/Cheirolepidiaceae; figure 26C). *Classopollis* is a dominant group of conifers during the Mesozoic (Kürschner and others, 2013). The genus was not found in the Salt Wash or Brushy Basin Members of the Morrison Formation in Utah (Tschudy and others, 1980, 1988); however, the Morrison Formation of Arizona and New Mexico is dominated by *Classopollis* (Hotton, 1986). Cheirolepidiaceae are drought-resistant xerophytes (Vakhrameyev, 1982; Zhang, 2022).

*Eucommiidites troedssonii* (Gnetopsida/Erdtmanithecales/Erdtmanitheceae; figure 26B). This pollen mimics angiosperm pollen, although a recent review of the exine ultrastructure assigned this pollen to the Family Erdtmanitheceae in the Order Erdtmanithecales (Tekleva and others, 2006). *Eucommiidites* are present in the Salt Wash and Brushy Basin Members of the Morrison Formation in Utah (Tschudy and others, 1980, 1988). Erdtmanitheceae are considered xerophytes and eurythermic plants (Zhang, 2022).

*Vitreisporites pallidus* (Ginkgoopsida/Caytoniales/Caytoniaceae). Caytoniaceae is an extinct cosmopolitan seed fern family of small trees. Caytoniaceae fossils are found in deltaic and floodplain environments in subtropical regions suggesting they were hygrophytes and megathermic trees (Zhang, 2022).

**Cycadophyta:** *Cycadopites fragilis* (Bennettitales, Ginkgoales, or Cycadales; figure 26D). Extant cycads are generally in tropical and subtropical zones occurring in the rainforest and open woodland habitats. They are mesophytic, megathermic plants (Zhang, 2022).

**Pteridophyta:** *Cicatricosisporites* sp. (Polypodiopsida/Schizaeales/Anemiaceae). The genus is found elsewhere in the Morrison Formation (Chure and others, 2006) and the Lourinhã Formation of Portugal (Mateus, 2006). Extant Anemiaceae mostly live in subtropical to tropical regions and are considered mesophytes and megathermic plants (Zhang, 2022).

*Concavissimisporites montuosus* and *C. irroratus* (Polypodiopsida/Schizaeales/Lygodiaceae). The genus is also present in both the Salt Wash and Brushy Basin Members of the Morrison Formation in Utah (Tschudy and others, 1980, 1988), the Upper Jurassic Lourinhã



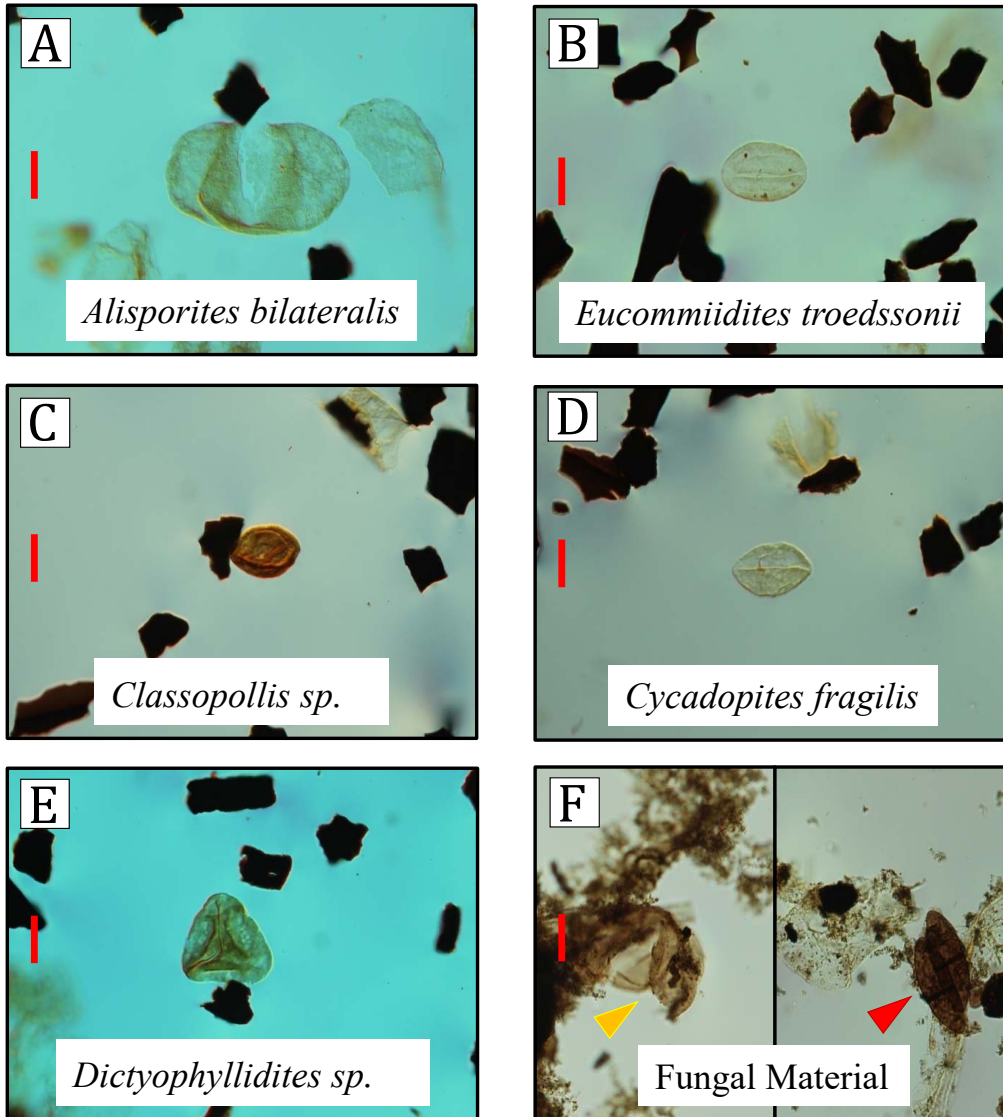


Figure 26. Photomicrographs of the pollen and spores were recovered from a mudstone bed (section F) at 38 m above the Swift Formation. (A) *Alisporites bilateralis* (Pinaceae). Extant Pinaceae prefer moist and cool environments. (B) *Eucommiidites troedssonii* (Erdtmanitheceae). The family is considered to favor drier environments with a wide range of temperatures. (C) *Classopollis* (Cheirolepidiaceae). Cheirolepidiaceae also favor drier environments and are drought-resistant xerophytes. (D) *Cycadopites fragilis* has uncertain cycad affinities. Extant cycads prefer mesic and warm environments. (E) *Dictyophyllidites* sp. (Dipteridaceae.) Extant Dipteridaceae prefers mesic and warm environments. (F) Unidentified fungal body (yellow arrow – 19 m above the Swift Formation) and spores (red arrow – 55 m above the Swift Formation). Fungal spores require moisture to grow and prefer warm environments. Red bars are 20  $\mu$ m for all samples.

Formation of Portugal (Mateus, 2006), and the Lower Cretaceous Yellow Cat Member of the Cedar Mountain Formation in Utah (Joeckel and others, 2019). Extent Lygodiaceae are hygrophytes and megathermic plants (Zhang, 2022).

*Cyathidites concavus* (Polypodiopsida/Cyatheaales/Cyatheaaceae). The genus is present in both the Salt Wash and Brushy Basin Members of the Morrison Formation in Utah (Tschudy and others, 1980, 1988). Extant Cyatheaaceae are tropical tree ferns that generally grow in the undergrowth of moist forests and are considered hygrophytes and megathermic ferns.

*Dictyophyllidites* sp. (Polypodiopsida/Gleicheniales/Dipteridaceae; figure 26E). Dipteridaceae are commonly known as umbrella ferns. Extant species are found

in tropical and warm-temperate regions from Asia to Australia, implying they are hygrophytes and megathermic plants.

*Todisporites minor* (Polypodiopsida/Osmundales/Osmundaceae). The genus is also present in the Salt Wash and Brushy Basin Members of the Morrison Formation in Utah (Tschudy and others, 1980, 1988). Extent Osmundaceae are mesophytic plants generally found in tropical climatic zones (Tryon and Tryon, 1982), implying they are hygrophytes and megathermic plants.

*Granulatisporites dailyi* (Polypodiopsida/uncertain pteridophyte, Ludvigson and others, 2010; Zhang, 2022).

*Inapertisporites pseudoreticulatus* (Polypodiopsida/uncertain pteridophyte, Chure and others, 2006; Lud-

vigson and others, 2010). The genus is also known from the Kootenay Formation of southeastern British Columbia, Canada (Rouse, 1959) and the Lourinhã Formation of Portugal (Mateus, 2006). Hotton (National Museum of Natural History, written communication, 2022) believes that the genus may be a “wastebasket” category for fungal, algal, or bryophytic taxa.

?*Gleicheniidites* (Polypodiopsida/Gleicheniales/Gleicheniaceae).

?*Ischyosporites* (uncertain Pteridophyta).

*Neoraistrickia* sp. (Lycopsida/Selaginellales/Selaginellaceae). *Neoraistrickia*, a lycopsid, is an herbaceous vascular plant related to the club mosses. Extant Selaginellaceae are considered euryphytes and eurythermic plants (Zhang, 2022).

**Bryophyta:** *Stereisporites* sp. (Sphagnopsida/Sphagnales/Sphagnaceae). Extant sphagnum mosses are cosmopolitan and are commonly found in wetlands. They are considered hydrophytes and eurythermic plants (Zhang, 2022).

The Morrison Formation palynology has thus far yielded several samples, but in those samples is recorded a diverse flora including seven gymnosperm families, one cycad, five pteridophyte families, and a single bryophyte family. The paleoenvironmental interpretation derived for the more mobile gymnosperm pollen shows a xeric preference, whereas the locally disseminated pteridophyte spores exhibit wet conditions (column S on figure 19). Most of the pteridophytes were identified in Litwin and others' (1998) samples, but no stratigraphic position was provided. Their sample implies the Morrison Formation in central Montana was, at one time, wet and warm. The upper stratigraphic samples (Newman, 1972; present study) signify that the climate of the upper section may have been more temperate.

**Fungi:** Unidentified fungal bodies and spores were found in the mudstones from 14 and 55 m stratigraphically above the Swift Formation (figure 10, columns H and F, respectively). Fungal spores require moisture to grow and prefer warm environments.

Uncertain Affinity: ?*Hymenozonotriletes mesozoicus* (?Marchantiopsida). No information can be provided for this Litwin and others (1998) specimen since no known affinities exist.

## Charophyta

Modern charophytes live in clear lentic oligotrophic freshwater environments. Charophytes in Morrison Formation limestone beds indicate standing water (Turner and Fishman, 1991). Charophytes are abundant in the calcareous shales and limestones of the central Montana Morrison (Peck, 1956, 1957, 1959). The most common and distinctive gyrogonites of the Morrison are *Latochara latitruncata* and *Aclistochara bransoni* (Peck, 1956). The Morrison biozones of *L. latitruncata* are 1 through 5, whereas the biozones *A. bransoni* are 1 through 4 (Schudack and others, 1998).

Charophyte gyrogonites of *Aclistochara latisulcata* are present in the micritic limestone beds (14.5 to 16.5 m). The micrite beds are interpreted to represent a small paleolake and wetland. In flood-splay mudstone beds (19 m), the charophyte genera *Aclistochara*, *Mesochara*, and *Porochara* have been reported (Richmond and others, 2017). The charophyte gyrogonites *P. minima* assign the bed to biozone 3. Based on the bivalve genera, the source of the splay bed was both lotic and lentic aquatic environments (Richmond and others, 2017). The Quarry 2 mudstone bone bed (47 m) yielded charophyte gyrogonites of the genus *Aclistochara complanata*, *Aclistochara latisulcata* (biozones 3 through 4), and *Mesochara voluta* (biozones 1 through 4) (Styles, 2014). Charophyte gyrogonites support the sedimentological and geochemical interpretation of a waterhole at the quarry (Richmond and Murphy, 2020). Charophyte gyrogonites of *Aclistochara latisulcata* are also present in the micritic limestone beds (60.5 m). The micrite beds are interpreted to represent a small paleolake, but the lateral extent of the beds is still being determined due to the lack of additional exposures. The presence of charophytes in these strata indicates a perennial water source and therefore an interval where precipitation is greater than evaporation (column T on figure 19).

## Algal and Cyanobacterial Buildups

An organic fabric was discovered in mound spring CM 13 (45 m above the Swift Formation) that may be the tufa-associated green algae *Oocardium stratum* Nägeli (see Richmond and others, 2021b, figure 7D). Tufas generally occur in regions with an annual rainfall

of over 500 mm/year (Pentecost, 1991; Ibarra and others, 2014). Tufas with associated *Oocardium* commonly have rainfall that exceeds 1000 mm/year (Ibarra and others, 2014; Richmond and others, 2021b). The presence of fossil *Oocardium* specifies a high rainfall during the deposition of this mound spring.

Additionally, banded cyanobacterial microbialite buildups were fortuitously discovered in thin section on the upper surfaces of the thin (5 cm) sandstone splay beds (50 m) capping the Quarry 2 pluvial/fluvial sequence (see figure 23, bed F). The banded buildups atop the sandstone beds indicate both a high-water table and the repeated reflooding of the distal crevasse splay beds (figure 4H). Cyanobacterial buildups are also found on dogtooth calcite crystals growing on the spring mounds (see Richmond and others, 2021b, figure 9A).

Carbonate spherulites, present in some of the spring mounds (48 to 50 m), were formed by a Jurassic variant of the betaproteobacteria *Ralstonia eutropha* H16 (see Richmond and others, 2021b, figures 9B and 9C). Cyanobacteria and *Ralstonia eutropha* H16 can grow over a wide temperature range. However, optimal growth occurs at warm temperatures (29 to 30° C; Lüring and others, 2013; Nowroth and others, 2016) (column U on figure 19).

## CONCLUSIONS

The Upper Jurassic Morrison Formation in central Montana had yet to be sufficiently studied. The historical stratigraphic measurements of the formation vary greatly. Recent field measurements in central Montana indicate the formation is 72 m thick. A review of well-log data over central Montana shows that formation does display variation, but the average thickness over the region is 71 m. The thickest part of the formation is in northeastern Wheatland County, suggesting a distributive fluvial system migrating from the southwest. There is no discernable well-log marker across the region nor consistent change in lithology to warrant a division of the formation into members. Although there is no distinguishable break in the formation to separate it into members, the lower mudstone interval is interpreted as the distal floodplain facies. The upper depositional facies marks a transition to a mudstone-dominated, anas-

tomosing fluvial depositional facies. The fluvial facies consist of small, isolated, fine-grained anastomosing channel beds, and thin crevasse and flood splay beds.

Based on climate models and lithologic proxies, many researchers have proposed the Morrison foreland basin experienced a semiarid to arid zonal climate. Climate proxies provide an interpretation over a short climate window; however, a comprehensive proxy assemblage compiled over a stratigraphic range and confined to a specific region delivers a full view of the climatic past. The retreat of the Sundance seaway and its proximity to the northern part of the Morrison foreland

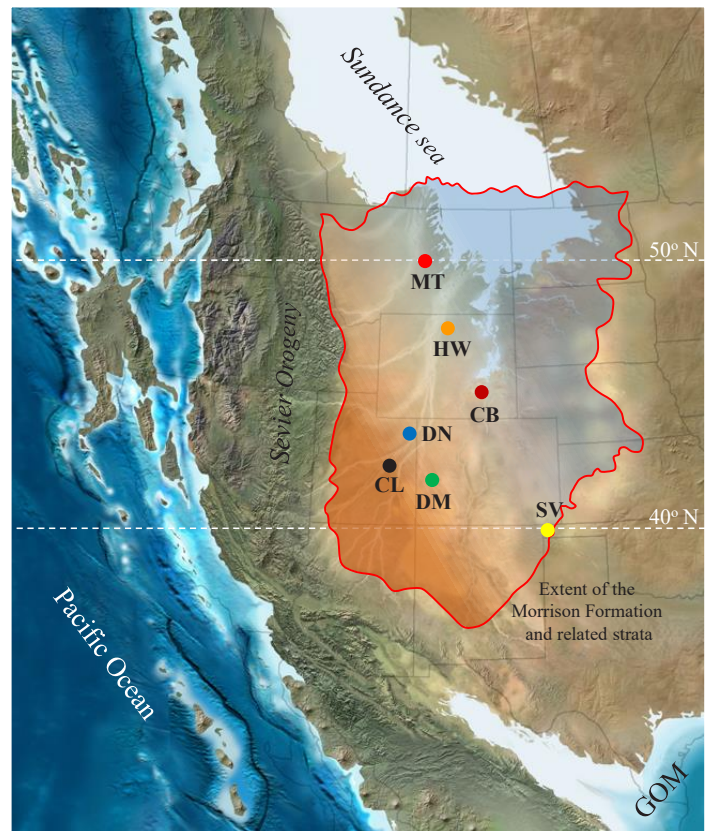


Figure 27. A modified paleogeography map of the Upper Jurassic of western North America. The dots represent well-known dinosaur quarries (MT–Montana quarries; HW–Howe quarries; CB–Como Bluff quarries; DN–Dinosaur National Monument quarry; CL–Cleveland-Lloyd quarry; DM–Dry Mesa quarry; and SV–Stovall quarries). Overlain on the Morrison foreland basin is an interpreted climatic map with the warm coloration representing a warmer and drier region and the cool coloration designating cooler and wetter areas. GOM–Gulf of Mexico. Source map © 2016 Colorado Plateau Geosystems Inc.

basin had a dramatic effect on the paleoclimate of the region. The compilation of lithologic, faunal, and floral proxies from the northern part of the basin recorded in sediments in central Montana demonstrates the climate in this region was wetter than in more southern parts of the Morrison foreland basin (figure 27). Based on the numerous climatic proxies, environmental conditions were not static but indicate that the Late Jurassic of central Montana experienced an overall subtropical humid/dry climate with intervals of temperate oceanic climate.

## ACKNOWLEDGMENTS

I am grateful to the Hein, Klakken, and Finkbinder families, who provided access to their ranches for a field review of the geology. With their permission and support, this research was accomplished. I especially thank David Hein of Billings, Montana, for his passion for this research and his assistance in many aspects of the research. I am grateful to Nate Murphy, who started me on this project and assisted in providing support and discussion. I appreciate Bethany Schatzke's (Rocky Mountain College, Billings, Montana) tireless efforts in finding research papers. For this project, TGS-NOPEC Geophysical Company donated access to the digital and raster well logs for Fergus County, Montana, and surrounding areas. A special acknowledgment is due to Harry Rowe, who completed the geochemical analysis of the mudstones and sandstones at the Bureau of Economic Geology at the University of Texas, Austin. I appreciate Katherine Huntington and Keith Hudson (University of Washington, Seattle) for performing the clumped isotope analysis. Richard Lupia (University of Oklahoma) and Carol Hotton (National Museum of Natural History) freely assisted with the paleobotany. Benjamin Sames (University of Vienna, Austria) aided with the identification of invertebrates. Quintin Carlson assisted with the GIS data in mapping the Morrison Formation. Jim Shaffer, Mitch Lukens, Serena Celestino, Linda Freeman, Deana and Michael Richmond assisted with the surveying and the stratigraphic measurements. And finally, I am grateful for all the field collectors who took their time to dig and study dinosaurs in Montana. As is often the case with a large project with such a

broad scope, many unmentioned contributed their time and talents in helping to accomplish this work. Kenneth Carpenter, University of Colorado Museum, Boulder, Colorado, and Thomas Chidsey, Utah Geological Survey Emeritus, and John Foster, Utah Field House of Natural History State Park Museum, carefully reviewed and significantly improved the manuscript. I am very grateful for Doug Sprinkel, Utah Geological Survey Emeritus, for his editing efforts and the time devoted to its publication.

## REFERENCES

- Ames, V., 1993, Cat Creek oil field, *in* Hunter, L.D.V., editor, Energy and mineral resources of central Montana: Montana Geological Society 1993 Field Conference Guidebook—Old Timers' Rendezvous Edition, p. 129–142.
- Ash, S.R., and Tidwell, W.D., 1998, Plant megafossils from the Brushy Basin Member of the Morrison Formation near Montezuma Creek Trading Post, southeastern Utah: *Modern Geology*, v. 22, p. 321–339.
- Baghai-Riding, N.L., and Hotton, C., 2009, Palynological evidence for conifer dominance and arid climate in the Late Jurassic Morrison Formation, U.S.A. [abs.]: *Geological Society of America Abstracts with Programs*, v. 41, no. 6, p. 40.
- Baghai-Riding, N.L., and Hotton, C., 2011, Regional climatic signals masked by local factors in the Late Jurassic Morrison palynoflora [abs.]: *Botanical Society of America Abstracts with Programs*, Abstract ID 1051.
- Baghai-Riding, N.L., Davis, K., Hotton, C., Myrow, P., and Dangles, L., 2014, Palynomorphs from the base of the Late Jurassic Morrison Formation, Colorado Springs, Colorado, U.S.A. [abs.]: *Botanical Society of America Abstracts with Programs*, Abstract ID 529.
- Baghai-Riding, N., Hotton, C., Davies, K., and Davidson, T., 2015, Palynological evidence for a latitudinal moisture gradient in the Late Jurassic Morrison Formation [abs.]: *Geological Society of America Abstracts with Programs*, v. 47, no. 7, p. 143.
- Baghai-Riding, N.L., Hotton, C., Gorman, M., and Davidson, T., 2013, A unique wetland ecosystem in the Late Jurassic Morrison Formation, U.S.A. [abs.]: *Botanical Society of America Abstracts with Programs*, Abstract ID 859.

- Baghai-Riding, N.L., Kirkland, J.I., Trujillo, K.C., Chamberlain, K.R., Hotton, C., Foster, J.R., and Hunt, R.K., 2018, Dispersed palynomorph and cuticle assemblages from the Late Jurassic Morrison Formation, southern Utah—floristic and paleoclimate implications [abs.]: Geological Society of America Abstracts with Programs, v. 50, no. 6. doi: 10.1130/abs/2018AM-322649
- Ballabio, C., Panagos, P., Lugato, E., Huang, J.-H., Orgiazzi, A., Jones, A., Fernández-Ugalde, O., Borrelli, P., and Montanarella, L., 2018, Copper distribution in European topsoils—an assessment based on LUCAS soil survey: *Science of the Total Environment*, v. 636, p. 282–298.
- Ballard, W.W., 1966, Petrology of Jurassic and Cretaceous sandstones north flank Little Belt Mountains, Montana, in Cox, J.E., editor, *Jurassic and Cretaceous stratigraphic traps—Sweetgrass Arch*: Billings Geological Society Guidebook 17th Annual Field Conference, p. 56–111.
- Batten, D.J., and Dutta R.J., 1997, Ultrastructure of exine of gymnospermous pollen grains from Jurassic and basal Cretaceous deposits in Northwest Europe and implications for botanical relationships: *Review of Palaeobotany and Palynology*, v. 99, p. 25–54.
- Beck, H.E., Zimmermann, N.E., McVicar, T.R., Vergopolan, N., Berg, A., and Wood, E.F., 2018, Present and future Köppen-Geiger climate classification maps at 1-km resolution: *Scientific Data*, v. 5, article 180214, p. 1–12.
- Bell, W.A., 1956, Lower Cretaceous flora of western Canada: *Geological Survey of Canada Memoir*, 285 p.
- Berry, E.W., 1929, Mesozoic paleontology of the Blairmore region, Alberta—the Kootenay and Lower Blairmore floras: *National Museum of Canada Bulletin*, v. 58, p. 28–54.
- Binkley, D., and Fisher, R.F., 2019, *Ecology and management of forest soils* (5th edition): John Wiley and Sons, New York, New York, p. 1–456.
- Bray, J.R., and Gorham, E., 1964, Litter production in forests of the world: *Advances in Ecological Research*, v. 2, p. 101–157.
- Bronzo, K.M., Fricke, H., Hoerner, M.E., Foster, J.R., and Lundstrom, C., 2017, Using oxygen, carbon and strontium isotope ratios of tooth enamel from dinosaurs to infer patterns of movement over the Late Jurassic landscape of CO, UT, and WY [abs.]: *Geological Society of America Abstracts with Programs*, v. 49, no. 6, paper 303-4.
- Brown, R.W., 1946, Fossil plants and Jurassic–Cretaceous boundary in Montana and Alberta: *American Association of Petroleum Geologists Bulletin*, v. 30, p. 238–248.
- Brown, J.T., 1972, *The flora of the Morrison Formation (Upper Jurassic) of central Montana*: Missoula, University of Montana, Ph.D. dissertation, 65 p.
- Burns, C.E., Mountney, N.P., Hodgson, D.M., and Colombera, L., 2019, Stratigraphic architecture and hierarchy of fluvial overbank splay deposits: *Journal of the Geological Society*, v. 176, p. 629–649.
- Calvert, W.R., 1909, *Geology of the Lewistown coal field Montana*: U.S. Geological Survey Bulletin 390, p. 1–83.
- Carpenter, K., 2022, *The lithostratigraphic Tidwell Member of the Morrison or Summerville Formation (Upper Jurassic)—who, what, where, when*: *Geology of the Intermountain West*, v. 9, p. 49–114.
- Chaudhri, A.R., and Singh, M., 2012, Clay minerals as climate change indicators—a case study: *American Journal of Climate Change*, v. 1, p. 231–239.
- Christie, H.H., 1961, *Geology of the southern part of the Gravelly Range southwestern Montana*: Corvallis, Oregon State University, M.S. thesis, 159 p.
- Chure, D.J., Litwin, R., Hasiotis, S., Evanoff, E., and Carpenter, K., 2006, The fauna and flora of the Morrison Formation, in Foster, J.R., and Lucas, S.G., editors, *Paleontology and geology of the Upper Jurassic Morrison Formation*: New Mexico Museum of Natural History and Science Bulletin 36, p. 233–249.
- Cobban W.A., 1945, *Marine Jurassic Formations of Sweetgrass Arch, Montana*: *American Association of Petroleum Geologists Bulletin*, v. 29, p. 1262–1303.
- Cobban, W.A., Erdmann, C.E., Lemke, R.W., and Maughan, E.K., 1976, *Type sections and stratigraphy of the member of the Blackleaf and Marias River Formations (Cretaceous) of the Sweetgrass Arch, Montana*: U.S. Geological Survey Professional Paper 974, 66 p.
- Collier, A.J., 1929, *The Kevin-Sunburst oil field and other possibilities of oil and gas in the Sweetgrass Arch, Montana*: U.S. Geological Survey Contributions to Economic Geology Part II, p. 57–189.
- Connely, M.V., 2002, *Stratigraphy and paleoecology of the Morrison Formation, Como Bluff, Wyoming*: Logan, Utah State University, M.S. thesis, 109 p.

- Connely, M.V., 2006, Preliminary results of the geological investigations for the Montana sauropod project: Wyoming, Casper College, unpublished report, 2 p.
- Cooley, J.T., 1993, Fluvial systems of the Upper Jurassic Morrison Formation, northern Beartooth and Gallatin Ranges, southwest Montana: Bozeman, Montana State University, M.S. thesis, 55 p.
- Cooley, J.T., and Schmitt, J.G., 1998, An anastomosed fluvial system in the Morrison Formation (Upper Jurassic) of southwest Montana: *Modern Geology*, v. 22, p. 171-208.
- Daniel, J.A., Bartholomew M.J., and Murray, R.C., 1992, Geological characteristics of the Stockett bed coal in the central Great Falls coal field Montana—coal geology of Montana: Montana Bureau of Mines and Geology Special Publication 102, p. 145-157.
- Dekalb, L.H., 1922, A guide to the geology of Fergus County, Montana: Argus Printing and Supply Company, Lewistown, Montana, p. 1-48.
- Demko, T.M., Currie, B.S., and Nicoll, K.A., 2004, Regional paleoclimatic and stratigraphic implications of paleosols and fluvial/overbank architecture in the Morrison Formation (Upper Jurassic), Western Interior, USA: *Sedimentary Geology*, v. 167, p. 115-135.
- Demko, T.M., and Parrish, J.T., 1998, Paleoclimatic setting of the Upper Jurassic Morrison Formation: *Modern Geology*, v. 22, p. 283-296.
- Deng, S., 2002, Ecology of the Early Cretaceous ferns of northeast China: Review of Palaeobotany and Palynology, v. 119, p. 93-112.
- Dickinson, W.R., and Suczek, C.A., 1979, Plate tectonics and sandstone compositions: *American Association of Petroleum Geologists Bulletin*, v. 63, p. 2164-2182.
- Dodson, P., Behrensmeyer, A.K., Bakker, R.T., and McIntosh, J.S., 1980, Taphonomy and paleoecology of the dinosaur beds of the Jurassic Morrison Formation: *Paleobiology*, v. 6, p. 208-232.
- Dott, R.H., Jr., 1964, Wacke, graywacke and matrix—what approach to immature sandstone classification?: *Journal of Sedimentary Petrology*, v. 34, p. 625-632.
- Dunagan, S.P., 1999, Paleosynecology and taphonomy of freshwater carbonate lakes and ponds from the Upper Jurassic Morrison Formation (Western Interior, U.S.A.) [abs.]: *Geological Society of America Abstracts with Programs*, v. 31, no. 7, p. 365.
- Dunagan, S.P., Driese, S.G., and Walker, K.R., 1997, Paleolimnological implications of Magadi-type cherts from lacustrine carbonates in the Morrison Formation (Upper Jurassic) Colorado, U.S.A. [abs.]: *Geological Society of America Abstracts with Programs*, v. 29, no. 6, p. 270.
- Dunagan, S.P., and Turner, C.E., 2004, Regional paleohydrologic and paleoclimatic settings of wetland/lacustrine depositional systems in the Morrison Formation (Upper Jurassic), Western Interior USA [abs.]: *Sedimentary Geology Abstracts with Programs*, v. 167, p. 269-296.
- Dupree, R.T., 2009, Provenance of Lower Kootenai (Lower Cretaceous) fluvial sandstone bodies, Sandy Hollow/Big Hole River area, southwestern Montana: Lafayette, University of Louisiana, M.S. thesis, 84 p.
- Emmons, S.F., Cross, W., and Eldridge, G.H., 1896, *Geology of the Denver Basin in Colorado*: U.S. Geological Survey Monograph 27, 556 p.
- Evanoff, E., Good, S.C., and Hanley, J.H., 1998, An overview of the freshwater mollusks from the Morrison Formation: *Modern Geology*, v. 22, p. 423-450.
- Falcon-Lang, H.J., Fensome, R.A., and Venugopal, D.V., 2003, The Cretaceous age of the Vinegar Hill silica sand deposit, southern New Brunswick—evidence from palynology and paleobotany: *Atlantic Geology*, v. 39, p. 39-46.
- Fisher, C.A., 1907, The Great Falls coal field, Montana: U.S. Geological Survey Bulletin 316—Contributions to Economic Geology, pt. 2., p. 161-211.
- Fisher, C.A., 1908, Southern extension of the Kootenai and Montana coal-bearing formation in northern Montana: *Economic geology and the Bulletin of the Society of Economic Geologists*, v. 3, p. 77-99.
- Fisher, C.A., 1909, *Geology of the Great Falls coal field Montana*: U.S. Geological Survey Bulletin 356, 85 p.
- Fisher, J.A., Krapf, C.B.E., Lang, S.C., Nichols, G.J., and Payenberg, T.H.D., 2008, Sedimentology and architecture of the Douglas Creek terminal splay, Lake Eyre, central Australia: *Sedimentology*, v. 55, p. 1915-1930.
- Folk, R.L., 1959, Practical petrographic classification of limestones: *American Association of Petroleum Geologist Bulletin*, v. 43, p. 1-38.
- Folk, R.L., and Ward, W.C., 1957, Brazos River Bar—a study in the significance of grain size parameters: *Journal of Sedimentary Petrology*, v. 27, p. 3-26.

- Fontaine, W.M., 1893, Description of some fossil plants from the Great Falls coal field of Montana: Proceedings of the United States National Museum, v. 15, p. 487–495.
- Foster, J., 2007, Jurassic West—the dinosaurs of the Morrison Formation and their world: Indiana University Press, 389 p.
- Foster, J.R., Gee, C.T., Ash, S.R., and Kirkland, J.I., 2023, Preliminary observations of the Jurassic Sald Bar, a new ginkgo-phyte-dominated flora from the Upper Jurassic Morrison Formation in southeastern Utah, USA: The Anatomical Record, v. 306, p. 96–101.
- Foster, J.R., Hunt, A.P., and Kirkland, J.I., 2022, Significance of a small *regurgitalite* containing *lissamphibian* bones from the Morrison Formation Upper Jurassic, within a diverse plant locality deposit in southeastern Utah, USA: PALAIOS, v. 37, p. 433–442.
- Francis, D.R., 1956, Some aspects of Jurassic stratigraphy in the Williston Basin area: First International Williston Basin Symposium, p. 179–185.
- Francis, D.R., 1957, Jurassic stratigraphy of Williston Basin area: American Association of Petroleum Geologists Bulletin, v. 41, p. 367–398.
- Fraser, G.D., Waldrop, H.A., and Hyden, H.J., 1969, Geology of the Gardiner area, Park County, Montana: U.S. Geological Survey Bulletin 1277, p. 1–118.
- Freeman, O.W., 1919, Geography and geology of Fergus County: Fergus High School Bulletin 2, p. 1–71.
- Fuentes, F., DeCelles, P.G., Constenius, K.N., and Gehrels, G.E., 2011, Evolution of the Cordilleran foreland basin system in northwestern Montana, U.S.A.: Geological Society of America Bulletin, v. 123, p. 507–533.
- Gaffney, E.S., 1979, The Jurassic turtles of North America: Bulletin of the American Museum of Natural History, v. 162, no. 3, p. 91–136.
- Gardner, L.S., 1950, Geology of the Button Butte–Forestgrove area, Fergus County, Montana: U.S. Geological Survey Oil and Gas Investigations Preliminary Map 106, scale 1:63,360.
- Gardner, L.S., 1959, Geology of the Lewistown area, Fergus County, Montana: U.S. Geological Survey Oil and Gas Investigations Map OM-199, scale 1:63,360.
- Gardner, L.S., Hendricks, T.A., Hadley, H.D., and Rogers, C.P., Jr., 1945, Columnar sections of Mesozoic and Paleozoic formation in the mountains of south-central Montana: U.S. Geological Survey Oil and Gas Investigations Preliminary Chart 18.
- Gardner, L.S., Hendricks, T.A., Hadley, H.D., and Rogers, C.P., Jr., 1946, Stratigraphic sections of Upper Paleozoic and Mesozoic rocks in south-central Montana: Montana Bureau of Mines and Geology Memoir 24, p. 40–42.
- Gee, C.T., Sprinkel, D.A., Bennis, M.B., and Gray, D.E., 2019, Silicified logs of *Agathoxylon hoodii* (Tidwell et Medlyn) comb. nov. from Rainbow Draw near Dinosaur National Monument, Uintah County, Utah, USA, and their implications for araucariaceous conifer forests in the Upper Jurassic Morrison Formation: Geology of the Intermountain West, v. 6, p. 77–92.
- Gibling, M.R., 2006, Width and thickness of fluvial channel bodies and valley in the geological records—a literature compilation and classification: Journal of Sedimentary Petrology, v. 76, p. 731–770.
- Giffen, E.B., Gabriel, D.L., and Johnson, R.E., 1988, A new Pachycephalosaurid skull (*Ornithischia*) from the Cretaceous Hell Creek: Journal of Vertebrate Paleontology, v. 7, p. 398–407.
- Good, S.C., 2004, Paleoenvironmental and paleoclimatic significance of freshwater bivalves in the Upper Jurassic Morrison Formation, Western Interior, USA: Sedimentary Geology, v. 167, p. 163–176.
- Gorman, M.A., II, 2007, A lacustrine Late Jurassic flora in the Morrison Formation [abs.]: Geological Society of America Abstracts with Programs, v. 39, no. 6, p. 89.
- Gorman, M.A., II, Miller, I.M., Pardo, J.D., and Small, B.J., 2008, Plants, fish, turtles, and insects from the Morrison Formation—a Late Jurassic ecosystem near Cañon City, Colorado: Geological Society of America Field Guide, v. 10, p. 295–310.
- Gregory, H.E., 1938, The San Juan County—a geographic and geologic reconnaissance of southeastern Utah: U.S. Geological Survey Professional Paper 188, p. 1–123.
- Gu, N., Jiang, W., Wang, L., Zhang, E., Yang, S., and Xiong, S., 2015, Rainfall thresholds for the precipitation of carbonate and evaporite minerals in modern lakes in northern China: Geophysical Research Letters, v. 42, p. 5895–5901.
- Guyette, R.P., and Cutter, B.E., 1994, Barium and manganese trends in tree-rings as monitors of sulfur deposition: Water, Air, and Soil Pollution, v. 73, p. 213–223.
- Hadley, H.D., 1956, Cat Creek oil field, in Foster, D.L., editor, Judith Mountains—central Montana: Billings Geological Society Guidebook 7<sup>th</sup> Annual Field Conference, p. 98–103.

- Hadley, H.D., and Milner, R.L., 1953, Stratigraphy of Lower Cretaceous and Jurassic, northern Montana—southwestern Saskatchewan, in Parker, J.M., editor, Little Rocky Mountains—Montana and southwestern Saskatchewan: Billings Geological Society Guidebook 4th Annual Field Conference, p. 85–86.
- Harland, M., Francis, J.E., Brentnall, S.J., and Beerling, D.J., 2007, Cretaceous (Albian–Aptian) conifer wood from Northern Hemisphere high latitudes—forest composition and palaeoclimate: Review of Palaeobotany and Palynology, v. 143, p. 167–196.
- Harris, J.D., 2006a, Cranial osteology of *Suuwassea emilieae* (Sauropoda: Diplodocoidea: Flagellicaudata) from the Upper Jurassic Morrison Formation of Montana, USA: Journal of Vertebrate Paleontology, v. 26, p. 88–102.
- Harris, J.D., 2006b, The axial skeleton of *Suuwassea emilieae* (Sauropoda: Flagellicaudata) from the Upper Jurassic Morrison Formation of Montana, USA: Palaeontology, v. 49, p. 1091–1121.
- Harris, J.D., 2007, The appendicular skeleton of *Suuwassea emilieae* (Sauropoda: Flagellicaudata) from the Upper Jurassic Morrison Formation of Montana (USA): Geobios, v. 40, p. 501–522.
- Harris, J.D., and Dodson, P., 2004, A new diplodocoid sauropod dinosaur from the Upper Jurassic Morrison Formation of Montana, USA: Acta Palaeontologica Polonica, v. 49, p. 197–210.
- Harris, W.L., 1966, The stratigraphy of the Upper Jurassic–Lower Cretaceous rocks in the Great Falls–Lewistown coal field, central Montana, in Cox, J.E., editor, Jurassic and Cretaceous stratigraphic traps—Sweetgrass Arch: Billings Geological Society Guidebook 17th Annual Field Conference, p. 164–177.
- Harris, W.L., 1968, Stratigraphy and economic geology of the Great Falls–Lewistown coal field: Missoula, University of Montana, M.S. thesis, 126 p.
- Hayden, F.V., 1869, Geological report of the exploration of the Yellowstone and Missouri Rivers, 1859–1860: U.S. War Department, Chapter 10, p. 85–94.
- Hecht, M.K., and Estes, R., 1960, Fossil amphibians from Quarry Nine: Postilla, v. 46, p. 1–19.
- Hobbs, B.B., 1967, Structure and stratigraphy of the Argenta area, Beaverhead County, Montana: Corvallis, Oregon State University, M.S. thesis, 164 p.
- Horne, D.J., 2002, Ostracod biostratigraphy and palaeoecology of the Purbeck Limestone Group in southern England: The Palaeontological Association, Special Papers in Palaeontology v. 68, p. 53–70.
- Horner, J.R., 1988, A new hadrosaur (Reptilia, Ornithischia) from the Upper Cretaceous Judith River Formation of Montana: Journal of Vertebrate Paleontology, v. 8, p. 314–321.
- Hotton, C.L., 1986, Palynology of the Morrison Formation: Proceedings of the Fourth North American Paleontological Convention, p. A20.
- Hotton, C.L., and Baghai-Riding, N.L., 2010, Palynological evidence for conifer dominance within a heterogeneous landscape in the Late Jurassic Morrison Formation, U.S.A., in Gee, C.T., editor, Plants in Mesozoic time: Bloomington, Indiana University Press, p. 295–328.
- Hotton, C.L., and Baghai-Riding, N.L., 2016, Palynology of the Late Jurassic Morrison Formation—new insights into floristics, paleoclimate, phytogeography and tetrapod herbivory [abs.]: Society of Vertebrate Paleontology Abstracts with Programs, p. 157.
- Hunt, T.C., and Richmond, D.R., 2018, The aquatic vertebrate community of a bone-dry pond—the historic Stovall Quarry 8, Morrison Formation in the panhandle of Oklahoma [abs.]: Society of Vertebrate Paleontology Abstracts with Programs, p. 152.
- Ibarra, Y., Corsetti, F.A., Cheetham, M.I., and Feakins, S.J., 2014, Were fossil spring-associated carbonates near Zaca Lake, Santa Barbara, California deposited under an ambient or thermal regime?: Sedimentary Geology, v. 301, p. 15–25.
- Imlay, R.W., 1954, Marine Jurassic Formation in the Pryor Mountains and northern Bighorn Mountains, Montana, in Richards, P.W., editor, Pryor Mountains—northern Bighorn Basin, Montana: Billings Geological Society Guidebook 5<sup>th</sup> Annual Field Conference, p. 54–64.
- Jackson, F.D., and Varricchio, D.J., 2010, Fossil eggs and eggshell from the lowermost Two Medicine Formation of western Montana, Sevenmile Hill Locality: Journal of Vertebrate Paleontology, v. 30, p. 1142–1156.
- Jansa, L. 1972, Depositional history of the coal-bearing Upper Jurassic–Lower Cretaceous Kootenay Formation, southern Rocky Mountains, Canada: Geological Society of America Bulletin, v. 83, p. 3199–3222.



- Jennings, D.S., Driese, S.G., and Dworkin, S.I., 2015, Comparison of modern and ancient barite-bearing acid-sulphate soils using micromorphology, geochemistry and field relationships: *Sedimentology*, v. 62, p. 1078–1099.
- Joeckel, R.M., Ludvigson, G.A., Moller, A., Hotton, C.L., Suarez, M.B., Suarez, C.A., Kirkland, J.I., and Henrix, B., 2019, Chronostratigraphy and terrestrial palaeoclimatology of Berriasian–Hauterivian strata of the Cedar Mountain Formation, Utah, USA, in Wagreich, M., Hart, M.B., Sames, B., and Yilmaz, I.O., editors, Cretaceous climate events and short-term sea-level changes: Geological Society of London Special Publications 498, <https://doi.org/10.1144/SP498-2018-133>.
- Johnson, E.A., 2005, Geologic assessment of undiscovered oil and gas resources in the Phosphoria total petroleum system, southwestern Wyoming province, Wyoming, Colorado, Utah: U.S. Geological Survey Digital Data Series, DDS-69-D, p. 1–46.
- Johnson-Carroll, A., 2014, Paleoenvironment and paleoclimate of the Jurassic Morrison Formation, Fergus County, central Montana: Rapid City, South Dakota School of Mines and Technology, M.S. thesis, 55 p.
- Kantor, D.C., 1995, Stratigraphy and sedimentology of the Upper Brushy Basin Member, Morrison Formation (Upper Jurassic), eastern central Utah: Madison, University of Wisconsin, M.S., thesis, 114 p.
- Khalid, M.E.A., 1990, Sedimentology of the Swift Formation (Jurassic) in the Little Rocky Mountains: Saskatoon, University of Saskatchewan, Canada, M.S. thesis, 107 p.
- Kirkland, J.I., 1987, Upper Jurassic and Cretaceous lungfish tooth plates from the Western Interior, the last dipnoan faunas of North America: *Hunteria*, v. 2, no. 2, p. 1–16.
- Knechtel, M.M., 1959, Stratigraphy of the Little Rocky Mountains and the encircling foothills Montana: U.S. Geological Survey Professional Paper 1072-N, p. 723–752.
- Knowlton, F.H., 1908, Description of a collection of Kootanie plants from the Great Falls coal field of Montana: Smithsonian Miscellaneous Collections, v. 50, p. 105–128.
- Kovada, I., and Mermut, A.R., 2010, Vertic features, in Stoops, G., Marcelino, V., and Mees, F., editors, Interpretation of micromorphological features of soils and regoliths: Amsterdam, Netherlands, Elsevier, p. 109–127.
- Kürschner, W.M., Batenburg, S.J., and Mander, L., 2013, Aberrant *Classopollis* pollen reveals evidence for unreduced (2n) pollen in the conifer family Cheirolepidiaceae during the Triassic–Jurassic transition: *Proceedings of the Royal Society B*, v. 280:20131708, p. 1–8, <http://dx.doi.org/10.1098/rspb.2013.1708>.
- LaPasha, C.A., 1982, Paleocology of the Lower Cretaceous Kootenai Formation flora in the Great Falls area, Montana: Missoula, University of Montana, Ph.D. dissertation, 222 p.
- LaPasha, C.A., and Miller, C.N., Jr., 1985, Flora of the Early Cretaceous Kootenai Formation in Montana, bryophytes and tracheophytes excluding conifers: *Palontographica—Beitrgte zur Naturgeschichte der Vorzeit*, v. 4–6, p. 111–145.
- Lindsey, D.A., 1980, Reconnaissance geologic map of the Big Snowies wilderness and contiguous RARE II study areas, Fergus, Golden Valley, and Wheatland counties, Montana: U.S. Geological Survey Miscellaneous Field Studies Map MF-1243-A, scale 1:100,000.
- Litwin, R., Turner, C.E., and Peterson, F., 1998, Palynological evidence on the age of the Morrison Formation, Western Interior U.S.: *Modern Geology*, v. 22, p. 297–320.
- Lockley, M.G., Houck, K.J., and Prince, N.K., 1986, North America largest dinosaur trackway site—implications for Morrison Formation paleocology: *Geological Society of America Bulletin*, v. 103, p. 1163–1176.
- Lockley, M.G., Prince, N.K., Houck, K.J., and Carpenter, K., 1984, Reconstruction of a Late Jurassic lacustrine ecosystem [abs.]: *Geological Society of America Abstracts with Programs*, v. 16, no. 4, p. 228.
- Loucks, R.G., Reed, R.M., Ruppel, S.C., and Hammes, U., 2012, Spectrum of pore types and networks in mudrocks and a descriptive classification for matrix-related mudrock pores: *American Association of Petroleum Geologists Bulletin*, v. 96, p. 1071–1098.
- Ludvigson, G.A., Witzke, B.J., Joeckel, R.M., Ravn, R.L., Phillips, P.L., González, L.A., and Brenner, R.L., 2010, New insights on the sequence stratigraphic architecture of the Dakota Formation in Kansas–Nebraska–Iowa from a decade of sponsored research activity: *Current Research in Earth Sciences Bulletin* 258, pt. 2, p. 1–31.
- Lupton, C.T., 1914, Oil and gas near Green River, Grand County, Utah: U.S. Geological Survey Bulletin 541, p. 115–140.

- Lupton, C.T., and Lee, W., 1921, Geology of the Cat Creek oil field, Fergus and Garfield Counties, Montana: American Association of Petroleum Geologists Bulletin, v. 5, p. 252–275.
- Lürling, M., Eshetu, F., Faassen, E.J., Kosten, S., and Huszar, V.L.M., 2013, Comparison of cyanobacterial and green algal growth rates at different temperatures: Freshwater Biology, v. 58, p. 552–559.
- Maidment, S., and Muxworthy, A., 2019, A chronostratigraphic framework for the Upper Jurassic Morrison Formation, western U.S.A.: Journal of Sedimentary Research, v. 89, p. 1017–1038.
- Maidment, S., Woodruff, D.C., and Horner, J., 2016, Environmental partitioning and differential growth in species of the Thyreophoran dinosaur *Stegosaurus* in the Upper Jurassic Morrison Formation, USA [abs.]: The Palaeontological Association Abstracts with Programs, p. 40.
- Maidment, S.C.R., Woodruff, D.C., and Horner, J.R., 2018, New specimen of the ornithischian dinosaur *Hesperosaurus mjosi* from the Upper Jurassic Morrison Formation of Montana, U.S.A., and implications for growth and size in Morrison stegosaurs: Journal of Vertebrate Paleontology, v. 38, 22 p., <https://doi-org.ezproxy.lib.ou.edu/10.1080/02724634.2017.1406366>
- Malone, A.E., and Suttner, L.J., 1991, Deposition of the Morrison Formation (Jurassic), northern Tobacco Root Mountains, Montana with evidence against recurrent movement along the Willow Creek fault zone: The Mountain Geologist, v. 28, p. 47–64.
- Marynowski, L., Philippe, M., Zaton, M., and Hautevelle, Y., 2008, Systematic relationships of Mesozoic wood genus *Xenoxylon*—integrative biomolecular and palaeobotanical approach: Neues Jahrbuch für Geologie und Paläontologie-Abhandlungen, v. 247, p. 177–189.
- Mateus, O., 2006, Late Jurassic dinosaurs from the Morrison Formation (USA), the Lourinhã and Alcobaça Formations (Portugal), and the Tendaguru Beds (Tanzania)—a comparison, in Foster, J.R., and Lucas, S.G., editors, Paleontology and geology of the Upper Jurassic Morrison Formation: New Mexico Museum of Natural History and Science Bulletin 36, p. 223–231.
- Maxwell, W.D., 1993, Neonate dinosaur remains and dinosaur eggshells from the Lower Cretaceous Cloverly Formation, Montana: Journal of Vertebrate Paleontology, v. 13, p. 49.
- McMannis, W.J., 1965, Résumé of depositional and structural history of western Montana: American Association of Petroleum Geologists Bulletin, v. 49, p. 1801–1823.
- Miller, C.N., Jr., 1987, Land plants in the northern Rocky Mountains before the appearance of flowering plants: Annals of the Missouri Botanical Garden, v. 74, p. 692–706.
- Miller, R.N., 1954, Geology of the south Moccasin Mountains, Fergus County Montana: Butte, Montana School of Mines, M.S. thesis, 108 p.
- Milnes, R.M., and Thiry, M., 1992, Silcrete, in Martini, I.P., and Chesworth, W., editors, Weathering, soils and paleosols, chapter 14: Amsterdam, Netherlands, Elsevier Science, p. 349–377.
- Moritz, C.A., 1951, Triassic and Jurassic stratigraphy of southwestern Montana: American Association of Petroleum Geologist Bulletin, v. 35, p. 1781–1814.
- Moritz, C.A., 1960, Summary of the Jurassic stratigraphy of southwestern Montana, in Campau, D.E., and Anisgard, H.W., editors, West Yellowstone—earthquake area: Billings Geological Society 11<sup>th</sup> Annual Field Conference, p. 239–243.
- Morris, T.H., and Richmond, D.R., 1992, A predictive model of reservoir continuity in fluvial sandstone bodies of a lacustrine deltaic system, Colton Formation, Utah, in Fouch, T.D., Nuncio, V.F., and Chidsey, T.C., Jr., editors, Hydrocarbon and mineral resources of the Uinta Basin, Utah and Colorado: Utah Geological Association Publication 20, p. 227–236.
- Mullens, T.E., and Freeman, V.L., 1957, Lithofacies of the Salt Wash Member of the Morrison Formation, Colorado Plateau: Geological Society of America Bulletin, v. 68, p. 505–526.
- Myers, T.S., 2009, Late Jurassic paleoclimate of Europe and Africa: Dallas, Texas, Southern Methodist University, Ph.D. dissertation, 204 p.
- Myers, T.S., Rosenau, N.A., and Tabor, N.J., 2012b, Mean annual precipitation estimates for the Morrison Formation [abs.]: Geological Society of America Abstracts with Programs, v. 44, no. 7, p. 83.
- Meyers, J.H., and Schwartz, R.K., 1994, Summary of the depositional environments, paleogeography, and structural control on sedimentation in the Late Jurassic (Oxfordian) Sundance foreland basin, western Montana, in Caputo, M.V., Peterson, J.A., and Franczyk, K.J., editors, Mesozoic systems of the Rocky Mountain region, USA: Society of Sedimentary Geology (SEPM), Rocky Mountain Section, p. 331–349.

- Myers, T.S., Tabor, N.J., Jacobs, L.L., and Mateus, O., 2012a, Palaeoclimate of the Late Jurassic of Portugal—comparison with the Western United States: *Sedimentology*, v. 59, p. 1695-1717.
- Myers, T.S., Tabor, N.J., and Rosenau, N.A., 2014, Multiproxy approach reveals evidence of highly variable paleoprecipitation in the Upper Jurassic Morrison Formation (western United States): *Geological Society of America*, v. 126, p. 1105-1116.
- Nanson, G.C., Rust, B.R., and Taylor, G., 1986, Coexistent mud braids and anastomosing channels in an arid-zone river—Cooper Creek, central Australia: *Geology*, v. 14, p. 175-178.
- Neese, D.G., and Pigott, J.D., 1987, Ooid genesis at Brown's Cay, Bahamas—in situ diurnal observations: Liverpool, England, 8th Bathurst Meeting of Carbonate Sedimentologists Papers with Programs, p. 1-31.
- Newberry, J.S., 1888, The coal of Colorado: The School of Mines Quarterly, v. 9, p. 327-341.
- Newberry, J.S., 1891, The flora of the Great Falls coal field, Montana: *American Journal of Science*, v. 41, p. 191-201.
- Newman, K.R., 1972, A review of Jurassic, Cretaceous, and Paleocene stratigraphic palynology, in Lynn, J., Balster, C., and Warne, J., editors *Montana, Crazy Mountains Basin: Montana Geological Society 21st Annual Geological Conference*, p. 81-84.
- North, C.P., Nanson, G.C., and Fagan, S.D., 2007, Recognition of the sedimentary architecture of dryland anabranching (anastomosing) rivers: *Journal of Sedimentary Research*, v. 77, p. 925-938.
- Norwood, E.E., 1965, Geological history of central and south-central Montana: *American Association of Petroleum Geologist Bulletin*, v. 49, p. 1824-1832.
- Nowroth, V., Marquart, L., and Jendrossek, D., 2016, Low temperature-induced viable but not culturable state of *Ralstonia eutropha* and its relationship to accumulated polyhydroxybutyrate: *FEMS Microbiology Letters*, v. 363, no. 23, p. 1-8.
- Owen, A., 2014, Analyses of the Salt Wash fluvial system; quantification of a distributive fluvial system in the Late Jurassic Morrison Formation, SW USA: United Kingdom, University of London, Ph.D. dissertation, 362 p.
- Owen, A., Nichols, G.J., Hartley, A.J., Weissmann, G.S., and Scuderi, L.A., 2015, Quantification of a distributive fluvial system—the Salt Wash DFS of the Morrison Formation, SW U.S.A.: *Journal of Sedimentary Research*, v. 85, p. 544-561.
- Parrish, J.T., and Peterson, F., 1988, Wind directions predicted from global circulation models and wind directions determined from eolian sandstone of the western United States—a comparison, in Kocurek, G., editor, *Late Paleozoic and Mesozoic eolian deposits of the Western Interior of the United States: Sedimentary Geology*, v. 56, p. 261-282.
- Parrish, J.T., Peterson, F., and Turner, C.E., 2004, Jurassic “savannah”—plant taphonomy and climate of the Morrison Formation (Upper Jurassic, Western USA): *Sedimentary Geology*, v. 167, p. 137-162.
- Parrish, J.T., Ziegler, A.M., and Scotese, C.R., 1982, Rainfall patterns and the distribution of coals and evaporites in the Mesozoic and Cenozoic: *Palaeogeography, Palaeoclimatology, Palaeoecology*, v. 40, p. 67-101.
- Peck, R.E., 1956, Rocky Mountain Mesozoic and Cenozoic nonmarine microfossils, in Berg, R.R., and Strickland, J.W., editors, *Jackson Hole: Wyoming Geological Association 11th Annual Field Conference Guidebook*, p. 95-98.
- Peck, R.E., 1957, North America Mesozoic Charophyta: U.S. Geological Survey Professional Paper 294-A, p. 1-44.
- Peck, R.E., 1959, Stratigraphic distribution of Charophyta and nonmarine ostracod, in Williams, N.C., editor, *Guidebook to the geology of the Wasatch and Uinta Mountains—transition area: Intermountain Association of Petroleum Geologists Tenth Annual Field Conference*, p. 115-121.
- Pentecost, A., 1991, A new and interesting site for the calcite-encrusted desmid *Oocardium stratum* Naeg. in the British Isles: *British Phycological Journal*, v. 26, p. 297-301.
- Pester, M., Knorr, K.-H., Friedrich, M.W., Wagner, M., and Loy, A., 2012, Sulfate-reducing microorganisms in wetlands—fameless actors in carbon cycling and climate change: *Frontiers in Microbiology*, v. 3, article 72, p. 19, <https://www.frontiersin.org/articles/10.3389/fmicb.2012.00072/full>.
- Peterson, F., 1988, Pennsylvanian to Jurassic eolian transportation systems in the western United States: *Sedimentary Geology*, v. 56, p. 207-260.
- Peterson, F., and Turner-Peterson, C.E., 1987, The Morrison Formation of the Colorado Plateau—recent advances in sedimentology, stratigraphy, and paleotectonics: *Hunteria*, v. 2, p. 1-18.

- Peterson, F., and Turner, C.E., 1993, Relative age of dinosaur quarries in the Upper Jurassic Morrison Formation—a stratigraphic approach [abs.]: *Journal of Vertebrate Paleontology*, v. 13, p. 2A.
- Peterson, J.A., 1966, Sedimentary history of the Sweetgrass Arch, in Cox, J.E., editor, *Jurassic and Cretaceous stratigraphic traps—Sweetgrass Arch: Billings Geological Society Guidebook 17th Annual Field Conference*, p. 112-134.
- Peterson, J.A., 1981, General stratigraphy and regional paleostructure of the western Montana overthrust belt, in Aram, R.B., Brinker, W.F., and Grabb, R.F., Jr., editors, *Guidebook to southwest Montana: Montana Geological Society Field Conference and Symposium* p. 5-35.
- Philippe, M., Jiang, H.-E., Kim, K., Oh, C., Gromyko, D., Harland, M., Paik, I.-S., and Thévenard, F., 2009, Structure and diversity of the Mesozoic wood genus *Xenoxylon* in Far East Asia—implications for terrestrial palaeoclimates: *Lethaia*, v. 42, p. 393-406.
- Philippe, M., Puijalon, S., Suan, G., Mousset, S., Thévenard, F., and Mattioli, E., 2017, The paleolatitudinal distribution of fossil wood genera as a proxy for European Jurassic terrestrial climate: *Palaeogeography, Palaeoclimatology, Palaeoecology*, v. 466, p. 373-381.
- Philippe, M., and Thévenard, F., 1996, Repartition and palaeoecology of the Mesozoic wood genus *Xenoxylon*—palaeoclimatological implications for the Jurassic of Western Europe: *Review of Palaeobotany and Palynology*, v. 91, p. 353-370.
- Pipiringos, G.N., and O'Sullivan, R.B., 1978, Principal unconformities in Triassic and Jurassic rocks, Western Interior United States—a preliminary survey: *U.S. Geological Survey Professional Paper 1035-A*, 29 p.
- Porter, K.W., Wilde, E.M., and Vuke, S.M., 1996, Preliminary geologic map of the Big Snowy Mountains 30' x 60' quadrangle, central Montana: *Montana Bureau of Mines and Geology Open-File Report MBMG 341*, scale 1:100,000.
- Prieto-Marquez, A., and Guenther, M.F., 2018, Perinatal specimens of *Maiasaura* from the Upper Cretaceous of Montana (USA)—insights into the early ontogeny of saurolophine hadrosaurid dinosaurs: *PeerJ*, p. 1-31, doi:10.7717/peerj.4734.
- Raigemborn, M.S., Gómez-Peral, L.E., Krause, J.M., and Matheos, S.D., 2014, Controls on clay mineral assemblages in an early Paleogene nonmarine succession—implications for the volcanic and paleoclimatic record of extra-Andean Patagonia, Argentina: *Journal of South American Earth Sciences*, v. 52, p. 1-23.
- Reeves, F., 1927, Geology of the Cat Creek and Devils Basin oil fields and adjacent areas in Montana: *U.S. Geological Survey Contributions to Economic Geology, Part II*, 786B, p. 39-98.
- Richardson, J.B., 2017, Manganese and Mn/Ca ratios in soil and vegetation in forests across the northeastern US—insights on spatial Mn enrichment: *Science of the Total Environment*, v. 581-582, p. 612-620.
- Richmond, D.R., 2022, The tidal-flat parasequence of the Oxfordian Swift Formation of central Montana [abs.]: *Geological Society of America Abstracts with Programs*, v. 54, no. 2, p. 45-46.
- Richmond, D.R., 2023, A strange wood in a strange land—the paleoecology of the fossil wood *Xenoxylon* in the Late Jurassic of North America: *The Anatomical Record*, v. 306, p. 218-220.
- Richmond, D.R., Hunt, T.C., and Cifelli, R.L., 2020, Stratigraphy and sedimentology of the Morrison Formation in the western panhandle of Oklahoma with reference to the historical Stovall dinosaur quarries: *Journal of Geology*, v. 129, p. 477-515.
- Richmond, D.R., Hunt, T.C., and Elmore, R.D., 2019a, Petrology of evaporite-associated cherts of the Upper Jurassic Morrison Formation, Oklahoma Panhandle and their climatic implication [abs.]: *Geological Society of America Abstracts with Programs*, v. 51, no. 5, paper 297-5.
- Richmond, D.R., Lukens, M.W., and Celestino, S.M., 2017, Upper Jurassic Morrison Formation clams on the half shell, central Montana [abs.]: *Geological Society of America Abstracts with Programs*, v. 49, no. 5, paper 4-2.
- Richmond, D.R., Lupia, R., Hunt, T.C., and Philippe, M., 2018, The first fossil woods from the Upper Jurassic Morrison Formation of western Oklahoma [abs.]: *Geological Society of America Abstracts with Programs*, v. 50, no. 1, paper 5-3.
- Richmond, D.R., Lupia, R., and Philippe, M., 2019b, First report of the fossil wood *Piceoxylon* from the North American Jurassic (Morrison Formation, central Montana) [abs.]: *Geological Society of America Abstracts with Programs*, v. 51, no. 2, paper 38-12.
- Richmond, D.R., Lupia, R., and Philippe, M., 2019c, *Circoporoxyton* from the Upper Jurassic Morrison Formation of central Montana [abs.]: *Geological Society of America Abstracts with Programs*, v. 51, no. 5, paper 271-15.

- Richmond, D.R., Lupia, R., and Philippe, M., 2021a, The northernmost Jurassic occurrences of *Cupressinoxylon* from the Morrison Formation of central Montana [abs.]: Botanical Society of America Abstracts with Programs, no. P3PB002, id. 96.
- Richmond, D.R., Lupia, R., Philippe, M., and Klimek, J., 2019d, First occurrence of the boreal fossil wood *Xenoxylon meisteri* from the Jurassic of North America: Morrison Formation of central Montana, USA: Review of Paleobotany and Palynology, v. 267, p. 39-53.
- Richmond, D.R., and Morris, T.H., 1996, The dinosaur death trap of the Cleveland-Lloyd Dinosaur Quarry, Emery County, Utah—the continental Jurassic: Museum of Northern Arizona Bulletin 60, p. 533-545.
- Richmond, D.R., and Morris, T.H., 1998, Stratigraphy and cataclysmic deposition of the Dry Mesa Dinosaur Quarry, Mesa County, Colorado: Modern Geology, v. 22, p. 121-143.
- Richmond, D.R., and Murphy, N., 2020, Stratigraphy, sedimentology, and depositional facies of the Morrison Formation 5ES Quarry of central Montana [abs.]: Geological Society of America Abstracts with Programs, v. 52, no. 6, paper 3-12.
- Richmond, D.R., Philippe, M., and Lupia, R., 2022, The first report of the fossil wood *Protocedroxylon scoticum* from the Upper Jurassic Morrison Formation of central Montana [abs.]: Geological Society of America Abstracts with Programs, v. 54, no. 2, paper 22-1.
- Richmond, D.R., Pigott, J., Lupia, R., Behm, M., and Hein, D., 2021b, Carbonate mound springs of the Upper Jurassic Morrison Formation of central Montana and their paleoclimatic significance for the northern foreland basin: Geology of the Intermountain West, v. 8, p. 1-26.
- Richmond, D.R., and Stadtman, K.L., 1996, Sedimentology of a *Ceratosaurus* site in the San Rafael Swell, Emery County, Utah: Brigham Young University Geology Studies, v. 41, p. 117-124.
- Rouse, G.E., 1959, Plant microfossils from Kootenay coal-measures strata of British Columbia: Micropaleontology, v. 5, no. 3, p. 303-324.
- Rust, B.R., 1981, Sedimentation in an arid-zone anastomosing fluvial system—Cooper's Creek, central Australia: Journal of Sedimentary Petrology, v. 51, p. 745-755.
- Sahni, A., 1972, The vertebrate fauna of the Judith River Formation, Montana: Bulletin of the American Museum of Natural History, v. 147, p. 323.
- Saitta, E.T., 2015, Evidence for sexual dimorphism in the plated dinosaur *Stegosaurus mjosi* (Ornithischia, Stegosauria) from the Morrison Formation (Upper Jurassic) of Western USA: PLoS One, <https://doi.org/10.1371/journal.pone.0123503>.
- Sames, B., Cifelli, R.L., and Schudack, M.E., 2010, The nonmarine Lower Cretaceous of the North American Western Interior foreland basin—new biostratigraphic results from ostracod correlations and early mammals, and their implications for paleontology and geology of the basin—an overview: Earth-Science Reviews, v. 101, p. 207-224.
- Sames, B., Schudack, M.E., and Cifelli, R.L., 2008, Western Interior Early Cretaceous hiatus likely to be much shorter than previously reported—new biostratigraphic results derived from nonmarine ostracod correlations [abs.]: Geological Society of America Abstracts with Programs, v. 60, p. 540.
- Scarberry, K.C., Yakovlev, P.V., and Schwartz, T.M., 2020, Mesozoic magmatism in Montana: Montana Bureau of Mines and Geology Special Publication 122—Geology of Montana, v. 1, p. 1-30.
- Schrank, E., 2010, Pollen and spores from the Tendaguru Beds, Upper Jurassic and Lower Cretaceous of southeast Tanzania—palynostratigraphical and paleoecological implications: Palynology, v. 34, p. 3-42.
- Scholten, R., Keenmon, K.A., and Kupsch, W.O., 1955, Geology of the Lima region, southwestern Montana and adjacent Idaho: Geological Society of America Bulletin, v. 66, p. 346-404.
- Schott, R.K., Evans, D.C., Williamson, T.E., Carr, T.D., and Goodwin, M.B., 2009, The anatomy and systematics of *Colepiocephale lambei* (Dinosauria: Pachycephalosauridae): Journal of Vertebrate Paleontology, v. 29, p. 771-786.
- Schudack, M.E., Turner, C.E., and Peterson, F., 1998, Biostratigraphy, paleoecology and biogeography of charophytes and ostracodes from the Upper Jurassic Morrison Formation, Western Interior, USA: Modern Geology, v. 22, p. 379-414.
- Ségalen, P., 1971, Metallic oxides and hydroxides in soils of the warm and humid areas of the world—formation, identification, evolution: Environmental Science, Chapter 2, p. 25-38.

- Seward, A.C., 1900, Catalogue of the Mesozoic plants in the Department of Geology, British Museum (Natural History), Vol. 3—The Jurassic flora; I. The Yorkshire Coast; plates I-XXI, 341 p.
- Shen, Z., Törnqvist, T.E., Mauz, B., Chamberlain, E.L., Nijhuis, A.G., and Sandoval, L., 2015, Episodic overbank deposition as a dominant mechanism of floodplain and delta-plain aggradation: *Geology*, v. 43, p. 875–878.
- Shipman, P., 1975, Implications of drought for vertebrate fossil assemblages: *Nature*, v. 257, p. 667–668.
- Silverman, A.J., and Harris, W.L., 1966, Economic geology of the Great Falls-Lewistown coal field west-central Montana, in Cox, J.E., editor, *Jurassic and Cretaceous stratigraphic traps—Sweetgrass Arch: Billings Geological Society Guidebook 17th Annual Field Conference*, p. 149–163.
- Silverman, A.J., and Harris, W.L., 1967, Stratigraphy and economic geology of the Great Falls-Lewistown coal field Montana: *Montana Bureau of Mines and Geology Bulletin* 56, 20 p.
- Singer, A., 1980, The paleoclimatic interpretation of clay mineral in soils and weathering profiles: *Earth-Science Reviews*, v. 15, p. 303–326.
- Singer, A., 1984, The paleoclimatic interpretation of clay mineral in sediments—a review: *Earth-Science Reviews*, v. 21, p. 251–293.
- Slessarev, E.W., Lin, Y., Bingham, N.L., Johnson, J.E., Dai, Y., Schimel, J.P., and Chadwick, O.A., 2016, Water balance creates a threshold in soil pH at the global scale: *Nature*, v. 540, p. 567–569.
- Small, B.J., Gorman, M.A., Pardo, J., and Smith, D., 2007, A Late Jurassic lacustrine biota from the Morrison Formation of Colorado [abs.]: *Geological Society of America Abstracts with Programs*, v. 39, no. 6, p. 400.
- Smith, J.J., 2001, The stratigraphy and petrology of the Upper Jurassic Morrison Formation near Dillon, Montana: Atlanta, Georgia State University, M.S. thesis, 81 p.
- Smith, D.G., and Putnam, P.E., 1980, Anastomosed river deposits—modern and ancient examples in Alberta, Canada: *Canadian Journal of Earth Sciences*, v. 17, p. 1396–1406.
- Smith, D.G., and Smith, N.D., 1980, Sedimentation in anastomosed river systems—examples from alluvial valleys near Banff, Alberta: *Journal of Sedimentary Petrology*, v. 50, p. 157–164.
- Smith, J.J., Hasiotis, S.T., and Fritz, W.J., 2006, Stratigraphy and sedimentology of the Upper Jurassic Morrison Formation, Dillon, Montana, in Foster, J.R., and Lucas, S.G., editors, *Paleontology and geology of the Upper Jurassic Morrison Formation: New Mexico Museum of Natural History and Science Bulletin* 36, p. 1–7.
- Sprinkel, D.A., Bennis, M.B., Gray, D.E., and Gee, C.T., 2019, Stratigraphic setting of fossil log sites in the Morrison Formation (Upper Jurassic) near Dinosaur National Monument, Uintah County, Utah, USA: *Geology of the Intermountain West*, v. 6, p. 61–76.
- Staaf, H., 1980, Release of plant nutrients from decomposing leaf litter in a south Swedish beech forest: *Holarctic Ecology*, v. 3, p. 129–136.
- Stoops, G., Marcelino, V., and Mees, F., 2010, Micromorphological features and their relation to processes and classification—general guidelines and keys, in Stoops, G., Marcelino, V., and Mees, F., editors, *Interpretation of micromorphological features of soils and regoliths*, Chapter 2: Amsterdam, Netherlands, Elsevier, p. 15–34.
- Storrs, G.W., Oser, S.E., and Aull, M., 2012, Further analysis of a Late Jurassic dinosaur bone-bed from the Morrison Formation of Montana, USA, with a computed three-dimensional reconstruction: *Earth and Environmental Science Transactions of the Royal Society of Edinburgh*, v. 103, p. 443–458.
- Styles, E., 2014, The Little Snowy Mountains Sauropod—a taphonomical study: Devon, United Kingdom, School of Geography, Earth and Environmental Sciences, University of Plymouth, Unpublished report, 47 p.
- Summerfield, M.A., 1983, Silcrete as a palaeoclimatic indicator—evidence from southern Africa: *Palaeogeography, Palaeoclimatology, Palaeoecology*, v. 41, p. 65–79.
- Surdam, R.C., Eugster, H.P., and Mariner, R.H., 1972, Magadi-type cherts in Jurassic and Eocene to Pleistocene rocks, Wyoming: *Geological Society of America Bulletin*, v. 83, p. 2261–2266.
- Suttner, L.J., 1969, Stratigraphic and petrographic analysis of Upper Jurassic-Lower Cretaceous Morrison and Kootenai Formations, southwest Montana: *American Association of Petroleum Geologists*, v. 53, p. 1391–1410.
- Taylor, G., and Eggleton, R.A., 2017, Silcrete—an Australian perspective: *Australian Journal of Earth Sciences*, v. 64, p. 987–1016.

- Tekleva, M.V., Krassilov, V.A., Kvaček, J., van Konijnenburn-van Cittert, J.H.A., 2006, Pollen genus *Eucommiidites*: ultrastructure and affinities: *Acta Palaeobotanica*, v. 46, p. 137-155.
- Tian, N., Wang, Y.-D., Philippe, M., Li, L.-L., Xie, X.-P., and Jiang, Z.-K., 2016, New record of fossil wood *Xenoxylon* from the Late Triassic in the Sichuan Basin, southern China and its paleoclimatic implications: *Palaeogeography, Palaeoclimatology, Palaeoecology*, v. 464, p. 65-75.
- Tidwell, W., 1990, Preliminary report on the megafossil flora of the Upper Jurassic Morrison Formation: *Hunteria*, v. 2, no. 8, p. 3-12.
- Towse, D., 1954, Jurassic system in Williston Basin: *American Association of Petroleum Geologists Bulletin*, v. 38, no. 4, p. 454-462.
- Trewin, N.H., and Fayers, S.R., 2005, Chert, in Selley, R.C., Cocks, L.R.M., and Plimer, I.R., editors, *Encyclopedia of geology, sedimentary rocks*: Amsterdam, Netherlands, Elsevier, , p. 51-62.
- Trujillo, K.C., 2006, Clay mineralogy of the Morrison Formation (Upper Jurassic-?Lower Cretaceous), and its use in long distance correlation and paleoenvironmental analyses, in Foster, J.R., and Lucas, S.G., editors, *Paleontology and geology of the Upper Jurassic Morrison Formation*: New Mexico Museum of Natural History and Science Bulletin 36, p. 17-23.
- Tschudy, R.H., Tschudy, B.D., and Van Loenen, S., 1980, Illustrations of plant microfossils from the Morrison Formation. I. Plant microfossils from the Brushy Basin Member: U.S. Geological Survey Open-File Report 81-35, 20 p.
- Tschudy, R.H., Tschudy, B.D., and Van Loenen, S., 1988, Illustrations of plant microfossils from the Morrison Formation. IV. Plant microfossils from the Salt Wash Member: U.S. Geological Survey Open-File Report 88-235, 25 p.
- Turner, C.E., and Fishman, N.S., 1991, Jurassic Lake T'ood'ichi'—a large alkaline, saline lake, Morrison Formation, eastern Colorado Plateau: *Geological Society of America Bulletin*, v. 103, p. 538-558.
- Turner, C.E., and Peterson, F., 1999, Biostratigraphy of dinosaurs in the Upper Jurassic Morrison Formation of the Western Interior, U.S.A.: Utah Geological Survey Miscellaneous Publication 99-1, p. 77-114.
- Turner-Peterson, C.E., and Fishman, N.S., 1986, Geologic synthesis and genetic models for Uranium mineralization in the Morrison Formation, Grants uranium region New Mexico, in Turner-Peterson, C.E., Santos, E.S., and Fishman, N.S., editors, *A basin analysis case study—Morrison Formation, Grants uranium region, New Mexico*: American Association of Petroleum Geologists Studies in Geology 22, p. 357-388.
- Tryon, R.M., and Tryon, A.F., 1982, Ferns and allied plants with special reference to tropical America: New York, Springer-Verlag, p. 1-857.
- Uhlir, D.M., Akers, A., and Vondra, C.F., 1988, Tidal inlet sequence, Sundance Formation (Upper Jurassic), north-central Wyoming: *Sedimentology*, v. 35, p. 739-752.
- Valdes, P.J., and Sellwood, B.W., 1992, A palaeoclimate model for the Kimmeridgian: *Palaeogeography, Palaeoclimatology, Palaeoecology*, v. 95, p. 47-72.
- Vaez-Javadi, F., 2018, Middle Jurassic flora from the Hojedk Formation in Tabas, central east Iran—biostratigraphy and palaeoclimate implications: *Rivista Italiana de Paleontologia e Stratigraphia*, v. 124, p. 299-316.
- Vakhrameyev, V.A., 1964, Jurassic floras of the USSR: *The Palaeobotanist*, v. 14, p. 118-123.
- Vakhrameyev, V.A., 1982, *Classopollis* pollen as an indicator of Jurassic and Cretaceous climate: *International Geology Review*, v. 24, p. 1190-1196.
- Vine, J.D., 1956, Geology of the Stanford-Hobson area central Montana: U.S. Geological Survey Bulletin 1027-J, p. 405-470.
- Walker, T.F., 1974, Stratigraphy and depositional environments of the Morrison and Kootenai Formations in the Great Falls area, central Montana: Missoula, University of Montana, Ph.D. dissertation, 113 p.
- Wang, Y., 2002, Fern ecological implications from the Lower Jurassic in western Hubei, China: *Review of Palaeobotany and Palynology*, v. 119, p. 125-141.
- Weed, W.H., 1892, Two Montana coal fields: *Geological Society of America Bulletin*, v. 3, p. 301-330.
- White, P.M., Fastovsky, D.E., and Sheehan, P.M., 1998, Taphonomy and suggested structure of the dinosaurian assemblage of the Hell Creek Formation (Maastrichtian), eastern Montana and western North Dakota: *PALAIOS*, v. 13, p. 41-51.

- Woodruff, C.D., and Foster, J.R., 2017, The first specimen of *Camarasaurus* (Dinosauria: Sauropods) from Montana—the northernmost occurrence of the genus: PLoS ONE 12 (5), e0177423, <https://doi.org/10.1371/journal.pone.0177423>.
- Woodruff, C.D., Trexler, D., and Maidment, S.C.R., 2019, Two new stegosaur specimens from the Upper Jurassic Morrison Formation of Montana, USA: *Acta Palaeontologica Polonica*, v. 64, p. 461–480.
- Wosik, M., Goodwin, M.B., and Evans, D.C., 2017, A nestling-sized skeleton of *Edmontosaurus* (Ornithischia, Hadrosauridae) from the Hell Creek Formation of northeastern Montana, U.S.A., with an analysis of ontogenetic limb allometry: *Journal of Vertebrate Paleontology*, v. 37, p. 1–26.
- Wu, Y., Qiu, S., Fu, S., Roa, Z., and Zhu, Z., 2018, Pleistocene climate change inferred from multi-proxy analyses of a loess-paleosol sequence in China: *Journal of Asian Earth Sciences*, v. 154, p. 428–434.
- Xin, C., Wang, L., Du, D., Zhang, Y., and Wang, J., 2018, Cuticles and spores in situ of *Coniopteris hymenophylloides* from the Middle Jurassic in Gansu, northwestern China: *Acta Geologica Sinica*, v. 92, p. 904–914.
- Yen, T.-C., 1952, Molluscan fauna of the Morrison Formation: U.S. Geological Survey Professional Paper 233-B, 49 p.
- Yuan, X.-C., Xiong, C.-H., Sun, F.-K., Wang, Z.-X., Moa, T., Li, Y.-J., Liu, C.-H., Sun, M.-X., Dong, J.-L., and Sun, B.-N., 2018, The geological significance of a new species of *Coniopteris* from the Middle Jurassic of northwestern China: *Historical Biology*, v. 32, p. 267–280.
- Zhang, J., 2022, Quantitative analysis of Triassic-Jurassic pollen and spores for paleoenvironmental and paleoclimate reconstructions: Germany, Institute of Applied Geosciences of the Technischen Universität Darmstadt, Ph.D. dissertation, 113 p.
- Zhang, Y., Lui, B., and Liang, F., 2019, A new species of *Coniopteris moguqiensis* sp. nov. from the Middle Jurassic Wanbao Formation in eastern Inner Mongolia, China: *Acta Geologica Sinica*, v. 93, p. 1317–1324.
- Zhao, L., Hong, H., Fand, Q., Yin, K., Wang, C., Li, Z., Torrent, J., Cheng, F., and Algeo, T.J., 2017, Monsoonal climate evolution in southern China since 1.2 Ma—new constraints from Fe-oxide records in red earth sediments from the Shenglia section, Chengdu Basin: *Palaeogeography, Palaeoclimatology, Palaeoecology*, v. 473, p. 1–15.